NEW MEXICO DEPARTMENT OF TRANSPORTATION

RESEARCH BUREAU

Innovation in Transportation

Evaluation of Plus Grades of Performance Graded (PG) Asphalt Binder (Phase II)

Final Report

Prepared by:
University of New Mexico
Department of Civil Engineering
Albuquerque, NM 87131

Prepared for:
New Mexico Department of Transportation
Research Bureau
7500B Pan American Freeway NE
Albuquerque, NM 87109

In Cooperation with:
The US Department of Transportation
Federal Highway Administration

Report NM14MSC-01

JANUARY 26, 2019

THIS PAGE LEFT INTENTIONALLY BLANK

USDOT FHWA SUMMARY PAGE

1. Report No. NM14MSC-01	2. Recipient's Catalog No.
3. Title and Subtitle Evaluation of Plus Grades of Performance Graded (PG) Asphalt Binder (Phase II)	4. Report Date January 26, 2019
5. Author(s): Rafiqul A. Tarefder and Md Amanul Hasan	6. Performing Organization Report No. NM14MSC-01
7. Performing Organization Name and Address University of New Mexico Department of Civil Engineering MSC01 1070 1 University of New Mexico Albuquerque, NM 87131	8. Performing Organization Code 456A 9. Contract/Grant No. 456-482
10. Sponsoring Agency Name and Address Research Bureau New Mexico Department of Transportation (NMDOT) 7500B Pan American Freeway PO Box 94690 Albuquerque, NM 87199-4690	11. Type of Report and Period Covered Final Report January 27, 2016 – January 26, 2019 12. Sponsoring Agency Code New Mexico DOT
13. Supplementary Notes The research project is funded by NMDOT in cooperation with the FHWA	

14. Abstract

The current Performance Grade (PG) system utilizes Dynamic Shear Rheometer (DSR), Bending Beam Rheometer (BBR), and Direct Tension (DT) tests to specify the grades of a binder. Some past studies reported that these tests apply very small amount of loadings those are within the Linear Viscoelastic (LVE) limits of the binder, where polymer network may be inactive. Therefore, researchers recommend different performance-based tests for the Polymer Modified Binders (PMBs) along with the existing PG tests. This study explored the effectiveness of different binder tests for better characterization of PMBs. In the beginning, a neat binder was blended with Styrene-Butadiene- Styrene (SBS) polymer at three different percentages: 1%, 3%, and 5%. The blended binders were used to develop a calibration curve using Fourier Transform Infrared (FTIR) spectroscopy for detecting SBS content in an unknown PMB. The laboratory produced binders were also used to prepare the mixture samples for performance tests. Next, Hamburg Wheel Track Device, Beam Fatigue, and Thermal Stress Restrained Specimen Test tests were performed on mixture samples made with different PMB binders to investigate the rutting, fatigue cracking and low-temperature performance respectively. Binder performance was evaluated through current PG tests. In addition to the PG tests, other binder tests such as Elastic Recovery, Forced Ductility, Multiple Stress Creep Recovery (MSCR), Time Sweep (TS), and Linear Amplitude Sweep (LAS) tests were conducted to evaluate which binder tests were more appropriate for PMBs. Results show that the traditional existing PG tests failed to characterize the PMBs properly. It is found that the MSCR test is most suitable for representing rutting performance. Both TS and LAS tests can successfully evaluate the fatigue cracking performance of a PMB. For thermal cracking, the critical cracking temperature calculated from BBR and DT tests' data can be a good option for characterizing the low-temperature cracking performance of a PMB.

15. Key Words Polymer, PMBs, Performance, PG Tests, PG Plus Tests, FTIR, MSCR, TS, LAS, Critical Temperature		16. Distribution Statement Available from NMDOT Research Bureau	
17. Security Classi. of the Report None	18. Security Classi. of this page None	19. Number of Pages 91	20. Price N/A

THIS PAGE LEFT BLANK INTENTIONALLY

PROJECT NO. NM14MSC-01

EVALUATION OF PLUS GRADES OF PERFORMANCE GRADED (PG) ASPHALT BINDER (PHASE II)

FINAL REPORT

January 27, 2016 – January 26, 2019

A Report on Research Sponsored by:

Research Bureau
New Mexico Department of Transportation
7500B Pan American Freeway NE,
PO Box 94690
Albuquerque, NM 87199-4690
(505)-841-9145
Research.bureau@state.nm.us
http://NMDOTRearch.com

Prepared by:
Rafiqul A. Tarefder and Md Amanul Hasan
Department of Civil Engineering
University of New Mexico
MSC01 1070, 1 University of New Mexico
Albuquerque, NM 87131

PREFACE

The research reported herein provides an in-depth literature search on the materials' properties, specifications, test procedures, and performance of polymer modified binders (also known as PG plus binders). This includes the materials' collection, literature review, and laboratory testing needed to carry out this goal.

NOTICE

The United States Government and the State of New Mexico do not endorse products or manufacturers. Trade or manufactures' names appear herein solely because they are considered essential to the object of this report. This information is available in alternative accessible formats. To obtain an alternative format, contact the NMDOT Research Bureau, 7500B Pan American Freeway NE, PO Box 94690, Albuquerque, NM 87199-4690, (505) 841-9145.

DISCLAIMER

This report presents the results of research conducted by the authors and does not necessarily reflect the views of the New Mexico Department of Transportation. This report does not constitute a standard or specification.

ABSTRACT

The current Performance Grade (PG) system utilizes Dynamic Shear Rheometer (DSR), Bending Beam Rheometer (BBR), and Direct Tension (DT) tests to specify the grades of a binder. Some past studies reported that these tests apply very small amount of loadings those are within the Linear Viscoelastic (LVE) limits of the binder, where polymer network may be inactive. Therefore, many researchers recommend different performance-based tests for the Polymer Modified Binders (PMBs) along with the existing PG tests. This study explored the effectiveness of available different binder tests for better characterization of PMBs. In the beginning, a neat binder was blended with Styrene-Butadiene- Styrene (SBS) polymer at three different percentages: 1%, 3%, and 5%. The blended binders were used to develop a calibration curve using Fourier Transform Infrared (FTIR) spectroscopy for detecting SBS content in an unknown PMB. The lab produced binders were also used to prepare the mixture samples for performance tests. After that, Hamburg Wheel Track Device, Beam Fatigue and Thermal Stress Restrained Specimen Test tests were performed on mixture samples made with different binders to investigate the rutting, fatigue cracking and low-temperature performance respectively. Binder performance was evaluated through current PG tests. In addition to the PG tests, other binder tests such as Elastic Recovery, Forced Ductility, Multiple Stress Creep Recovery (MSCR), Time Sweep (TS), and Linear Amplitude Sweep (LAS) tests were conducted to evaluate which binder tests were more appropriate for PMBs. Results show that the PG tests failed to characterize the PMBs properly. It is found that the MSCR test is most suitable for representing rutting performance. Both TS and LAS tests can successfully evaluate the fatigue cracking performance of a PMB. For thermal cracking, the critical cracking temperature calculated from BBR and DT tests' data can be a good option for characterizing the low-temperature cracking performance of a PMB.

ACKNOWLEDGEMENTS

This project was funded by the New Mexico Department of Transportation (NMDOT) Research Bureau.

The authors would like to express their sincere gratitude and appreciation to Mr. James Gallegos, Materials Bureau Chief, NMDOT, for being the sponsor of this project and for his regular support, sponsorship, and suggestions. The authors express their gratitude to MR. Parveez Anwar, former NMDOT's State Asphalt Engineer, for being advocate for this project. The UNM research team appreciates the valuable service and time of the Project Manager, Mr. Virgil Valdez for this project. Virgil's kind help in field work, material collection and so on are highly appreciated.

The UNM research team would like to thank the Project Technical panel members for their valuable suggestions during the quarterly meetings. Special thanks go to several Project Panel members namely, Mr. Jeff Mann, Pavement Management and Design Bureau Chief, Mr. Jeremy Rocha and Ms. Kelly Montoya of Materials Bureau, and Mr. Shawn Hammer, Fisher Sand & Gravel New Mexico, Inc. for their assistance and suggestions for this project.

The authors would like to thank several members and personnel at UNM for their support.

TABLE OF CONTENTS

LIST OF FIGURES

LIST OF TABLES

INTRODUCTION

RESEARCH NEED AND SIGNIFICANCE

An asphalt pavement mainly experiences three major distresses during its life time. These distresses are rutting (permanent deformation), fatigue cracking, and low-temperature cracking. The rutting primarily occurs in newly constructed pavements at higher temperature when the binders are soft enough to deform easily. When pavements become older, binders lose their flexibility and become brittle due to oxidizing aging. The fatigue cracking occurs in old pavements due to repetitive traffic loading at normal or intermediate temperature when the binders are neither too soft nor to stiff. The low-temperature cracking also occurs at freezing temperature in old pavements when thermal stress exceeds the tensile strength of the materials. Since binder is the main bonding material in the asphalt concrete pavement, the binder grade is an important factor for the mix design because it directly describes how the binder will survive against traffic loads at different climatic conditions. The Superpave Performance Grade (PG) system represents a binder by specifying a high-temperature grade and a low-temperature grade (*1*). The high-temperature grade indicates the maximum allowable temperature at which binder is strong enough to prevent rutting for the traffic loads. On the other hand, the low-temperature grade indicates the lowest temperature at which the binder has enough flexibility to prevent low-temperature cracking. The PG specification uses the rheological parameters of binder tested from Dynamic Shear Rheometer (DSR) test (*2*) to determine the high-temperature grade. It uses the $G^*/\sin\delta$ as the rutting parameter where G^* is the complex shear modulus, and δ is the phase angle of the binder. The high-temperature grade is selected in such a way when the $G^*/\sin\delta$ value is at least 1.00 kPa for unaged binder and 2.20 kPa for short-term-aged binder. The laboratory short term aging is done by Rolling Thin Film Oven (RFTO) aging procedure according to AASHTO T 240 (*3*). For the low-temperature, the PG uses the Bending Beam Rheometer (BBR) test (*4*) on small long-term-aged binder samples to determine the stiffness, *S* and the slope of the rate of stress relaxation, *m*-value. The laboratory long term aging is done by Pressure Aging Vessel (PAV) aging procedure according to AASHTO R 28 (*5*). The low-temperature grade is selected in such a way when the *S* is lower than 300 MPa, and the *m*-value is at least 0.30. If S is greater than 300 MPa, it is recommended to perform the Direct Tension (DT) test (*6*) to ensure minimum failure strain. For fatigue cracking, the PG uses another parameter, $G^*\sin\delta$ to represent as the fatigue parameter at an intermediate temperature, and the intermediate temperature is the average of high-and low-temperature grades plus four. The PG specification limits the $G^*\sin\delta$ value maximum of 5000 kPa at the intermediate temperature of binder to perform well against fatigue cracking. It is worth it to mentioned that these specifications are developed for neat binders.

The rapid growth of traffic, the extreme climatic condition, and the thickness reduction enthusiasm lead to the increase in polymer modification nowadays (*7, 8*). If polymers are added in asphalt binders for better performance, the polymer modified binders (PMBs) are also called PG plus binders, and they have different morphological structures than the neat binders (*9–13*). Therefore, many researchers have questioned on the applicability of existing PG tests for characterizing of performance of PMBs (or PG plus binders). Bahia et al. (*14*) reported that the current PG fatigue test failed to provide satisfactory results for the PMBs, because the applied strain amplitude is too small that is within the linear viscoelastic (LVE) range of the binders where the polymer network may be inactive (*15*). To overcome this problem, many of the states that uses PMBs employ “PG

plus" tests (i.e., elastic recovery, toughness) in addition to PG testing to ensure the presence of polymers and to measure the elastic recovery properties. The main problem with these tests only confirms the presence of polymers but is not specific to what percentage of polymer is being used. Most importantly, these PG plus tests are only an indicator of polymer being used in the binder, not related to rutting, fatigue, and low-temperature field pavement performance nor asphalt mixtures' laboratory performance.

During the last ten plus years, researchers have made significant efforts to replace the elastic recovery (PG plus) test. Recently, Multiple Stress Creep Recovery (MSCR) test (*16*) has shown to be a good potential to replace elastic recovery test. The MSCR test has been added to AASHTO M 320 (*1*) to take care of the drawbacks of the rutting parameter, $G^*/\sin\delta$ of PG plus binders. In the MSCR test, higher levels of stress and strain are applied to the binder. By using the higher levels of stress and strain in the MSCR test, the response of the asphalt binder captures not only the stiffening effects of the polymer but also the elastic effects. In the MSCR test, two separate parameters are determined: a non-recoverable creep compliance (J_{nr}) and a percentage of recovery (*%R*) during each loading cycle. The J_{nr} parameter has been shown through numerous field and laboratory studies to better correlate with rutting potential than $G^*/\sin\delta$, particularly for modified asphalt binders.

Though AASHTO has adopted the MSCR test for characterization of rutting behavior, still no test has been approved for the fatigue cracking, and low-temperature cracking. During the NCHRP 9-10 project, a new binder fatigue test named Time Sweep (TS) test was proposed to characterize the binder fatigue performance (*17*). In the TS test, the binder is subjected to a constant repeated cyclic loading until specific criterion (such as threshold stiffness limit) met. The main drawback of this test is that it takes too much time to complete a test. Therefore, researchers are now proposing a new accelerated test named Linear Amplitude Sweep (LAS) test (*18*) to characterize the fatigue behavior of the binder. In this test, the binder is subjected to a certain number of repetitive strains where strain amplitudes are systematically increased to accelerate the rate of damage accumulation. Finally, the simplified viscoelastic continuum damage (S-VECD) model is used to characterize the fatigue performance of the binder (*19–25*). Although few research studies have been undertaken in this area, PMBs have still to be comprehensively characterized, due to the complex interaction of the binder and polymer system. In addition, the relationship between S-VECD based binder fatigue parameter and mixture fatigue performance is still unclear and has to be thoroughly investigated. For low-temperature cracking, a few studies have shown that binder critical temperature based on the BBR and DT tests data can be a good option for the PMBs (*26, 27*). However, validities of these findings need to be thoroughly investigated due to lack of enough proven studies.

The contents of plastomeric and elastomeric polymers are usually 2 to 6%, while the content of crumb rubber is typically 15 to 20% by weight of asphalt binder content. The vast majority of states have focused on elastomers or crumb rubber as polymer modifier. The elastomeric polymers are Styrene-Butadiene-Styrene (SBS), Styrene-Butadiene (SB) and Styrene-Butadiene-Rubber (SBR) etc. A few states also use plastomeric modified such as Elvaloy (EVA). It is also required to determine the compatibility of the base binder and different polymer types and content. In addition, the quantity or percent polymer used in binders is often unknown because this a proprietary information to the binder producer or supplier, but not to the user, paving contractors,

or agencies. Therefore, a calibration curve needs to be developed to determine the polymer content in a PMB, and this will be done in this study.

Like the PG binders, the performance of PG plus binder should be evaluated in three main categories: rutting, fatigue cracking and thermal cracking distresses in the pavement. These categories represent three primary temperature ranges: high-, intermediate- and low-temperature. Therefore, the proposed research will explore different laboratory binder testing methods and evaluation procedures, which are currently in practice and are newly developed. In order to develop PG plus binder testing parameters, it is important to relate polymer modified binder properties with laboratory and field performances of asphalt concrete made out of those PMBs. Therefore, mixture tests pavement performances are proposed to be determined for evaluating the current tests for PG plus binders. Test procedures and analysis methods, which show better correlation to the pavement performances and highest potential to improve pavement design, will be adapted for developing New Mexico's PG plus binder specification.

OBJECTIVES

The main goal of this research is to determine what properties of a polymer modified binder best predict a pavement performance. The objective is to develop a PG plus binder specification suitable to traffic and climate zones in New Mexico. Specific objectives are to:

a) Assess the current state-of-the-practice regarding the use of PMBs with special emphasis on type of modification and newly developed test procedures, specification, guidelines, and parameters from national and local perspective.
b) Develop a correlation between polymer content (amount) and binder property (e.g., MSCR recovery) and use that correlation to find polymer content (which is proprietary to the supplier, and therefore unknown to users) in PMBs.
c) Develop correlations of binder performances (high-, intermediate-, low-temperature parameters) with asphalt mix or mastic performances (rut, fatigue, low-temperature cracks) in the laboratory simulating New Mexico's field conditions. Pavement performance can be complicated by some uncontrollable/un-documented factors in the field. Therefore, it is important to correlate laboratory binder testing results with laboratory mix or mastic performance results, as a first step.
d) Develop correlations between binder laboratory performance parameters (high-, intermediate-, low-temperature parameters) with actual or field pavement performances.
e) Evaluate the predicted performance for use of the PMBs through the pavement ME design software.
f) Assess the performance of the pavement sections made with the PMBs.
g) Document the literature and survey information generated in this research and provide recommendations for PG plus testing specification to be used in New Mexico.

RESEARCH METHODOLOGY

The proposed research methodology is presented in Figure 1. At the beginning, PMBs were prepared in the lab with different polymer contents. A Fourier Transform Infrared (FTIR)

spectroscopy-based calibration curve was developed using the lab produced PMBs. The lab produced binders were also used to prepare the mixture samples for investigation of mixture performance. The rutting, fatigue cracking, and low-temperature performance of the mixture samples were investigated through Hamburg Wheel Tracking Device (HWTD) test, Beam Fatigue (BF) test, and Thermal Stress Restrained Specimen Test (TSRST). After that, PMBs were tested for traditional PG grade system parameters such as G*/sinδ, G*.sinδ, and BBR stiffness and *m*-value, and DT percentage strain. In addition to the PG tests, the MSCR tests was performed to specify PMB's rutting. For fatigue cracking, Elastic Recovery (ER), Forced Ductility (FD), non-linear MSCR, TS, and LAS tests were used. For thermal cracking, the critical cracking temperatures for tested PMBs were computed from BBR and DT tests' data. Finally, this study evaluated the correlations between these binder tests with the respective the mixture performance to select the most appropriate tests for characterizing the PMBs.

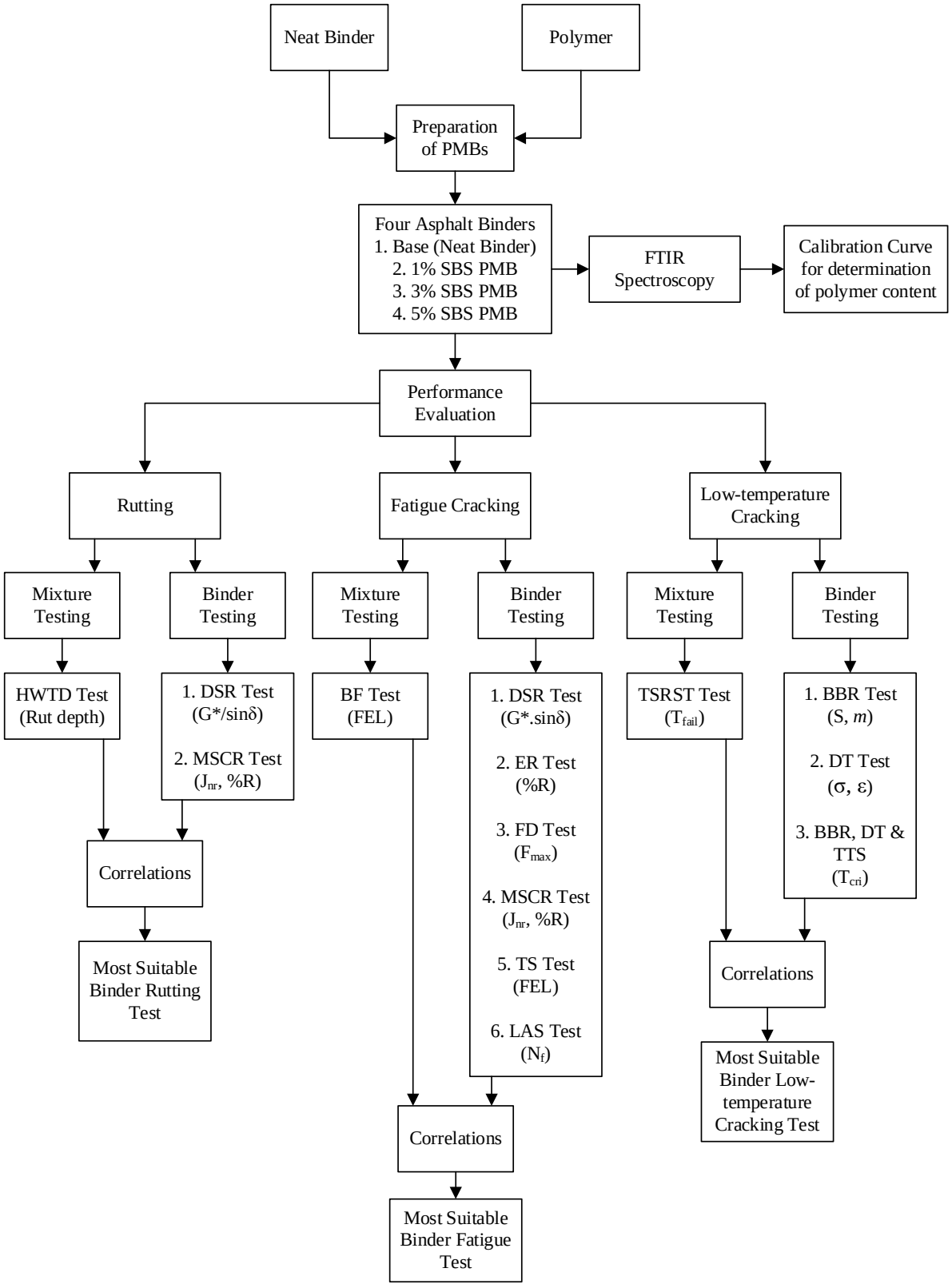

FIGURE 1 Research Methodology

REPORT ORGANIZATION

This report is comprised of seven sections. These can be summarized as follows:

Section 1 describes the research need and objectives of this research.

Section 2 contains the literature review on the past studies related to PMBs. It also covers the current practices of different state departments of transportation (DOTs) on PMBs.

Section 3 describes about the development of calibration curve based on the FTIR spectroscopy to determine the polymer content in a PMB.

Section 4 presents the performance of mixture samples made with laboratory produced PMBs. There are mainly three different distresses experience by an asphalt pavement: rutting, fatigue cracking, and low-temperature cracking. All these three performances of the polymer modified mixtures are investigated here. It also explored the effectiveness of alternative binder tests to characterize these performances.

Section 5 discusses the predicted performance for the PMBs through the pavement ME design software.

Section 6 illustrates the performance of the pavement sections made with the PMBs.

Section 7 concludes with the findings from this research and provides recommendations for future studies.

THIS PAGE LEFT BLANK INTENTIONALLY

LITERATURE REVIEW

INTRODUCTION

This section provides the information about the current state-of-the-practice regarding the use of PMB with special emphasis on the type of modification and the newly developed test perspective. The research team conducted a comprehensive study on PMBs and its performance while used as a pavement material. Based on this study, this section provides details about the polymer modification, classification, advantages, and disadvantages of different polymer modifiers. It also summarizes the in-depth findings from the previous research related to PMBs. The properties, specifications, and test procedures for PMB used by other state DOTs are also discussed here. It also describes the current specification and practice in New Mexico related to PMB. Finally, this section presents the major findings of the various studies and performance evaluation of the reviewed studies, which are discussed herein.

POLYMER MODIFICATION

Due to increased traffic volume and load, the conventional asphalt binder is unable to ensure the desired service life of pavements. As a result, asphalt binder is now being modified with different types of polymer in order to improve its mechanical properties so that it can minimize the potential pavement distresses or increase the service life.

Classification of Modifiers

There are mainly three different types of polymer modifier are currently used as shown in Figure 2. They are elastomer, plastomer, and rubber.

Elastomer

Typical elastomer modifiers are SBS, SB, SBR, styrene-ethylene/butylene-styrene (SEBS), and styrene-isoprene-styrene (SIS) etc. The most commonly used elastomer modifier is SBS. Lu and Isacsson (*28*) showed that SBS modified aged binder shows better rheological properties than the base binder. Tarefder and Zaman (*29*) reported that the SBS modified binders are less sensitive to moisture damage. Molenaar et al. (*30*) showed that the elastomer modifier protects the bituminous binder form aging more than the plastomer modifier. Naskar et al. (*31*) reported that modified bituminous binders are more resistant to heat and radiation. Tarefder and Yousefi (*32*) showed that SBS improves the stiffness at high and intermediate temperature.

Plastomer

Typical plastomers modifiers are polyethylene (PE), polypropylene (PP), EVA, ethylene-butyl acrylate (EBA), and ethylene-methacrylate (EMA). Plastomer modifiers cannot improve elastic recovery properties of asphalt pavement (*7*). Most used plastomer modifiers are EVA and EBA. Sengoz and Isikyakar (*12*) concluded that improvement due to EVA is lesser than improvement

due to SBS. Ameri et al. (*33*) reported that EVA improves the pavement resistance against distresses. Bulatovic et al. (*34*) showed that the addition of EVA improves the elastic response.

Rubber

Rubber modifier can be either natural rubber latex or crumb rubber. This type of modifier has multiple advantages relative to neat asphalt pavement, including enhanced mechanical properties, increased riding quality, decreased traffic noise, and increased rutting and cracking resistance (*35–37*). However, crumb rubber is not reactive, and it is thus difficult to dissolve or fully disperse the crumb rubber particles in the asphalt matrix. In addition, crumb rubber is prone to decomposition and oxygen absorption. Furthermore, there is an environmental issue associated with rubber modifier.
Figure 2 shows the physical appearance of a typical elastomer (SBS), a typical plastomer (EVA), and natural rubber latex (*38*).

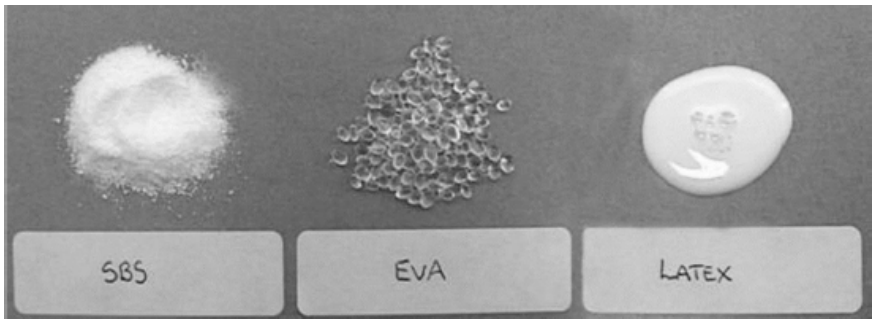

FIGURE 2 Samples of polymers used in asphalt modification (***38***)

Effect of Polymer Type

Different types of polymer have different advantages and disadvantages. Table 1 summarizes these based on the specific type of polymer modifier.

TABLE 1 Summary of different types of polymer modifiers

Type	Examples	Advantages	Disadvantages
Elastomer	SBS, SBR, SIS, SEBS	• Increases stiffness. • Reduces temperature sensitivity. • Improves elastic response.	• Relatively high cost. • Compatibility problems in some asphalt
Plastomer	PE, EVA, EBA	• Relatively good storage stability. • High resistance to rutting. • Relatively low cost.	• Limited improvement in elastic recovery. • Improvement lesser than the Elastomer.
Rubber	Natural rubber or crumb rubber	• Improve mechanical properties.	• Compatibility issue. • Environmental issues.

Effect of Polymer Content

Past studies also showed that the polymer content affects the binder properties. For example, Ameri et al. (*33*) shows that the resistance to low-temperature cracking increased with increased EVA content in the range of 2 wt.% to 4 wt.% but decreased with 6 wt.% EVA addition. Tarefder and Yousufi (*32*) showed that increasing of SBS content improves the mechanical properties of the binder. However, a high content of SBS increases the viscosity and reduces the workmanship. For, rubber modifier Navarro et al. (*39*) showed that thermal susceptibility of the binder reduces with the increase of additional rubber. However, they suggested to use a maximum amount of 9% rubber content for a binder paving application.

Summary

After reviewing the previous studies, it can be concluded that the types of polymer modifiers and polymer content affect the improvement of the binder. Among all polymer modification, SBS modification performs the best. In addition, it is very important to select the appropriate modifier content.

REVIEW OF PAST STUDIES

In this subsection, a comprehensive literature review was conducted to achieve the knowledge of polymer modification in the asphalt industry.

Past Studies

The asphalt modification by plastomers has a longer history than that by elastomers, as many plastomer modifications were commercially implemented before 1960 (*40*). One well-known

early example is neoprene (polychloroprene) latex, which became increasingly used for bitumen modification in North America in the 1950s. The first commercially acceptable SBS product was developed in the USA in 1965 and has been widely used in Europe since the 1970s. Few studies were performed to evaluate the effect of using a modified binder. Rostler et al. (*41*) showed that modification of asphalt improves the wear resistance. Chaffin et al. (*42*) showed that SBS modified asphalt improves the rutting resistance. During the 1980s, more polymers were developed with an increasing demand for thickness reduction in the pavement layer. Piazza et al. (*43*) found that the mechanical and viscoelastic properties of asphalt binder, both at high and low-temperatures, was noticeably improved by modification. In late 1987, the Strategic Highway Research Program (SHRP) developed the performance-based specification for neat asphalt based on rheology. Reese and Predoehl (*44*) reported that the resistance to aging and cracking improves by the modification after a two-year field test in California.

By the 1990s, many researchers performed systematic investigations to evaluate the effects of various polymers on asphalt performance. The mechanical properties, temperature sensitivity, storage stability, rheology, morphology, thermal performance, aging resistance, and durability were studied in many countries. Krutz et al. (*45*) used static creep test to investigate the rutting potential of PMB and found that SBS modification provides high rutting resistance. Stock and Arand (*46*) showed that polymer modification provides high cracking resistance at low-temperature. However, some drawbacks were proven, such as the thermal instability of some polymer modifiers and phase separation problems of some PMBs (*47*). Since the 2000s, researchers are focusing on developing new methods to mitigate disadvantages and clarifying the modification mechanisms. Wen et al. (*48*) reported that sulfur vulcanization can improve the stability problem. Later, Li et al. (*49*) showed that aging resistance can be improved by adding antioxidants. Navarro et al. (*50*) recommended using of rubber particle sizes lower than 0.35 mm and high shear rates during manufacturing of rubber modified asphalt to improve the storage stability. The concentration of rubber modifier also affects the rheological properties.

Furthermore, some researchers focused on the detailed evaluation of PMBs and their applicability in the pavement industry. Lu and Isacsson (*41–53*) performed chemical and rheological evaluation of aging properties of elastromeric as well as plastromeric PMBs. They found that in all cases, the aged modified binders showed better rheological properties than aged base binders. Khattak and Baladi (*54*) reported that polymer modified asphalts have more the fatigue and rutting resistance than regular asphalt. Airey (*9, 10*) performed dynamic mechanical analysis (DMA) using a DSR to see the effect of polymer modification. The investigation indicated that EVA polymer modification increases binder stiffness and elasticity at high service temperatures and low loading frequencies. Navarro et al. (*55*) showed that rubber modified modification improves the rutting resistance. Ruan et al. (*56*) showed that polymer modification resulted in increased asphalt complex modulus at high temperatures, decreased asphalt complex modulus at low-temperatures, broadened relaxation spectra, and improved ductility. Tarefder and Zaman (*29*) showed that SBS modified binders perform well against the moisture damage than the unmodified binders.

In addition to the laboratory test, some field investigations were also performed to evaluate the advantage of polymer modification. Glaszman (*57*) performed a survey on 20 experts representing 18 states to quantify the benefits of PMBs. Approximately 70 percent of the responses indicated that there was a benefit in using PMBs to extend the pavement's service life; 58 percent also said that the use of PMBs significantly reduced maintenance costs. Quintus et al. (*58*) studied the Long-

Term Pavement Performance (LTPP) sections and found modified pavements featured less rutting, less cracking. Another study by Dreessen et al. (*59*) showed that modified pavement is affected by the weather. In addition, a decrease in mechanical properties with aging is relatively low for modified pavement.

The binders become stiffer due to the high content of the polymer. As a result, Bahia et al. (*60*, *61*) reported that Superpave test protocol failed to test the extreme grades required by the new, modified binders, resulting in the initiation of new testing protocols for modified binders. Therefore, the elastic recovery test in addition to PG tests is being used by many DOTs. However, MSCR test is found to be more promising by many researchers to evaluate the high-temperature binder (*62*). Therefore, AASHTO adopted this test in addition to existing PG tests.

Summary

From the literature review, it can be concluded that PMBs significantly improve the rheological properties of the binder. In addition, PMBs are less susceptible to moisture, temperature, and age. Modifier concentration also affects the rheological properties of modified asphalt. On the other hand, they have some drawbacks such as storage stability and phase separation. Sulfur vulcanization or addition of antioxidants can eliminate the phase separation problem of SBS modifier. Reduced particle sizes and high shear rates during manufacturing improves the storage stability of rubber modified asphalt. Field evaluation also shows that modified asphalt pavements show better resistance to distresses. However, high content of modifier makes the binder stiffer and reduces the workmanship.

REVIEW OF CURRENT PRACTICE

This subsection presents detailed information of specification, and guidelines regarding polymer modified asphalt pavement used by other states.

Arizona

Arizona DOT (ADOT) uses the crumb rubbers rather than elastomer or plastomer for asphalt modification. PG 64-16 was used in a hot climate area (Phoenix), PG 58-22 was used in a moderate climate area (Prescott, Flagstaff), and PG52-28 was used in a cold climate area (Alpine). A minimum of 20 % (wt) crumb rubber is required by weight of asphalt to make the pavement more durable and less noisy. The crumb rubber was added to asphalt at 180 °C-205 °C and cured for at least one hour for the reaction between asphalt and crumb rubber to occur at 165 °C-190 °C under agitation. For the PG 76-22 TR+ binder, a minimum 2 % (wt) of SBS and 8 % (wt) of crumb rubber are required. The benefits of crumb rubber modification to the asphalt pavement include: a) reduced reflective cracking via improved elastic properties; b) increased aging resistance; c) increased durability; d) reduced noise; and e) improved cost-effectiveness. The specification specified by ADOT for crumb rubber modified asphalt is listed in Table 2.

TABLE 2 ADOT specification for polymer modified binders

Modified Binder Specifications	CRA-1	CRA-2	CRA-3	GTR+SBS 1	GTR+SBS 2
Base Binder	PG 52-28	PG 58-22	PG 64-16	PG 70-22	PG 76-22
Original Binder					
Flash Point Temp, T48: Min °C	230	230	230	230	230
Viscosity, T316: Max, 3 Pa-s, Temp, °C	135	135	135	135	135
DSR, T315: G*/sinδ, Min, at required Temp @ 10 rad/s, KPa	1.00	1.00	1.00	1.00	1.00
RTFO aged Binder					
Mass Loss, Max, %	1.00	1.00	1.00	1.00	1.00
DSR, T315: G*/sinδ, Min, at required Temp @ 10 rad/sec, KPa	2.20	2.20	2.20	2.20	2.20
PAV aged Binder					
PAV Aging Temp, °C	90	100	100	100	100
DSR, T315: G*sinδ, Max, at required Temp @ 10 rad/sec, KPa	5000	5000	5000	5000	5000
BBR Stiffness, T313: S, Max, at required Temp, @ 60 sec, MPa	300	300	300	300	300
m-value, Min	0.300	0.300	0.300	0.300	0.300
DT, T314: Failure Strain, Min at required Temp @ 1.0 mm/min, Percent	1.00	1.00	1.00	1.00	1.00
Polymer Modified Binder					
Modification details	Min 20 % GTR	Min 20 % GTR	Min 20 % GTR	Min 8 % GTR + 2% SBS	Min 8 % GTR + 2% SBS
Resilience, Percent, D5329: 25 °C, Min	15	20	25		
Elastic Recovery, T301: Percent, 10 °C, Min				55	55
Rotational Viscosity, T316: Pa-s	1.50-4.00	1.50-4.00	1.50-4.00		
Penetration Depth, D5: 0.1 mm, 4 °C, Min	25	15	10		
Solubility, D2042: Percent, Min				97.5	97.5
Softening Point, T53: Temp °C, Min	52	54	57	54	60
Phase angle, Max at 76°C Temp @ 10 rad/sec, KPa				75	75

California

California Department of Transportation (Caltrans) has adopted three PMBs: PG58-34PM, PG64-28PM and PG76-22PM (PM indicates polymer modified). The different grades are suited for different climatic applications. It also incorporates additional specifications for the elastic recovery and phase angle. The specification specified by Caltrans for the modified asphalt is listed in Table 3.

TABLE 3 Caltrans specification for polymer modified binders

Modified Binder Specifications	Type I	Type II	Type III
Base Binder	PG 58-34	PG 64-28	PG 76-22
Original Binder			
Flash Point Temp, T48: Min °C	230	230	230
Viscosity, T316: Max, 3 Pa-s, Temp, °C	135	135	135
DSR, T315: c G*/sinδ, Min, at required Temp @ 10 rad/s, KPa	1.00	1.00	1.00
RTFO aged Binder			
Mass Loss, Max, %	0.60	0.60	0.60
DSR, T315: G*/sinδ, Min, at required Temp @ 10 rad/sec, KPa	2.20	2.20	2.20
PAV aged Binder			
PAV Aging Temp, °C	100	100	100
DSR, T315: G*sinδ, Max, at required Temp @ 10 rad/sec, KPa	5000	5000	5000
BBR Stiffness, T313: S, Max, at required Temp, @ 60 sec, MPa	300	300	300
m-value, Min	0.300	0.300	0.300
DT, T314: Failure Strain, Min at required Temp @ 1.0 mm/min, Percent	1.00	1.00	1.00
Additional requirement for Polymer Modified Binder			
Modification details	2-6 % GTR	2-6 % GTR	2-6 % GTR
Elastic Recovery, T301: Percent, 10 °C after RTFO	75	75	65
Rotational Viscosity, T316: at 135^0C Pa-s, Max	3.00	3.00	3.00
Solubility, D2042: Percent	99.0	99.0	99.0
Phase angle, Max at required Temp @ 10 rad/sec, kPa after RTFO	80	80	80

Colorado

In Colorado, three types of polymers were used as the modifiers for asphalt modifications. Type I was neat asphalt mixed with styrene block copolymer; Type II was neat asphalt mixed with SBR or neoprene latex; and Type III was neat asphalt mixed with EVA. The rutting resistance of pavement constructed by PMBs was not remarkably increased. In contrast, the cracking resistance was remarkably enhanced in the sections constructed with modified asphalt binders. Compared with the control sections, the cracks in the modified sections decreased about 50 percent for longitudinal and transverse cracking (*63*). The specification specified by Colorado DOT (CDOT) for the modified asphalt is listed in Table 4.

TABLE 4 CODOT specification for polymer modified binders

Modified Binder Specifications	Type I	Type II	Type III
Base Binder	PG 64-28	PG 70-28	PG 76-28
Original Binder			
Flash Point Temp, T48: Min °C	230	230	230
Viscosity, T316: Max, 3 Pa-s, Temp, °C	135	135	135
DSR, T315: c G*/sinδ, Min, at required Temp @ 10 rad/s, KPa	1.00	1.00	1.00
RTFO aged Binder			
Mass Loss, Max, %	1.00	1.00	1.00
DSR, T315: G*/sinδ, Min, at required Temp @ 10 rad/sec, KPa	2.20	2.20	2.20
PAV aged Binder			
PAV Aging Temp, °C	90	100	100
DSR, T315: G*sinδ, Max, at required Temp @ 10 rad/sec, KPa	5000	5000	5000
BBR Stiffness, T313: S, Max, at required Temp, @ 60 sec, MPa	300	300	300
m-value, Min	0.300	0.300	0.300
DT, T314: Failure Strain, Min at required Temp @ 1.0 mm/min, Percent	1.00	1.00	1.00
Polymer Modified Binder			
Modification details	Three types of modifier, SBS, SBS + neoprene and latex, and EVA		
Ductility, T51: Min, cm at 4°C 5cm/min	50	50	
Toughness, CP L2210: Min at 25°C	110	110	
Elastic Recovery, T301: Percent, 10 °C after RTFO			50
Ductility, T51: Min, cm at 4°C 5cm/min after RTFO	20	20	

Florida

In Florida, SBS modified PG 76-22 (at about 3 wt.%), and SBS modified PG82-22 (at about 6 wt.%) were used to evaluate for rutting resistance and fatigue resistance. The rutting and fatigue cracking performance of hot-mix-asphalt (HMA) mixtures were both improved by the SBS modification. The PG82-22 binder remarkably reduced the damage rate of HMA, and it showed a relatively higher energy ratio than the PG76-22 binder, which indicates a relatively higher cracking resistance (*64*). The Specification specified by Florida DOT (FDOT) for modified asphalt is listed in Table 5.

TABLE 5 FDOT specification for polymer modified binders

Modified Binder Specifications	PMA-1	ARB-1	PMA-2
Base Binder	PG 76-22	PG 76-22	PG 82-22
Original Binder			
Flash Point Temp, T48: Min °C	230	230	230
Viscosity, T316: Max, 3 Pa-s, Temp, °C	135	135	135
DSR, T315: c G*/sinδ, Min, at required Temp @ 10 rad/s, KPa	1.00	1.00	1.00
RTFO aged Binder			
Mass Loss, Max, %	1.00	1.00	1.00
DSR, T315: G*/sinδ, Min, at required Temp @ 10 rad/sec, KPa	2.20	2.20	2.20
PAV aged Binder			
PAV Aging Temp, °C	100	100	100
DSR, T315: G*sinδ, Max, at required Temp @ 10 rad/sec, KPa	5000	5000	5000
BBR Stiffness, T313: S, Max, at required Temp, @ 60 sec, MPa	300	300	300
m-value, Min	0.300	0.300	0.300
DT, T314: Failure Strain, Min at required Temp @ 1.0 mm/min, Percent	1.00	1.00	1.00
Polymer Modified Binder			
Modification details	3% SBS	7% GTR	6% SBS
Flash Point Temp, T48: Min °C	450		
Solubility, D2042: Percent	99.0		
DSR, Phase angle, Maximum	75		
Multiple Stress Creep Recovery, $J_{nr,}$ TP 70-12: at 67°C after RTFO, Maximum, kPa^{-1}	1.00		0.50
MSCR, %Recovery, %R, TP 70-12: at 67°C after RTFO	$\%R_{3.2} > 29.37\ (J_{nr,3.2})^{-0.2633}$		

Oklahoma

Three different modified binders are used in Oklahoma. They are PG 64-22, PG 70-28, and PG 76-28. An elastomer modifier (i.e., SBS) and two anti-stripping additives (Adhere HP-Plus and Perma Tac Plus) were used to evaluate the modification effects. The testing results show that the grade changes of the PG 70-28 and PG 76-28 modified asphalt are more significant than the neat PG 64-22 asphalt with various anti-striping additives. The PG 64-22 binder increased 1.5°C on high grade temperature, while the PG 70-28 increased 3.2°C and the PG 76-28 increased 3.6°C. After the change of grade, the PG 76-28 can closely reach the level of PG 82-28. The Specification specified by Oklahoma DOT (ODOT) for modified asphalt is listed in Table 6.

Summary

After reviewing the specification of other states, it can be concluded that all of the states have additional requirements for PMBs than the neat asphalt binders. Furthermore, different states have different requirements on the elastic recovery, flash point, solubility, and DSR parameters, but the requirements for rotational viscosity, creep stiffness and *m*-value, and mass change are similar. Florida specified a maximum phase angle value from the DSR test and a maximum J_{nr} from MSCR test for the PMBs. This subtask concludes that additional specifications are required for PMBs in addition to current PG grading system.

TABLE 6 ODOT specification for polymer modified binders

Modified Binder Specifications	Type I	Type II	Type III
Base Binder	PG 64-22	PG 70-28	PG 76-28
Original Binder			
Flash Point Temp, T48: Min °C	230	230	230
Viscosity, T316: Max, 3 Pa-s, Temp, °C	135	135	135
Dynamic Shear, T315: c G*/sinδ, Min, at required Temp @ 10 rad/s, KPa	2.50	2.50	2.50
RTFO aged Binder			
Mass Loss, Max, %	1.00	1.00	1.00
Dynamic Shear, T315: G*/sinδ, Min, at required Temp @ 10 rad/sec, KPa	5.50	5.50	5.50
PAV aged Binder			
PAV Aging Temp, °C	100	100	100
Dynamic Shear, T315: G*sinδ, Max, at required Temp @ 10 rad/sec, KPa	5000	5000	5000
Creep Stiffness, T313: S, Max, at required Temp, @ 60 sec, MPa	300	300	300
m-value, Min	0.300	0.300	0.300
Direct Tension, T314: Failure Strain, Min at required Temp @ 1.0 mm/min, Percent	1.00	1.00	1.00
Polymer Modified Binder			
Modification details	Type IV Polymer Modified Asphalt Binder is normally produced by modifying neat asphalt binders with polymer content (SBS-solid base) 3 wt.% min, and tire rubber 5 wt.% min.		
Elastic Recovery, T301: Percent, 25 °C, Min		65	75
Flash Point Temp, T48: Min °C	260	260	260
Separation, Max, percent		10	10
Solubility, D2042: Percent	99.0	99.0	99.0
Dynamic Shear, T315: c G*/sinδ, Max, at required Temp @ 10 rad/s, KPa, Original	2.50	2.50	2.50
Dynamic Shear, T315: c G*/sinδ, Min, at required Temp @ 10 rad/s, KPa, RTFO	5.50	5.50	5.50
PAV DSR change in testing temperature, °C		77	77

REVIEW OF NM DOT SPECIFICATIONS

This subsection presents detailed information of specification and guidelines specified by NMDOT regarding PMBs. Currently, NMDOT does not use any PMB for structural sections. However, two different types of modified binder are being used for Open Graded Friction Coarse (OGFC) layer. One is polymer modified and another one is rubber modified. The specification specified by NMDOT for modified asphalt is listed in Table 7. Although the specification of PMB has been successfully applied in the OGFC of New Mexico, some requirements still need to be determined before the polymer modified asphalt can be optimized as dense graded mix binder. This is considering that the OGFC is only used as a highly porous surface and its stress condition, binder content, and porosity are considerably different from the dense graded mix.

TABLE 7 NMDOT specification for polymer modified binders

Modified Binder Specifications	Type I	Type II
Binder	PG 70-28+	PG 70-28R+
Original Binder		
Flash Point Temp, T48: Min °C	230	230
Viscosity, T316: Max, 3 Pa-s, Temp, °C	135	135
Dynamic Shear, T315: c G*/sinδ, Min, at required Temp @ 10 rad/s, KPa	1.00	1.00
RTFO aged Binder		
Mass Loss, Max, %	1.00	1.00
Dynamic Shear, T315: G*/sinδ, Min, at required Temp @ 10 rad/sec, KPa	2.20	2.20
PAV aged Binder		
PAV Aging Temp, °C	100	100
Dynamic Shear, T315: G*sinδ, Max, at required Temp @ 10 rad/sec, KPa	5000	5000
Creep Stiffness, T313: S, Max, at required Temp, @ 60 sec, Mpa	300	300
m-value, Min	0.300	0.300
Direct Tension, T314: Failure Strain, Min at required Temp @ 1.0 mm/min, Percent	1.00	1.00
Polymer Modified Binder		
Modification details		min 5% GTR + min 2% SBS
Elastic Recovery, T301: Percent, 10 °C	65	55
RTFO Mass Loss, Max, %	1.00	1.00
Flash Point Temp, T48: Min °C	230	230
Rotational Viscosity, T316: at 135^0C Pa-s, Max	3.00	3.00
Solubility, D2042: Percent	97.5	97.5

REVIEW OF LTPP DATABASE

Introduction

In this section, the Long-Term Pavement Performance (LTPP) database was reviewed to identify all polymer modified LTPP sections in the U.S. to quantify the benefits of using PG plus asphalt binders over the PG binders. After that, the performance of PMB pavements were compared with neat or non-polymer modified PG binder pavements for rutting, fatigue and low-temperature cracking.

Polymer Modified LTPP Sections

From LTPP database, 62 pavement sections were identified as modified sections. Table 8 lists the modified LTPP sections with their locations. Table 8 also includes the specific modifier that used was for each site.

TABLE 8 List of LTPP modified sections

SI No	Station ID	State	Types of Modifier used
1	0560	Arizona	Reclaimed Rubber
2	0662	Arizona	Reclaimed Rubber
3	0570	California	Reclaimed Rubber
4	8534	California	Reclaimed Rubber
5	8535	California	Reclaimed Rubber
6	1370	Florida	Reclaimed Rubber
7	3997	Florida	Reclaimed Rubber
8	4096	Florida	Antistrip Additive
9	4100	Florida	Reclaimed Rubber
10	4101	Florida	Reclaimed Rubber
11	0601	Illinois	SBS
12	0602	Illinois	SBS
13	0605	Illinois	SBS
14	9267	Illinois	Block Copolymer
15	0163	Kansas	Reclaimed Rubber
16	0164	Kansas	Reclaimed Rubber
17	0902	Kansas	Block Copolymer
18	0502	Maryland	Polyolefin
19	0503	Maryland	Polyolefin
20	0508	Maryland	Polyolefin
21	D310	Michigan	Silicone
22	5803	Mississippi	Fiber
23	0960	Missouri	SES
24	0962	Missouri	SES
25	0963	Missouri	SES
26	0964	Missouri	SES
27	0113	Montana	EVA
28	0114	Montana	EVA
29	0115	Montana	EVA
30	0116	Montana	EVA
31	0117	Montana	EVA
32	0118	Montana	EVA
33	0119	Montana	EVA
34	0120	Montana	EVA
35	0121	Montana	EVA
36	0122	Montana	EVA
37	0123	Montana	EVA
38	0124	Montana	EVA
39	1001	New Hampshire	Silicone
40	1024	North Carolina	Silicone
41	1028	North Carolina	Silicone
42	1030	North Carolina	Silicone

TABLE 8 (cont.) List of LTPP modified sections

SI No	Station ID	State	Types of Modifier used
43	1645	North Carolina	Silicone
44	1802	North Carolina	Silicone
45	1803	North Carolina	Silicone
46	1817	North Carolina	Silicone
47	1992	North Carolina	Silicone
48	2819	North Carolina	Silicone
49	2824	North Carolina	Silicone
50	2825	North Carolina	Silicone
51	3011	North Carolina	Silicone
52	C311	Tennessee	Polymer
53	0903	Texas	Synthetic Latex
54	1049	Texas	Silicone
55	A504	Texas	Synthetic Latex
56	A505	Texas	Synthetic Latex
57	A506	Texas	Synthetic Latex
58	A507	Texas	Synthetic Latex
59	0803	Utah	SBS
60	0804	Utah	SBS
61	1004	Utah	Block Copolymer
62	1006	Utah	Synthetic Latex

Modifier Type

Figure 3 shows the proportion of different modifiers used for the LTPP sections. The most common modifier is Silicon. About 24% of the sections were modified with Silicon modifier. EVA was used for 19% of the sections. Reclaimed rubber was used a modifier for 18% of the sections. Synthetic latex, SBS, SES and other polymers were used for 10%, 10%, 5% and 5% of the sections respectively. In addition, antistrip additives, polyolefin and fiber used as modifier for a few sections.

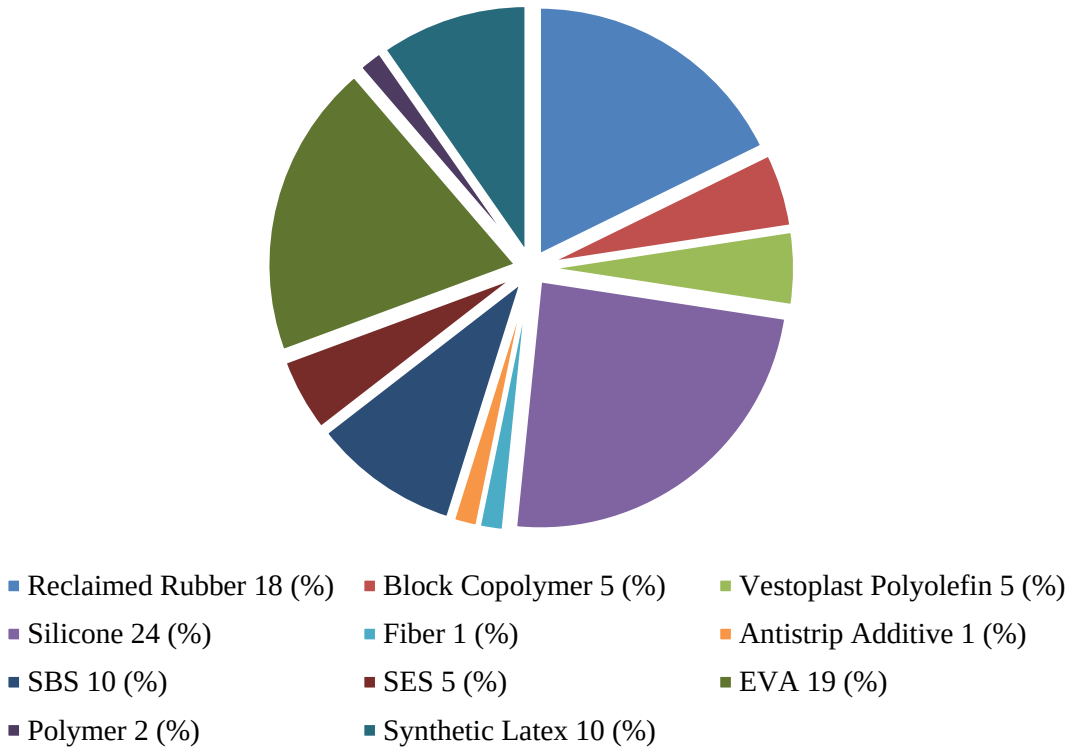

FIGURE 3 Proportion of section with different types of modifiers

Performance Improvement

In order to compare the performance improvement due to use of PMB, 32 sections from LTPP were compared where 16 sections have neat binders and 16 sections have PMBs. The sections were chosen in such a way that both neat and modified sections have the same traffic, the same section properties, and the same climatic locations (from the same route).

Rutting

Figure 4 compares the measured rutting for both non-PMB and PMB sections. In this figure every dot marker represents the pair sections (one with PMB binder and the other with neat binder). The line presented in the graph is the line of equality. The *x*-axis is the measured rutting in PMB modified sections whereas the *y*-axis is the measured rutting in non-PMB section. If a point is on the line of equality, then there is no difference in measured rutting for PMB and non-PMB sections. If a point is above the line of equality, then measured rutting for the non-PMB section is more than the PMB section. On the other hand, if a point is below the line of equality, then the measured rutting for the non-PMB section is less than the PMB section. It shows that out of 16 points, 12 points are above the line of equality, 2 points are on the line, and 2 points are below the line of equality. Therefore, it can be concluded that rutting can be reduced by using PMBs.

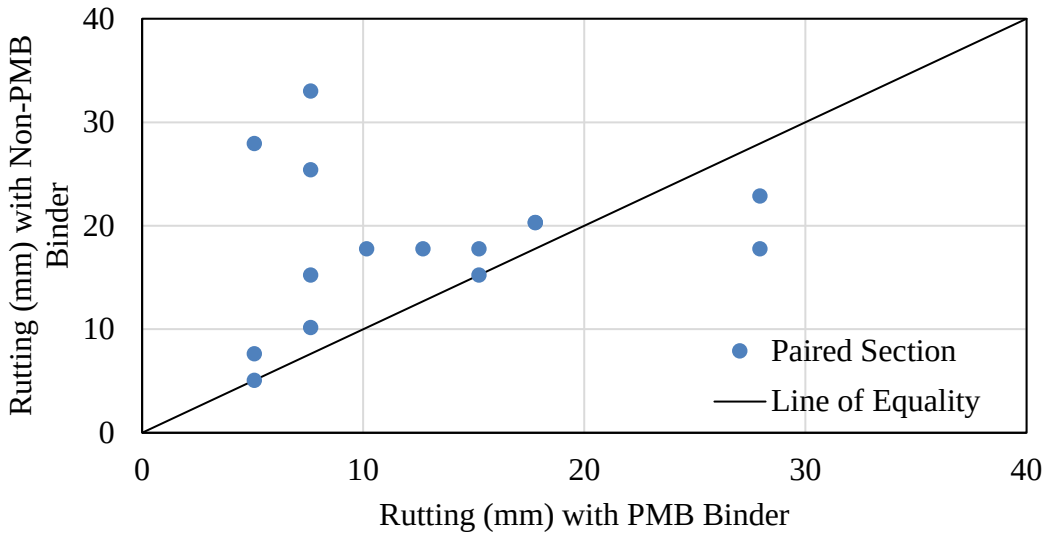

FIGURE 4 Comparison of rutting performance

Fatigue Cracking

Figure 5 compares the measured fatigue cracking for both non-PMB and PMB sections. It shows that measured fatigue cracking for the PMB sections are less than the measured fatigue cracking for non-PMB sections. However, improvement for fatigue cracking resistance is not as good as for rutting resistance.

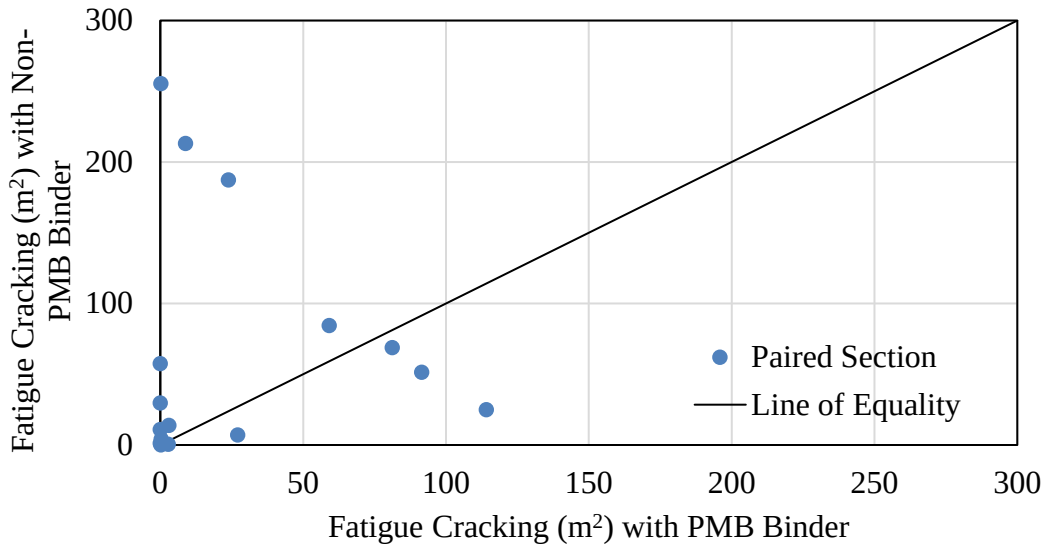

FIGURE 5 Comparison of fatigue cracking performance

Improvement in Transverse Cracking

Figure 6 compares the measured transverse cracking for both non-PMB and PMB sections. It shows that measured transverse cracking for PMB sections are less than the measured transverse cracking for non-PMB sections.

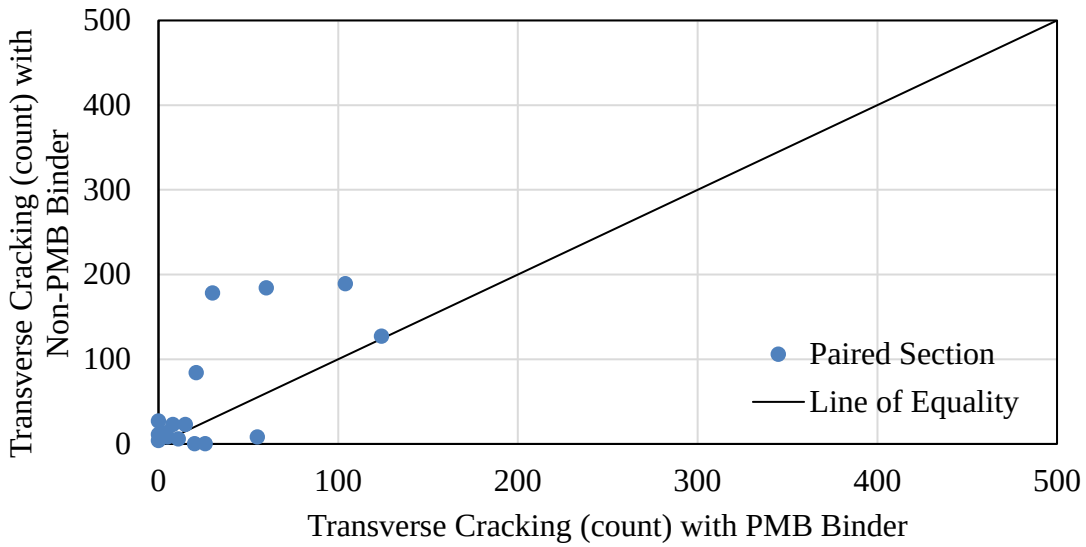

FIGURE 6 Comparison of low-temperature cracking performance

Statistical Tests

To see the difference in distresses for PMB and non-PMB section, paired *t*-test was performed for each type of distresses. The significance level for the *t*-test was chosen as 0.05. Table 9 shows the t-test results for all cases. From the *t*-test results, it can be concluded that measured rutting and transverse cracking for PMB sections are statistically different from the non-PMB sections. However, measured fatigue cracking for PMB section is not statistically different from the non-PMB sections.

TABLE 9 Effect of polymer modification on performance of LTPP sections

Distress Type	p-Value	Remarks
Rutting	0.023	Statistically significant
Fatigue Cracking	0.062	Not statistically significant
Transverse Cracking	0.040	Statistically significant

Summery

After reviewing the LTPP database, it can be concluded that modified binder can improve the rutting resistance, fatigue cracking resistance, and transverse cracking resistance of pavement sections. In addition, *t*-test analysis also shows that the improvement for rutting and transverse cracking are statistically significant. However, improvement for fatigue cracking resistance is not

as good as for rutting resistance. Moreover, the improvement for fatigue cracking is not statistically significant.

SURVEY OF NEW MEXICO ASPHALT SUPPLIERS

Introduction

In this task, a survey was conducted with the current New Mexico asphalt suppliers to determine the feasibility and cost associated with producing the various PG plus binders. Here, the most commonly used base binder, polymers, and PMBs are identified. A survey form consisting of questions with multiple choice and short answer was sent to the highway engineers, asphalt suppliers, and contractors of the state of New Mexico. The survey was distributed with the help of the NMDOT.

Survey on Polymer Modified Binder

The survey is divided into seven different sections. There were only 2 responses found from the survey participants.

Section 1: General Questions

In this section, general questions regarding use of PMBs are asked. The survey responses show that PMB is being used in New Mexico. Two common modified binders are 70-28+ and 70-28R+. However, they are only used in OGFC layer. The primary polymer used to modify the binder is SBS polymer. The PG 58-28 and the PG 64-22 are being used as base binders for modification. Typically, 3-6% SBS is being used depending on the specification.

Section 2: Binder and Mix Specifications

This section asks about the specific requirements for the PMB binder and PMB mixes. The survey responses show that the specification for PMB binder is mainly on the elastic recovery. Both respondents reported that PMB binders must meet at least 65% elastic recovery. However, one respondent reported that they use MSCR in addition to elastic recovery test. They also used some compatibility test as per owner agency requirements. For PMB mixes, there is still no specification developed.

Section 3: Polymer Mixing Specification

In this section, questions regarding mixing of polymer with binder are asked. One respondent reported that they use vigorous agitation with a high shear mixer to blend the polymer with the binder. However, the shear rate is not specified. Mixing temperature is ranged from 350 °F to 380 °F. One respondent said that they occasionally (not very often) encounter problems during mixing the polymers. The other respondent reported that viscosity curves are higher for PMB binders than non-PMB binders.

Section 4: Construction

Questions regarding construction processes with PMB mixes are asked in this section. Based on the survey response, it can be concluded that heavily PMB mixes need higher compaction temperatures and more compaction efforts during construction.

Section 5: Pavement Performance

In this section, questions regarding pavement performance improvement due to use of PMB are asked. Both respondents answered that PMB binder reduces the pavement distresses thus increases the pavement life.

Summery

After reviewing the LTPP database, it can be concluded that PMB can improve the rutting resistance, fatigue cracking resistance, and transverse cracking resistance of pavement sections. In addition, *t*-test analysis also shows that the improvement for rutting and transverse cracking are statistically significant. However, improvement for fatigue cracking resistance is not as good as for rutting resistance. Moreover, the improvement for fatigue cracking is not statistically significant.

THIS PAGE LEFT BLANK INTENTIONALLY

CALIBRATION CURVE FOR DETERMINING POLYMER CONTENT

INTRODUCTION

Past studies showed that the performance of a PMB depends on the type and amount of polymer used in it. Therefore, it is very important to know the chemical properties and the percentage of polymer content in order to characterize the PMB. However, most of the current specifications for asphalt binder currently available are performance based. These specifications lack the ability to accurately determine the polymer content in a PMB. Therefore, several studies were performed to determine the polymer content in an unknown PMB. Loucks and Seguin (*65*) provided a process for determining the polymer content in a polymer modified asphalt using gel permeation chromatography (GPC). This method determines the asphalt content based on the molecular weight distribution. However, the molecular weight of asphaltenes are close to the molecular weight of the polymer (*66*). Later, Kosińska et al. (*67*) developed a method using high performance GPC and size exclusion chromatography (SEC) to distinguish between modified binders and unmodified binders. On the other hand, Chen and Lin (*68*) found that elastic recovery provided a good means by which separate polymer-modified and neat binders. Han et al. (*69*) developed a method based on viscosity-temperature curve to determine polymer content in asphalt. These performance-based methods can identify the presence of polymer; however, these methods failed to determine the amount of polymer mixed with the neat binder. Finally, Molenaar et al. (*70*) reported that FTIR spectroscopy can be used to determine the presence of polymers in PMBs. However, they also stated that FTIR analysis is unsuitable for quantitative analysis without the availability of calibration curves. Therefore, this study develops a calibration curve in order to quantify the polymer content in an unknown SBS modified binder using FTIR analysis.

FOURIER TRANSFORM INFRARED (FTIR) SPECTROSCOPY

The FTIR spectroscopy is a technique which is widely used in organic chemistry to identify the presence of different functional groups in solid, liquid or gas sample based on the energy (light) absorption of infrared by the sample. Figure 7(a) shows the FTIR device used for this analysis. Figure 7(b) shows the working mechanism of FTIR device. The FTIR device passes light from a source through a beam splitter. The splitter splits the light into two beams. One beam goes to a stationary mirror and another beam goes to a moving mirror. Then both beams move back to the splitter to combine again. The moving length moves in order to create constructive and destructive interferences (an interferogram). Then, the recombined light passes through an attenuated total reflection (ATR) prism and hence, passes through the sample. The sample absorbs the lights of different wavelengths depending on the vibrations of existing different functional groups, and the remaining light is received by a detector. The detector then reports intensity of light versus time for all wavelengths simultaneously. Finally, a mathematical function called a Fourier transform is used to convert an intensity versus time spectrum into an intensity versus frequency spectrum with the help of a computer. The FTIR spectroscopy exploits the fact that molecules absorb specific frequencies that depends on their characteristic chemical structure. These absorbed frequencies are known as resonant frequencies which match the transition energy of the bond or group that vibrates. Depending on the shape of the molecular potential energy surfaces, the masses of the

atoms, and the associated vibrionic coupling, the bond energy is different for different functional groups. Therefore, each functional group has a distinct FTIR spectrum.

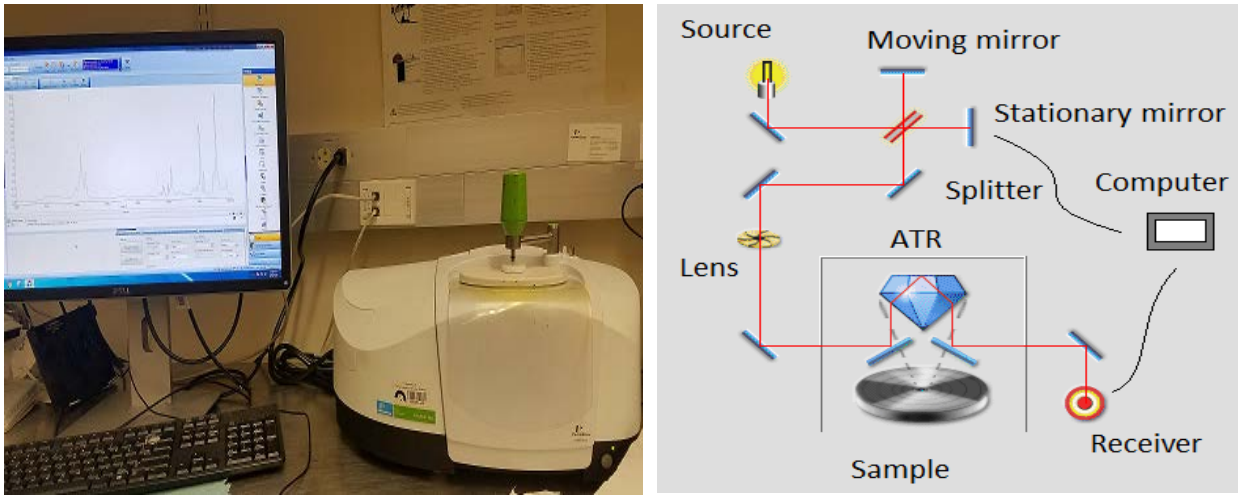

a) PerkinElmer FTIR device b) FTIR mechanism

FIGURE 7 FTIR device used in this study

CHEMICAL STRUCTURE OF SBS POLYMER

To utilize the FTIR analysis for PMB, it is very important to know the chemical structure of the polymer. The SBS is triblock copolymer of polystyrene and polybutadiene as shown in Figure 8(a).

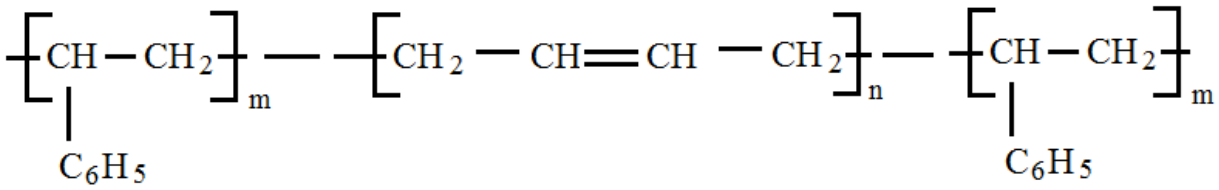

a) Styrene-butadiene-styrene (SBS)

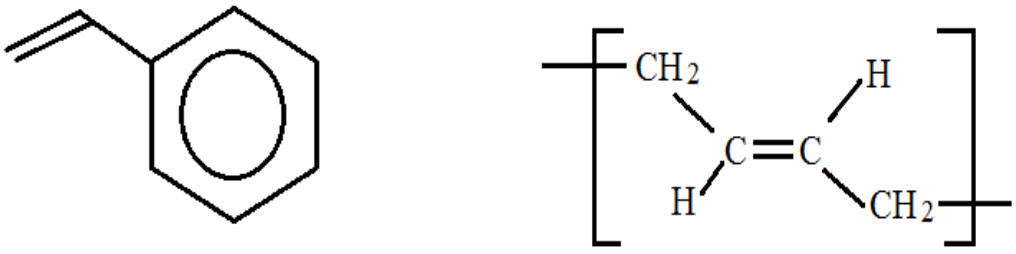

b) Styrene c) Butadiene

FIGURE 8 Chemical structure of SBS polymer (*71*)

The polystyrene (also known as ethenylbenzene) is an aromatic compound with the chemical formula of $C_6H_5CH=CH_2$. It a mono-substitute benzene where one hydrogen atom is replaced by an ethenyl functional group as shown in Figure 8(b). As a mono-substitute benzene, the polybutadiene generates two characteristic absorption peaks at wavenumber 699 cm^{-1} and at wavenumber 757 cm^{-1} respectively. On the other hand, the chemical formula of butadiene is $H_2C=CH-CH=CH^2$. The polybutadiene has a trans-alkene structure (Figure 8(c)) and generates characteristics peak at wavenumber 966 cm^{-1}. However, for terminal mono-substitute alkenes, it also generates two peaks at wavenumber 911 cm^{-1} and at wavenumber 993 cm^{-1} respectively. Figure 9 shows the absorption spectrum of SBS polymer.

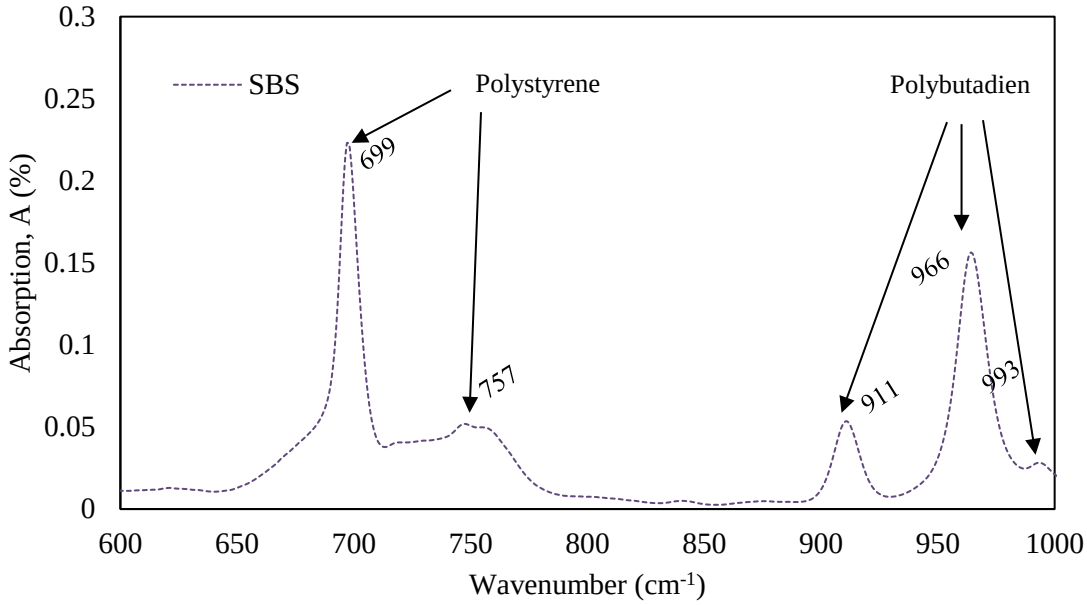

FIGURE 9 FTIR spectrum for SBS polymer

METHODOLOGY

Since SBS is the most popular polymer modifier because of its excellent elastic property, this study chose SBS as the primary and sole modifier for preparation of PMBs. This study also selected PG 64-22 as the base (neat binder) binder. The collected base binder was mixed with three different percentages of SBS polymer and FTIR spectroscopy was performed to develop the calibration curve.

DEVELOPMENT OF CALIBRATION CURVE

Preparation of PMBs

To ensure that the neat binder and the PMBs have the same origin, this study used lab produced PMBs. Therefore, the SBS polymer was blended with a base (neat) binder, PG 64-22 to prepare the PMBs at three different percentages: 1%, 3%, and 5%. Preparation of the PMBs is one of the major steps of this study. It is reported in the past literature that the blending should be done at a higher temperature range from 150 °C to 200 °C (*72*). A wide range of shear rate (from 5,000 rpm

to 10,000 rpm) for blending is also reported in several past studies (*73*–*77*). Therefore, this study chose 190 °C as the blending temperature that is within the previously specified range. Similarly, a shear rate of 8,000 rpm was selected for blending process. A high shear mixer, which has a slotted disintegrating head, was used in this study as shown in Figure 10. A thermocouple was also used for monitoring the temperature to prevent overheating. In addition, the mixing can (bucket) was covered with a foil paper to avoid any air entry to stop oxidizing aging. A maximum of 1500 gm binder was blended at a time. Sample tests using the DSR apparatus were done after one hour of mixing at a 15 minutes interval to ensure the quality of blending process. The mixing process was continued until the coefficient of variation (CV) of three consecutive test results was less than 2.3% (allowable single-operator precision for the DSR test). Since 5% is the maximum polymer content, the mixing time was determined for the 5% SBS PMB and applied to other percentages. The study found the optimum mixing time is 2 hrs.

a) High shear mixer b) Polymer mixing

FIGURE 10 Mixing of polymer with binder

Morphology of PMBs

The morphology of the lab produced PMBs were investigate through Fluorescence Microscopy (FM). The FM images give the idea about distributed SBS globules size in a binder matrix. This study also assumed that the required mixing homogeneity was achieved when the size and distribution of SBS globules of different samples for a specific PMB looks visually similar. Figure 11 shows the FM images of all tested binders. Figure 11(a) shows a complete dark field (asphalt phase) due to the absence of SBS polymer. On the other hand, PMBs have white globules (polymer phase), which indicate the presence of SBS particles, as shown in Figures 11(b)–(d). For all cases, the SBS globules are dispersed homogenously which indicates uniform mixing quality. Since the SBS polymer has higher failure strength compared to binder itself, these SBS globules may work as the reinforcement for the PMBs. In addition, the FM images show that density of the globules increases with polymer content. The 5% SBS PMB has dense polymer phase compared to the 3% and the 1% SBS PMBs. There are some long SBS globules are also observed that for the 5% SBS PMB. With the increase of reinforcement density, the strength of overall binder should be increased.

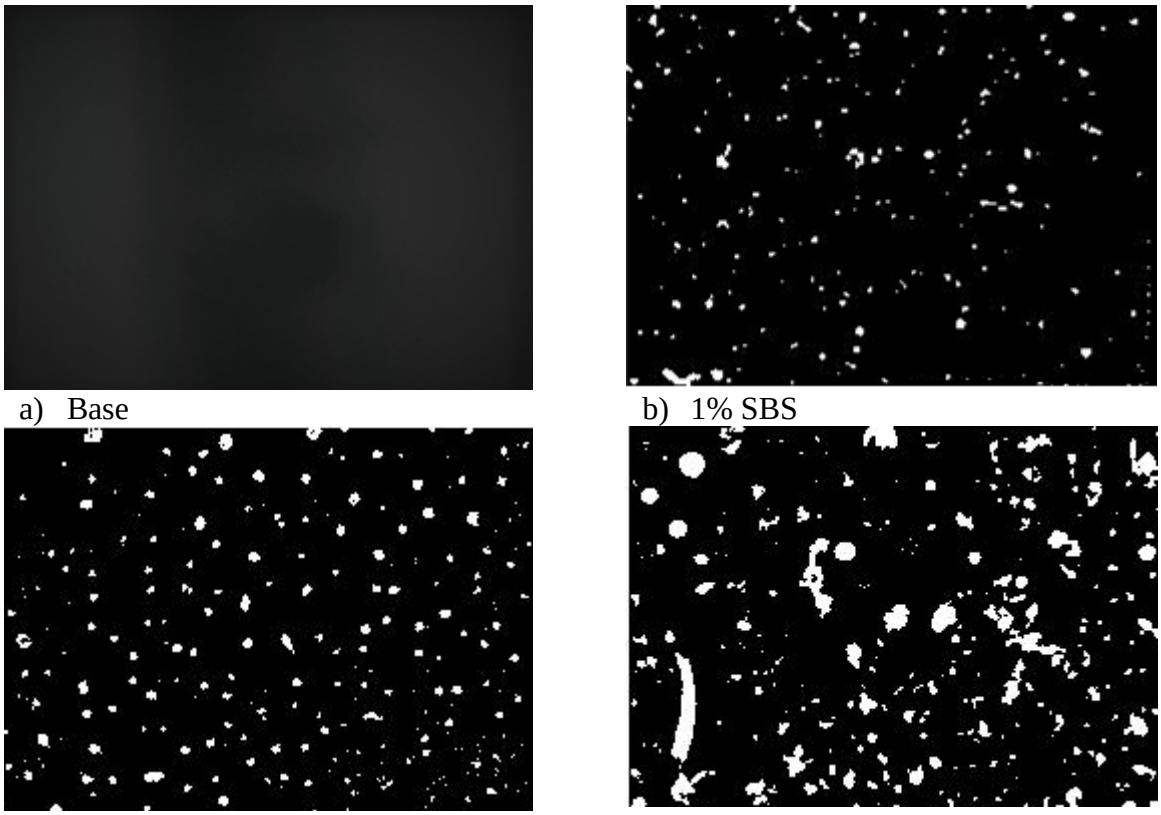

a) Base b) 1% SBS

c) 3 %SBS d) 5% SBS

FIGURE 11 Fluorescence images

Detection of SBS Polymer

Figure 12 shows the generated FTIR spectra for SBS polymer, neat binder and modified binder with 5% SBS. It shows that the neat binder has no peaks at wavenumber 699 cm^{-1} (for styrene) and peak at wavenumber 966 cm^{-1} (for butadiene), which indicates that the neat binder has no SBS polymer in it. On the other hand, modified binder with 5% SBS has two small peaks at wave number 699 cm^{-1} and 966 cm^{-1}, which indicates the presence of styrene and butadiene polymers (thus SBS polymer) in the mixture.

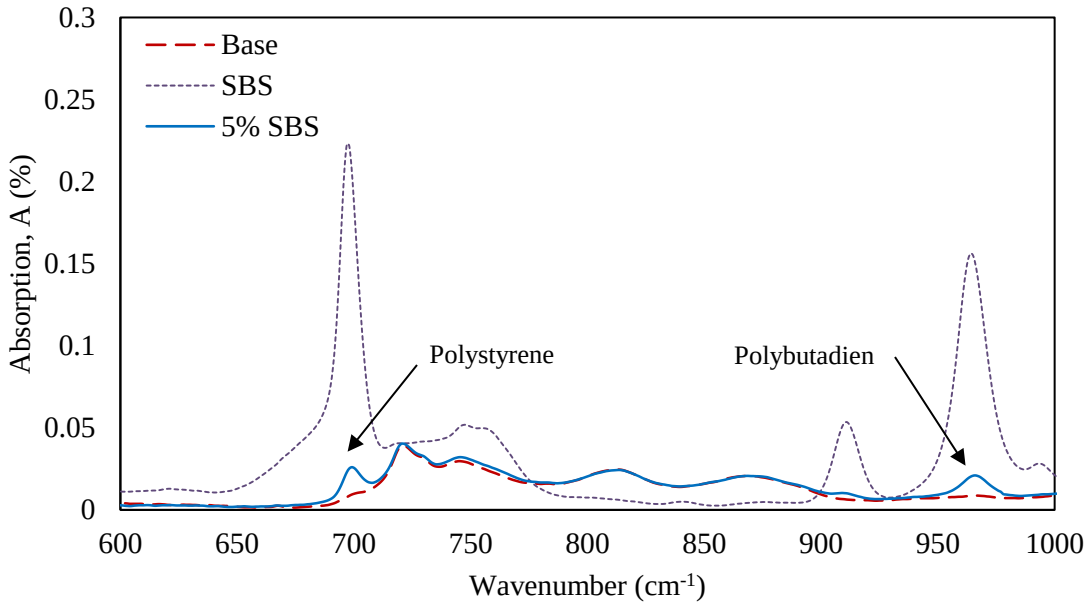

FIGURE 12 Use of FTIR to detect presence of polymer

Calibration Curve

Figure 13(a) shows the FTIR spectra of base binder and three other laboratory produced PMBs. It shows that all PMBs have noticeable peak values at wave number 699 cm^{-1} and 966 cm^{-1}. The peak values increase with increment of polymer content. For example, the 5% SBS PMB has highest peak values than the other binders. On the other hand, 1% SBS PMB has the smallest peak values among the modified binders. The neat binder has no peaks at those two locations. Figures 13(b) and 13(c) show that absorption peak values at wavenumber 699 cm^{-1} and 966 cm^{-1} increase linearly with an increment of polymer content. To make it simple, the final calibration curve (Eq. (1)) was generated by correlating the averaging of these two peaks with SBS content as shown in Figure 13(d).

$$\text{Combined Absorption} = 0.0029 \times \text{polymer content} + 0.0084 \quad (1)$$

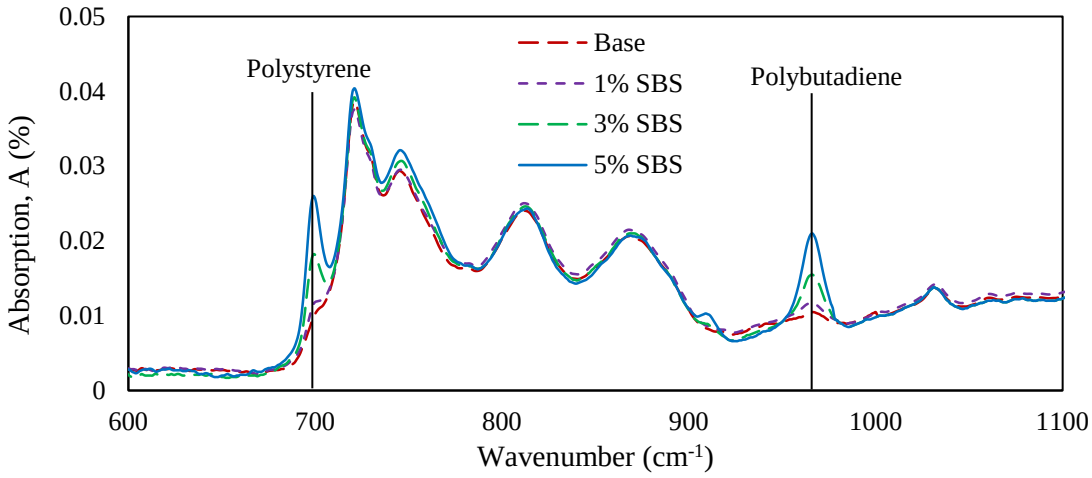

a) FTIR Spectrum

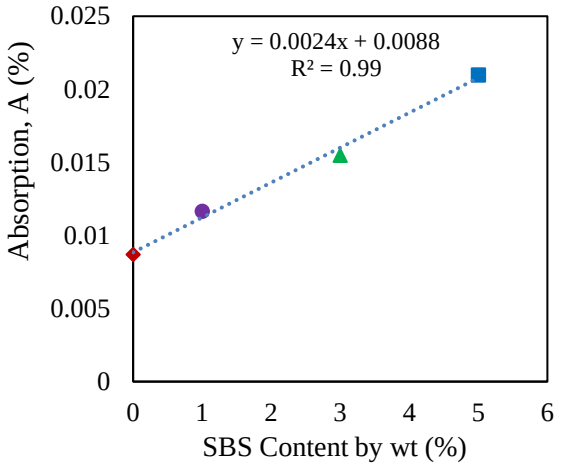

b) Absorbance peak for polystyrene

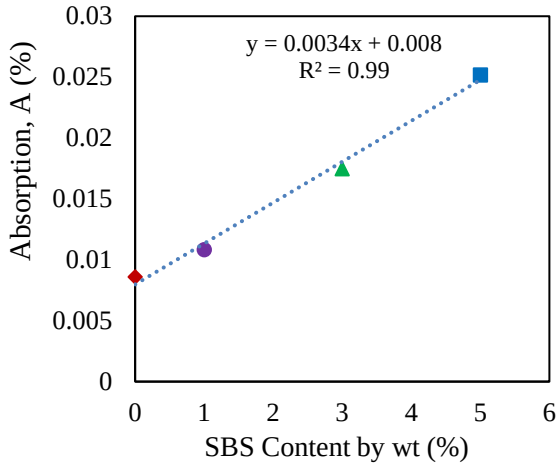

c) Absorbance peak for polybutadiene

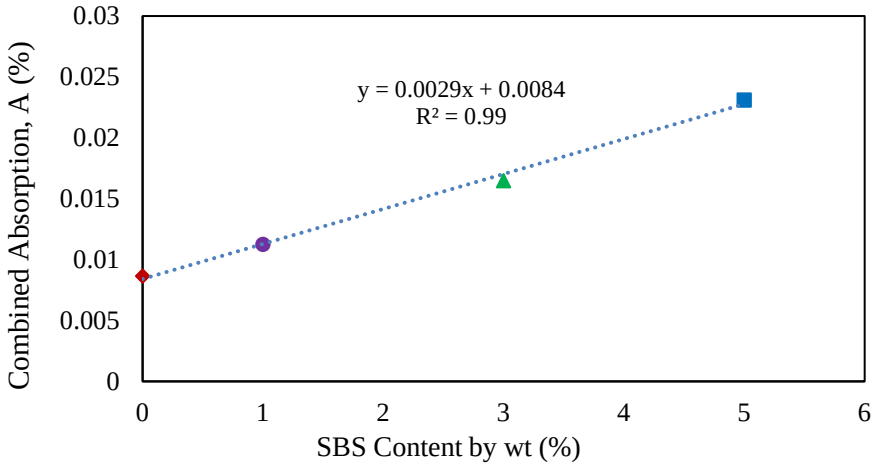

d) Final calibration curve

FIGURE 13 FTIR Calibration Curve

SUMMARY

Based on the results of this study, the following conclusions can be made:

- The FTIR can differentiate between a PMB and a neat binder. The SBS modified binders have noticeable peaks at wavenumber 699 cm^{-1} and at wavenumber 966 cm^{-1} respectively. Therefore, the FTIR spectroscopy can be a useful method to verify the presence of polymer in the binder.
- The developed calibration curve shows that there is a strong linear relationship between absorption peak ratio and the polymer content with an *R*-squared value closed to 1.0. Therefore, the developed calibration can be useful to determine the polymer content in an unknown binder.

THIS PAGE LEFT BLANK INTENTIONALLY

EXPLORING BINDER TESTS FOR PMBs

INTRODUCTION

There are three major distresses that an asphalt concrete pavement experiences during its lifetime. They are rutting, fatigue cracking, and low-temperature cracking. In this section, effectiveness of existing PG binder tests is evaluated by comparing respective test parameters with the respective mixture performance.

Binder Aging

The rutting primarily occurs in newly constructed pavements at high temperature when binders are soft enough to deform easily. Therefore, unaged or short-term aged binders are evaluated to characterize the rutting potential. The short-term aging can be simulated in lab by performing RTFO aging procedure according to AASHTO T 240 (*3*) as shown in Figure 14(a). On the other hand, both fatigue cracking and low-temperature cracking occur in old pavements when binders have significant oxidation aging. Thus, these performances are investigated on long-term aged binders. The long-term aging can be done by PAV aging procedure according to AASHTO R 28 (*5*) as shown in Figure 14(a). This study performed these two aging procedures on all test binders.

a) RTFO b) PAV

FIGURE 14 Binder aging procedures

Preparation of Mixture Samples

In this study, the lab blended PMBs were used to prepare the mixture samples. The aggregate gradation used in this study is shown in Figure 15. This is a SP-III aggregate gradation with a nominal maximum aggregate size of 19 mm. A 4.7% binder content was determined for the base binder and this binder amount was kept the same for other PMB mixtures to make the study simple and consistent. Air voids were tried to be kept the same (7.0±0.3%) for all the tested mixtures. Three replicate tests were done for all cases, and the average values are shown in this paper. To retain consistent aggregate gradation, aggregate was sieved first and then recombined with appropriate amounts from each sieve. At one time a total of 7000 gm sample was prepared. 1%

versa bind was added with the aggregate as specified with design requirement. Bucket mixing procedure was followed to mix the aggregate with binder. The mixing temperature was collected from the Rotational Viscosity (RV) test (*78*) result.

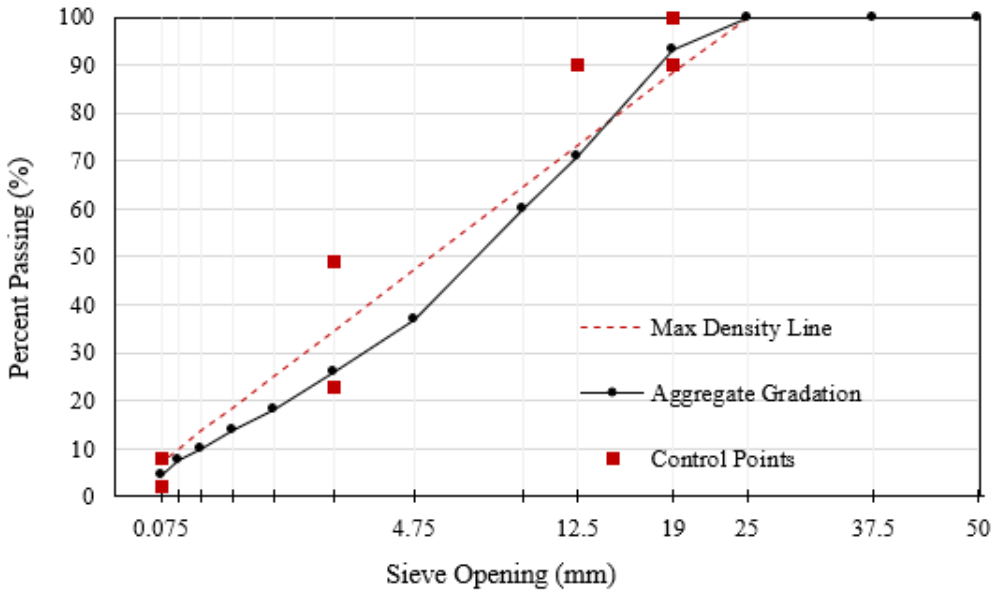

FIGURE 15 Aggregate gradation used in this study

Rotational Viscometer (RV) Test

The objective of RV test (also known as Brookfield viscometer) is to determine the temperature ranges for mixing and compaction of HMA. The viscosity or the coefficient of viscosity is the ratio between applied shear stress and rate of shear and it measures the resistance to flow. The viscosity of asphalt binder at high temperature is important as it controls the pump-ability, mix-ability, and workability. AASHTO T 316 (*78*) was followed to conduct the RV test. In a RV test, a spindle is rotated at 20 rpm rotational speed in 10 grams of hot binder (Figure 16). The viscosity is calculated based on the torque required to maintain the constant rotational speed. According to the Asphalt Institution, the viscosity ranges at Pa-s for mixing and compaction temperature are as follows:

- Range for mixing: 0.15 to 0.19 Pa-s.
- Range for compaction: 0.25 to 0.31 Pa-s.

(a) RV Test Instruments

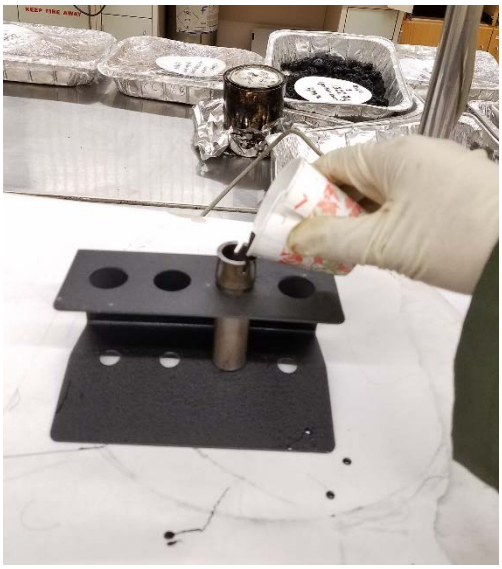

(b) Sample container

FIGURE 16 RV test setup

Table 10 shows the mixing and compaction temperature ranges for base (PG 64-22), 1% SBS, 3% SBS and 5% SBS modified binders respectively.

TABLE 10 Mixing and compaction Temperatures

Binder	Mixing Temperature Range	Compaction Temperature Range
Base (PG 64-22)	158 °C to 162 °C	149 °C to 155 °C
1% SBS	170 °C to 175 °C	160 °C to 164 °C
3% SBS	178 °C to 183 °C	168 °C to 172 °C
5% SBS	179 °C to 185 °C	169 °C to 173 °C

HIGH TEMPERATURE TEST

Rutting

It is known that asphalt binder becomes soft at higher temperature. Many asphalt pavements in the hot climate regions experience surface depression in the wheel path. This kind of distress is known as permanent deformation or rutting. To prevent rutting, binder must be strong enough to withstand against wheel load at elevated temperature. In this section, high temperature performance of the lab produced PMBs will evaluated.

Mixture Performance

Hamburg Wheel Tracking Device (HWTD) Test

To evaluate the performance of the PMBs in Asphalt Concrete (AC) against rutting or permanent deformation, widely used Hamburg Wheel Tracking Device (HWTD) test was conducted. Though the configuration inputs and samples parameters will affect the results of the HWTD, there is no

standard still available for this test. The most common setup for the HWTD used in most transportation agencies as follows:

- 20,000 passes along the test track
- 12.5 mm. (0.5 in.) maximum rutting depth
- 52 rpm
- 50 °C constant water bath temperature
- 158 lb. (700 N approx.)

Several departments of transportation (DOTs) have implemented HWTD test in their specifications as an alternative to Tensile Strength Ratio (TSR) test. Researchers found that binder PG is related to HWTD; stiffer asphalt binder showed better results. In their specifications, transportation agencies defined the water temperature test and number of passes according to the binder PG grade of the AC mixture. In addition, a maximum rutting depth was adopted when binder PG varies. Figure 17 shows the HWTD test setup.

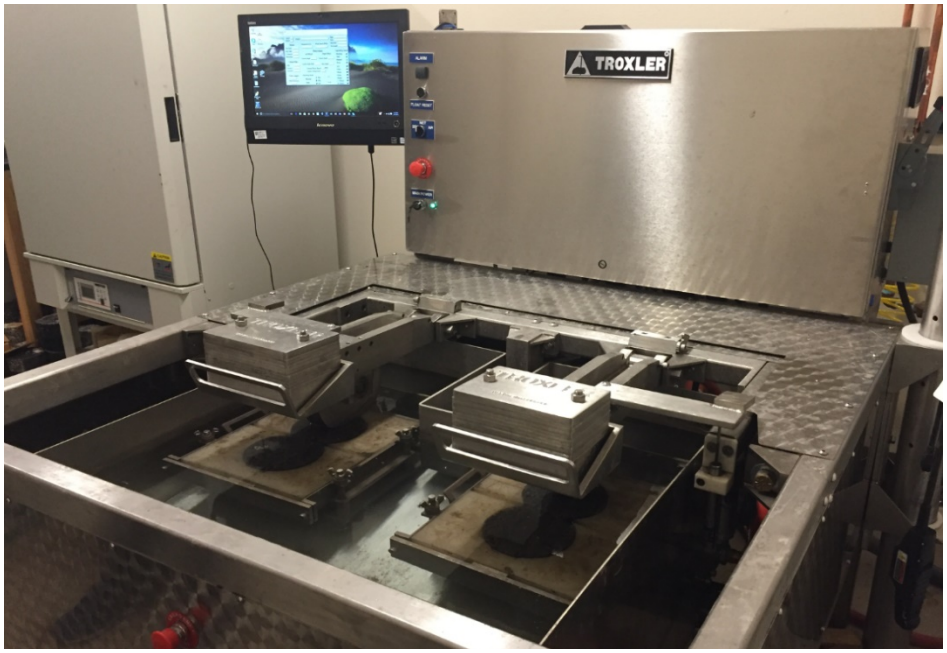

FIGURE 17 Hamburg Wheel Tracking Device Test Setup

A typical curve of rutting depth vs. number of wheel passes has been presented in Figure 18. As seen in the figure, there is one point termed as post compaction, what occurs at the very beginning of the test. This point appears at approximately 100-1000 wheel passes and it represents initial consolidation in several hours after traffic movement is allowed on pavement. Creep slope is the reciprocal of rate of deformation in the linear region of HWTD test results curve, and it starts once a sample reaches to post compaction consolidation. Again, stripping slope is the reciprocal of rate of deformation of linear curve that starts after creep slope. Creep slope is related with rutting potential of asphalt mixes, where stripping slope represents the moisture damage potential. A lower trend of creep and stripping slope represents a severe trend of rutting and moisture damage of

tested samples. If a curve includes both stripping and rutting slope, there is an intersection point of two tangents of these two slopes, which is referred as the Stripping Inflection Point (SIP). If there is no stripping slope, there is no SIP, what indicates the sample performs well against moisture damage. On the other hand, rutting potential is predicted based on maximum impression for 20,000 wheel passes. Several states such as Texas, Colorado, etc. have their own specification for HWTD tests, however, NMDOT does not have any developed specification. Based on other states' specification, if maximum impression lies below 12.5 mm, the mixture is considered to have adequate rutting resistance.

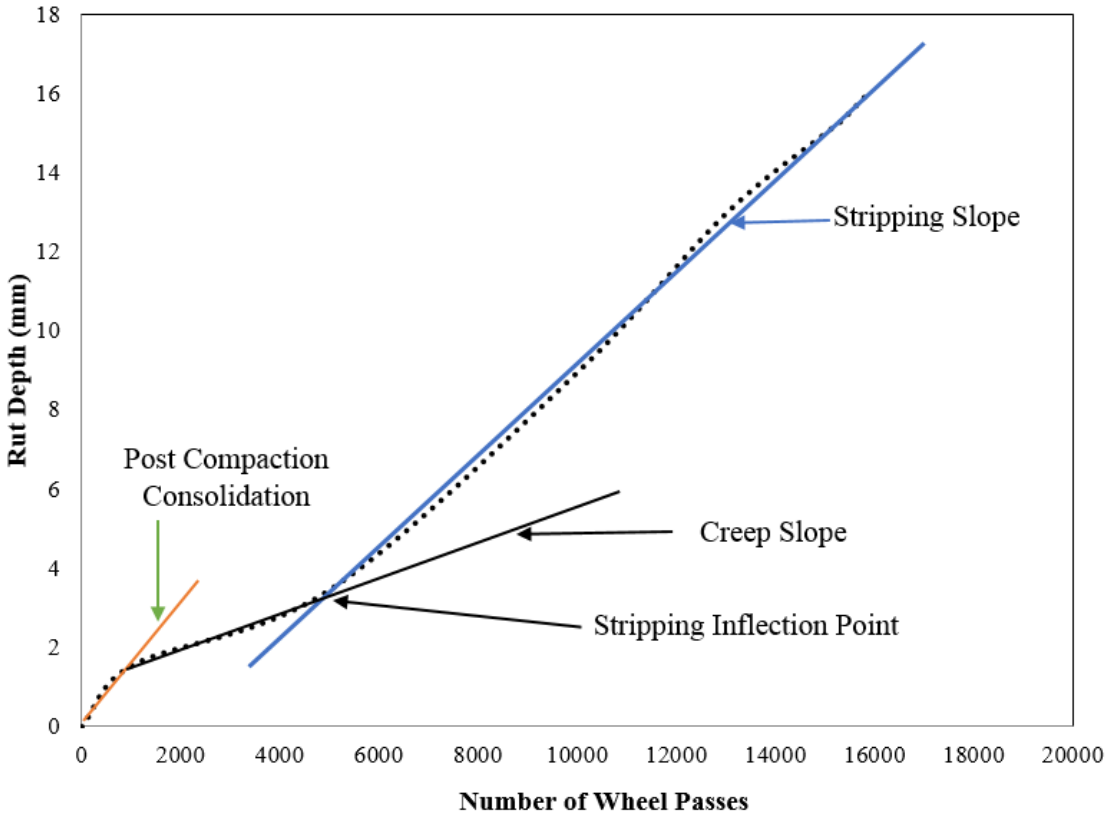

FIGURE 18 Typical Rut Depth Curve from HWTD test

Test Results

This study followed AASHTO T 324-11 (*79*) for the preparation of cylindrical test samples. The HWTD test was conducted on HMA mixture made with base binder and 3 PMBs. The void ratios of the samples were first determined by measuring the theoretical maximum specific gravity, G_{mm} of the loose mixes and the bulk specific gravity, G_{mb} of the compacted samples. The void ratio of the samples varies from 7.12 to 7.26 as shown in Table 11. Figure 19 shows the HWTD test results for all samples. Figure 19(a) shows the rut depth for each wheel passes. For all cases, the rut depth increases with increment of wheel passes. However, increment rate is higher for the base binder and lowest for the 5% SBS modified binder. The increment rate for 1% SBS and 3% SBS modified binder lies in between base and 5% SBS modified binder. It is also observed that base binder

experienced stripping after nearly 10,000 wheel passes. Figure 19(b) compares the final rut depth of all mixes. It shows that the final rut depth for base binder is close to 17 mm, which is above the limiting value of 12.5 mm. On the other hand, 5% SBS modified binder has the lowest rut depth followed by the 3% SBS and then 1% SBS modified binders. From this result, it can be concluded that the polymer content increases the rutting resistance of the binder. The HWTD results are also summarized in Table 11.

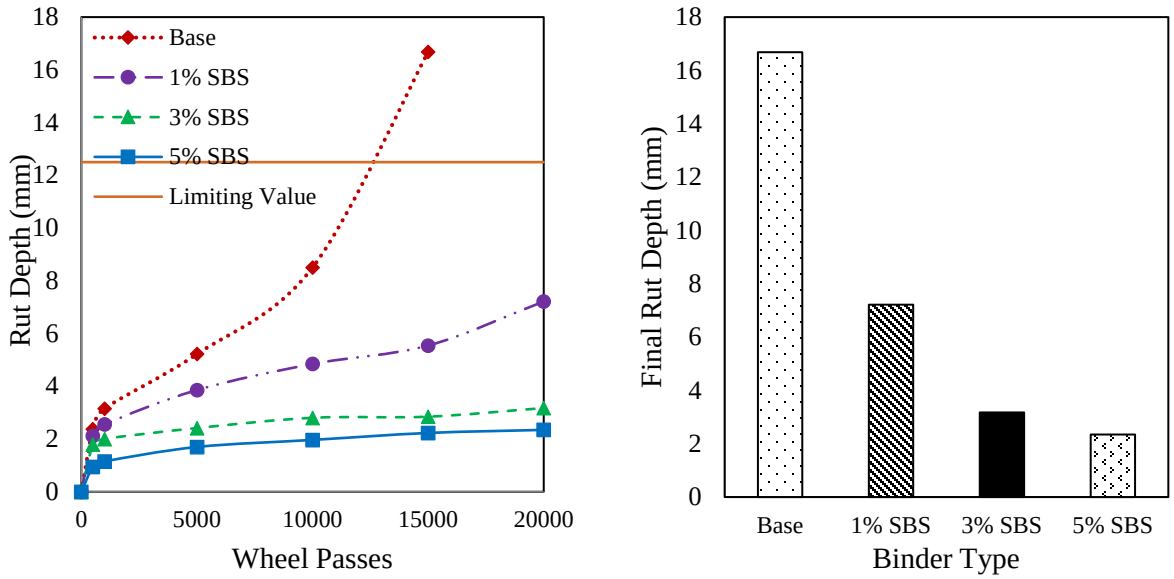

(a) Rut Depth vs. Number of Wheel Passes (b) Final Rut Depth

FIGURE 19 HWTD test results

TABLE 11 Generalized HWTD test results.

Mixture	Average Number of Passes	Maximum Impression (mm)	Samples Air Voids Average (%)	Post-Compaction Point Slope (pass/mm)	Creep Slope (pass/mm)	Stripping Slope (pass/mm)	SIP
Base	17,858	16.68	7.12	422	1,523	611	8,863
1% SBS	20,000	7.22	7.21	471	5,924	2995	14,623
3% SBS	20,000	3.18	7.32	560	12,850	N/A	N/A
5% SBS	20,000	2.34	7.26	1063	18,713	N/A	N/A

PG Rutting Parameter

Dynamic Shear Rheometer (DSR) Test

The PG specification uses the G*/sinδ from the DSR test as the rutting parameter where *G** is the complex shear modulus, and δ is the phase angle of the binder. The DSR test is performed on unaged (and RTFO-aged) binder cylindrical sample with 25 mm diameter and 1 mm height by applying a constant oscillating strain at 10 rad/s (Figure 20). The high-temperature grade is selected such a way when the G*/sinδ value is at least 1.00 kPa for original binder, and 2.20 kPa for RTFO-aged binder.

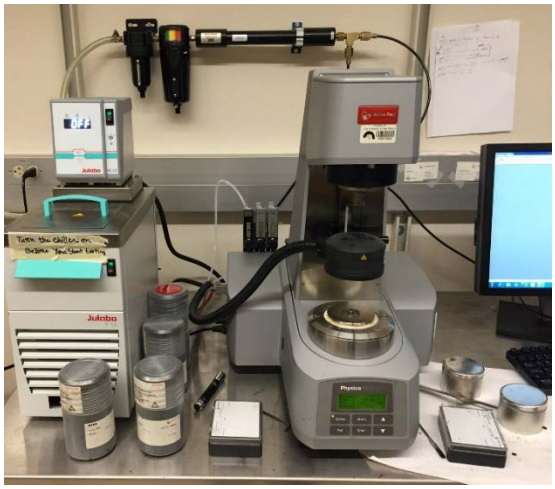

a) DSR device

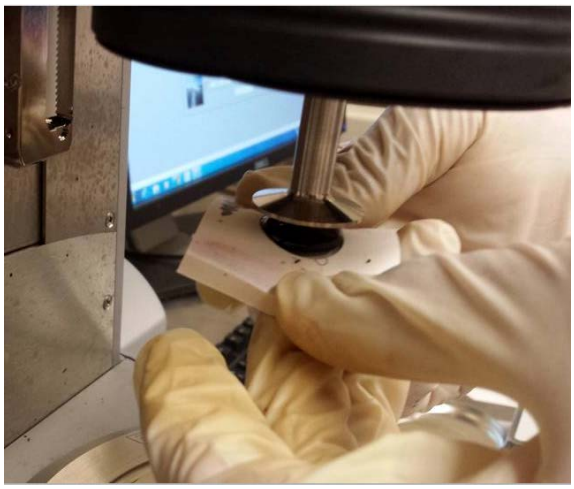

b) Sample in 25 mm parallel plates

FIGURE 20 DSR test setup

DSR Test Results

This study performed the DSR test to determine the high-temperature grades of the lab produced PMBs. Figure 21 shows the DSR result for tested unaged binders. Its shows that the G*/sinδ value increases with an increase of polymer content at each temperature. The unaged base binder meets the Superpave criteria at 69 °C as shown in Figure 21(a). Figures 21(b)-(d) show that the 1% SBS PMB meets the criteria at 75 °C, the 3% SBS PMB meets the criteria at 81 °C, and the 5% SBS PMB meets the criteria at 102 °C.

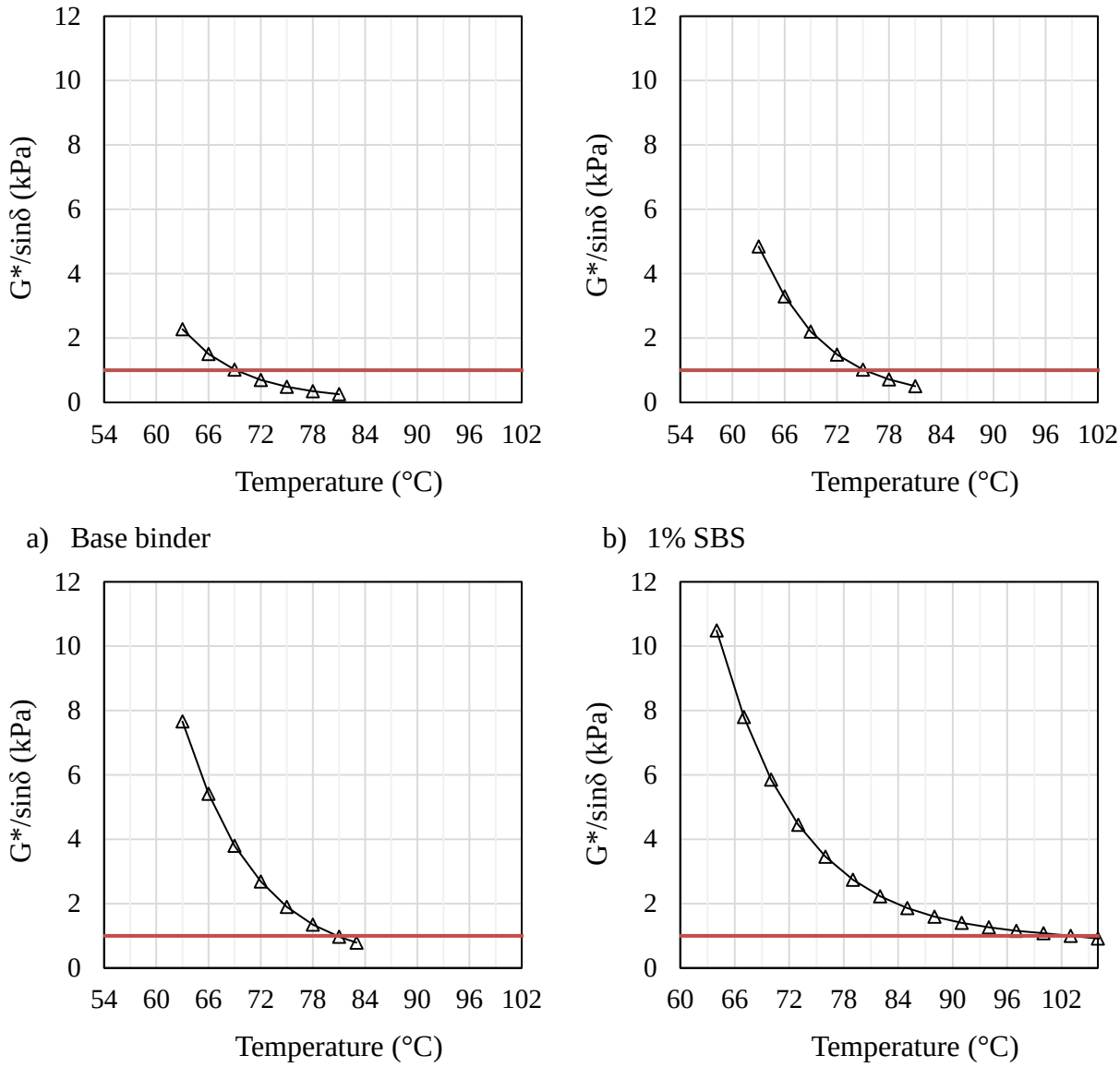

FIGURE 21 DSR results of unaged binders

Figure 22 shows the DSR result for tested RTFO aged binders. Similar to unaged binders, the G*/sinδ value of RTFO-aged binder increases with increase of polymer content. The RTFO aged base binder meets the Superpave criteria at 69 °C as shown in Figure 11(a). Figures 22(b)-(d) show that the 1% SBS PMB meets the criteria at 76 °C, the 3% SBS PMB meets the criteria at 85 °C, and the 5% SBS meets the criteria at 90 °C. The actual high grades of all binders are shown in Table 12. This result indicates that polymer content increases the high-temperature grade.

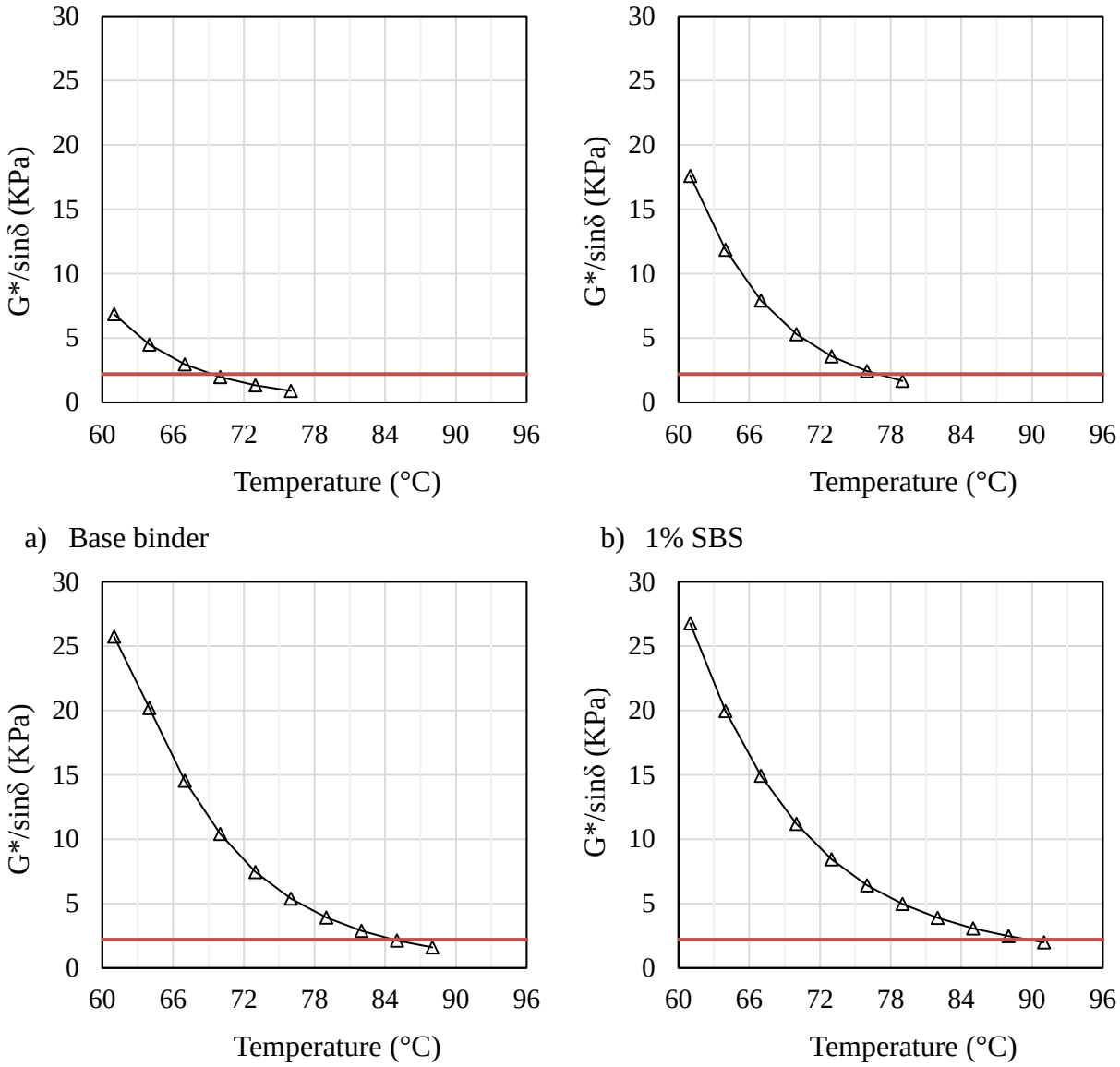

a) Base binder b) 1% SBS

c) 3% SBS d) 5% SBS

FIGURE 22 DSR results of RTFO aged binders

TABLE 12 Actual high-temperature grade of the tested binders

Binder type	High-temperature grade (°C)
Base binder (PG 64-22)	69
1 % SBS	75
3% SBS	81
5 % SBS	90

Correlation with G/sinδ*

According to current PG grading system, the rutting potential of a binder is determined by the G*/sinδ values of unaged and RTFO-aged binders at that temperature. Figure 23 shows the correlation between G*/sinδ values with rut depths of the binders. Figure 23(a) shows the relationship between G*/sinδ values of unaged binder and rut depths. It is found that the rut depth decreases with increment of G*/sinδ. A linear model was fitted with the data. It is found that the relationship is not too strong. The *R*-squared value is found as 0.67. Figure 23(b) shows the relationship between G*/sinδ values of RTFO-binder and rut depths. Similar observation was found. This result proves that the PG binder test failed to characterize the high-temperature performance of PMBs properly.

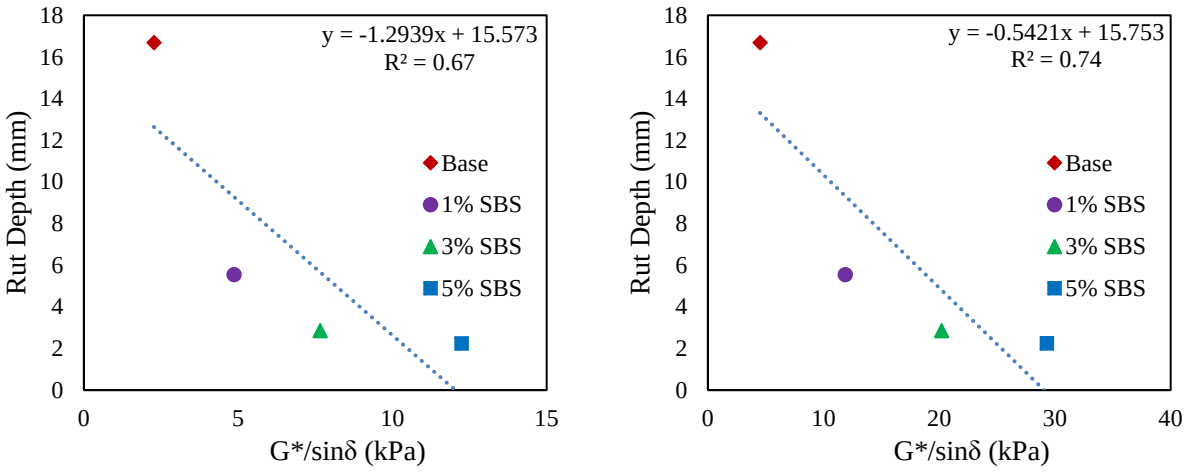

(a) Unaged binder (b) RTFO-aged binder

FIGURE 23 Correlation with DSR test

Alternative Binder Test

Multiple Stress Creep Recovery (MSCR) Test

The MSCR test method relies on asphalt binder creep-recovery performance. In this test, repeated number of loading is applied on the binder sample using the DSR apparatus at two different stress levels. The stress levels in the MSCR test are selected in such a way that one stress in within the LVE range of the binder and another is just outside of the LVE range. This test method also includes a recovery period (as shown in Figure 24) in between loadings, which evaluates the elastic response of asphalt binder.

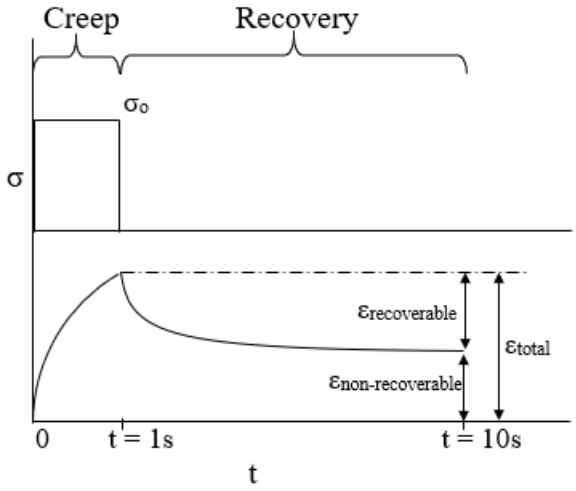

FIGURE 24 Strain history during MSCR testing

There are mainly two parameters that are being determined from the MSCR test: percentage recovery (*%R*) and non-recoverable creep compliance (J_{nr}). The past studies showed that the J_{nr} value measured from the MSCR test represents a better rutting potential than G*/sinδ factor from the conventional DSR test. In this study, AASHTO T 350-14 (*80*) was followed to conduct the MSCR test at temperature 64 °C on the RTFO aged binder. The *%R* and J_{nr} values at each cycle can be calculated using Eq. (2) and Eq. (3) respectively. Similarly, the final J_{nr} values for 0.1kPa and 3.2 kPa stress levels are the averaged J_{nr} of respectively cycles.

$$\%R = \frac{\varepsilon_{recoverable}}{\varepsilon_{total}} \cdot 100 \quad (\%) \tag{2}$$

$$J_{nr} = \frac{\varepsilon_{non-recoverable}}{\sigma_0} \qquad (1/\text{kPa}) \tag{3}$$

MSCR Test Results

Figure 25 shows the MSCR test results for the RTFO-aged binders. Figures 25(a) and 25(b) show the *%R* values of different binders at 0.1 kPa and 3.2 kPa stress levels respectively. It is found that the *%R* increases with increment of SBS content. This is due to the presence of SBS polymer particles in binder matrix, which may create a reinforcing network and enhance the elastic properties. A denser SBS particles may create more effective network, thus, the 5% SBS PMB has highest recovery or elastic property. It is also evident from the figures that the *%R* value decreases when the stress level increased. Figures 25(c) and 25(d) show the J_{nr} values at 0.1 kPa and 3.2 kPa stress levels respectively. In this case, J_{nr} decreases with the SBS content, which indicates that the rutting performance increases with SBS content. The base binder is more prone to accumulate the permanent deformation than the PMBs.

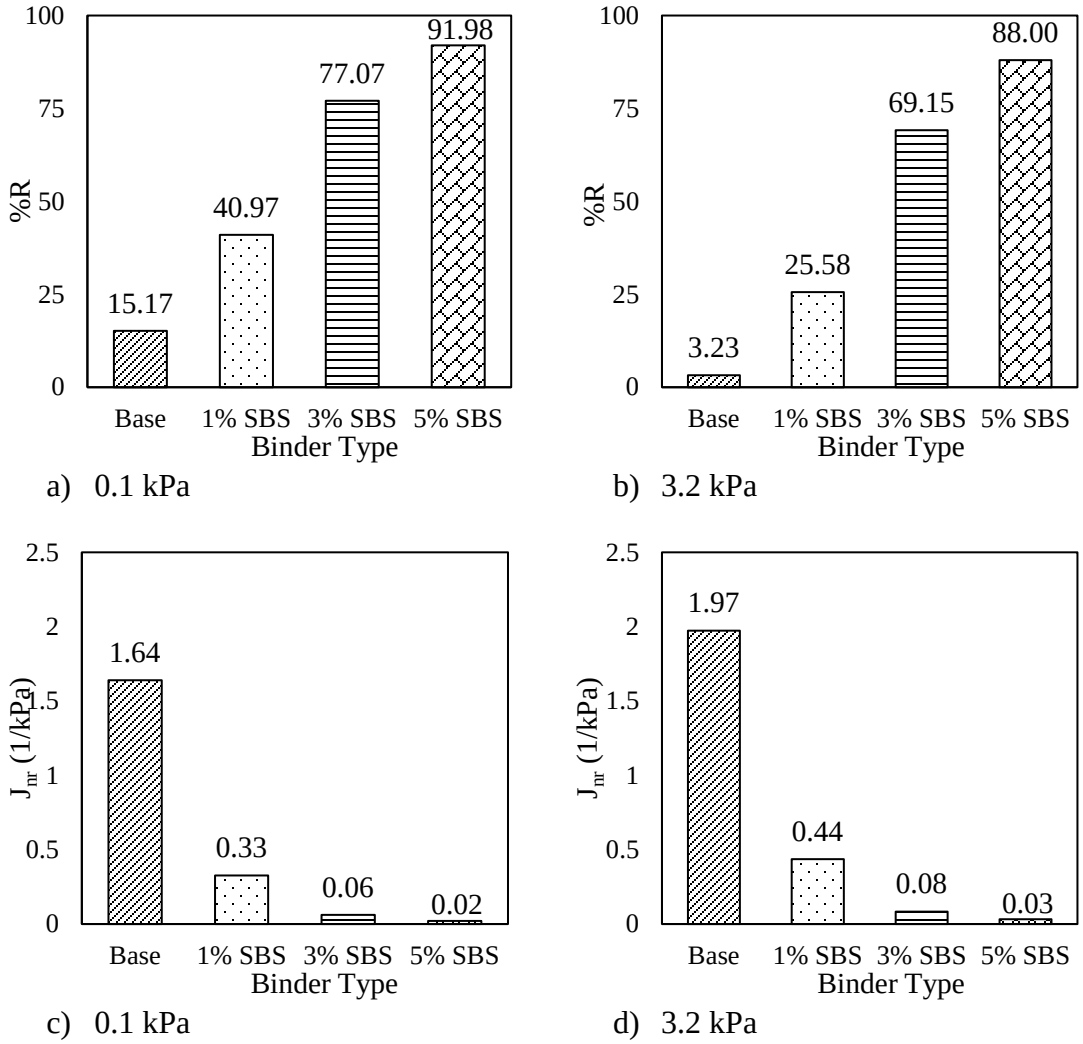

FIGURE 25 MSCR test results

Figure 26 shows the *%R* versus the J_{nr} at 3.2 kPa for the tested binders and compares them with AASHTO control limits. It shows that test points for the base binder and the 1% SBS PMB are below the control line, which indicates that these binders failed to meet the minimum recovery requirement according to MSCR test specification. On the other hand, both 3% SBS and 5% SBS PMBs meet the MSCR criteria as the test points are above the control line. For this section, it can be concluded that SBS modification improves the high temperature performance of the binder. However, enough SBS is needed to get the satisfactory performance.

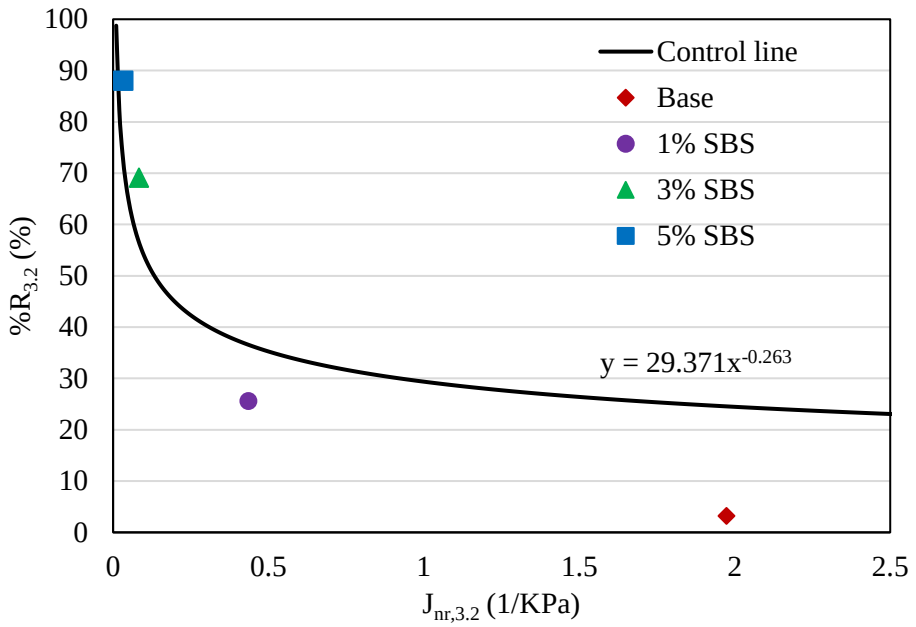

FIGURE 26 Comparison of *%R* versus J_{nr} for different binders

Correlation with MSCR test

Figure 27 shows the correlation between MSCR results and rut depths from HWTD test. Figure 27(a) shows the relationship between non-recoverable creep compliance, J_{nr} and rut depth. The relationship is found strong because the *R*-squared value is found as 0.93. Figure 27(b) shows the relationship between *%R* and rut depth. However, this relationship is not enough strong compared to the relationship between J_{nr} and rut depth.

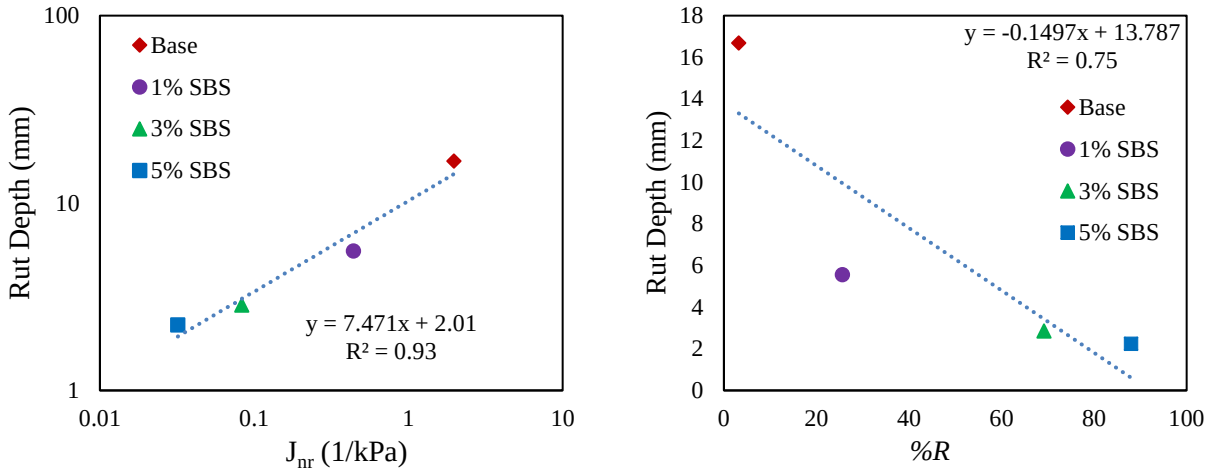

(a) J_{nr} versus rut depth (b) %Recovery vs rut depth

FIGURE 27 Correlation with MSCR test

Summary

From this analysis, it is found that the polymer content increases the rutting resistance. It is also found that the current PG grading system has a weak correlation with the rut depth from the HWTD test. On the other hand, the non-recoverable creep compliance from the MSCR test has the strong correlation with the rut depth. Therefore, this study recommends performing the MSCR test instead of DSR test for characterizing high-temperature performance of PMBs.

INTERMEDIATE TEMPERATURE TEST

Fatigue Cracking

Fatigue cracking is one of the major pavement distresses that generally initiates and propagates in binder/mastic phase of the asphalt concrete. The rapid growth of traffic, the extreme climatic condition, and the thickness reduction enthusiasm lead to a higher propensity of fatigue cracking in pavement nowadays. The fatigue cracking mainly occurs at the intermediate temperature when the pavement is neither too stiff nor too soft. Because, being a viscoelastic material, asphalt pavement dissipates some energy after each cycle of traffic loading and gets some fatigue damage. Fatigue cracking is the accumulation of damage caused by repeated loading. Since fatigue cracks generally initiate and propagate in the binder or mastic phase of an AC, proper asphalt binder should be selected to resist the cracking. This study assumed 20 °C is the intermediate temperature and performed all fatigue tests at this temperature.

Mixture Performance

Beam Fatigue (BF) Test

The BF test is the traditional approach to analysis the fatigue behavior of asphalt concrete. In this test, rectangular asphalt concrete beam sample is subjected to a constant repeated sinusoidal loading at constant frequency. After each cycle of loading, the beam sample has some damage and loses some stiffness. Therefore, due to repeated loading the flexural strength of the beam decreases over the time. The BF test records the change of stiffness over the cycle and determines the N_f. The N_f is considered as the number of cycles required for the 50% reduction of the initial stiffness (*81*). Figure 28(a) illustrates a schematic of the test setup. Because of its support and loading condition, sometimes it is referred as four-point bending test. Figure 28(b) shows a test setup for beam fatigue test.

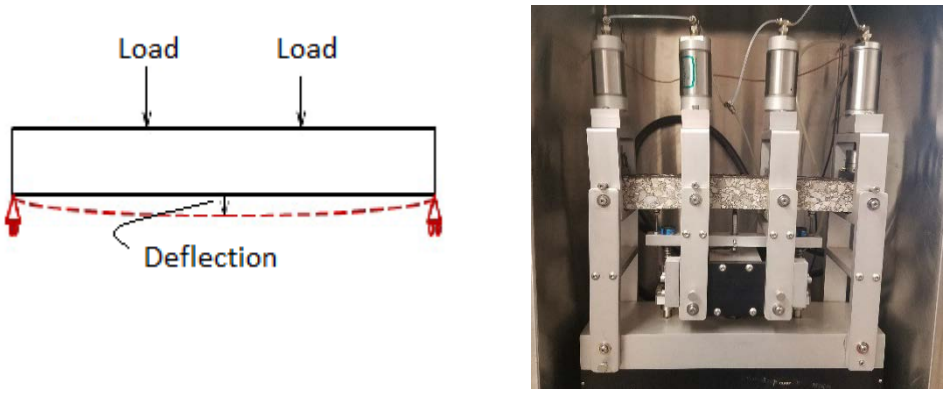

(a) Schematic of BF test (b) Beam sample in test setup

FIGURE 28 BF test setup

BF Test Results

The BF test was conducted in this study according to AASHTO T 321-14 (*82*) standard. It was done on mixture samples made from the base, and the other three lab-produced three PMBs at a frequency of 10 Hz. The test was conducted at three different strain levels: 400 με, 600 με and 800 με. Smaller micro-strains were avoided as the BF test takes more than 10 days at strain lower than 200 με (*s*). Figure 29 shows the BF test results for all tested binders. Figure 29(a) shows that the base mixture has the lowest fatigue life compared to the polymer modified mixtures at each different strain levels. On the other hand, the 5% SBS modified mixture has the highest fatigue life. These results indicate that polymer modification increases fatigue life. This probably because fatigue damage mainly occurs in the binder/mastic phase in an AC sample and the SBS reinforcement network might boost the elastic property of the binder. As such, polymer modification improves the mixture's fatigue life. There is a power relationship between applied strain, ε (or γ) and N_f as shown in Eq. (4).

$$N_f = a\varepsilon^{-b} \tag{4}$$

where a, b are the regression coefficients these material parameters depend on the loading frequencies. This study determined the Fatigue Endurance Limit (*FEL*) values for respective mixture samples using Eq. (4). The *FEL* is the maximum strain level to ensure 50 million fatigue life (*84*). The main purpose of calculating *FEL* is to use a unique fatigue performance parameter for each binder (or mixture) instead of multiple values for multiple strain levels. The calculated *FEL* values are presented in Figure 29(b). As expected, that the *FEL* value increases with an increment of SBS content. Found *FEL* for 5% SBS mixture has more than 1.5 times *FEL* than the base mixture that indicates that 5% SBS mixture can take similar numbers of 1.5 times greater traffic load than the base mixture. This section showed that the fatigue resistance different mixture samples with same mix-properties except the binder type are different, which proves that binder properties have a significant effect on fatigue performance of an AC pavement. Thus, a reliable test is very important that gives the proper binder property. In the following sections, different binder parameters will be evaluated from different binder tests to see which binder test is more reliable to represent the mixture performance.

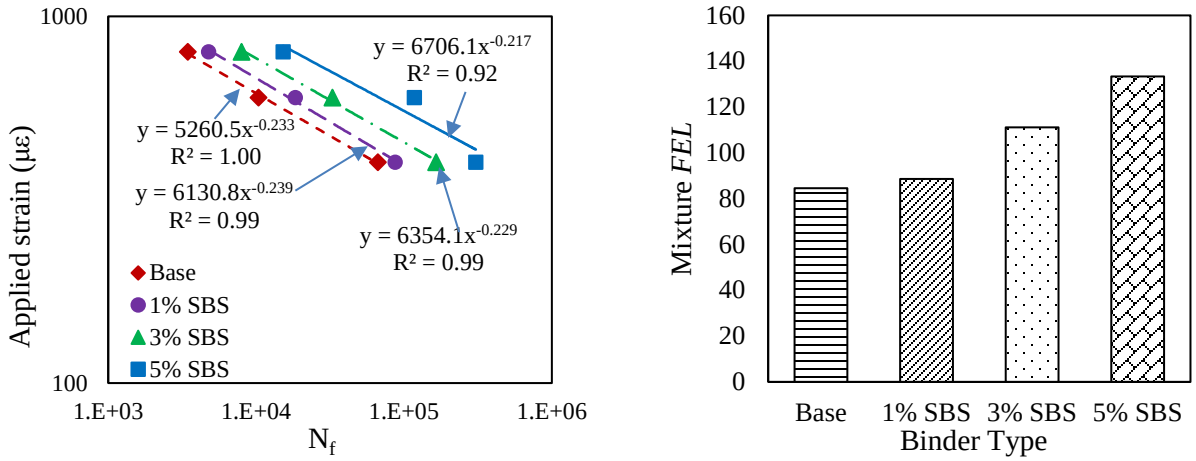

a) N_f versus applied strain b) Mixture *FEL*

FIGURE 29 BF test results

PG Fatigue Parameter

Dynamic Shear Rheometer (DSR) Test

The PG specification uses the G*sinδ from the DSR test as the fatigue parameter where *G** is the complex shear modulus, and δ is the phase angle of the binder. The DSR test is performed on PAV-aged binder cylindrical sample with 8 mm diameter and 2 mm height by applying a constant oscillating strain at 10 rad/s (Figure 30). The PG specification limits the G*sinδ value maximum of 5000 kPa at the intermediate temperature of binder to perform well against fatigue cracking.

a) DSR device b) 8 mm sample

FIGURE 30 DSR test setup

Correlation between BF Test and DSR Test Results

This study used the DSR test to determine the *G** and δ values of the all PAV aged binders at 20 °C. Figure 31 shows the G*sinδ values for respective binders and their correlation with the mixture

FELs. Figure 31(a) shows the found G*sinδ values for the PMBs are higher than the base binder. It also shows that G*sinδ decreases with SBS content. According to PG specification, a lower G*sinδ value represents higher fatigue resistance capability. However, all PMBs have higher G*sinδ as well as higher *FEL* values than the base binder which is opposite of basis of PG specification. Moreover, base binder and 5% SBS PMB have G*sinδ values closed to each other, but 5% SBS mixture has significant higher *FEL* than the base mixture. Therefore, no specific relationship was observed between mixture *FEL* and binder G*sinδ (Figure 31(b)). This section again confirms that G*sinδ is not a good indicator for fatigue performance of an asphalt binder.

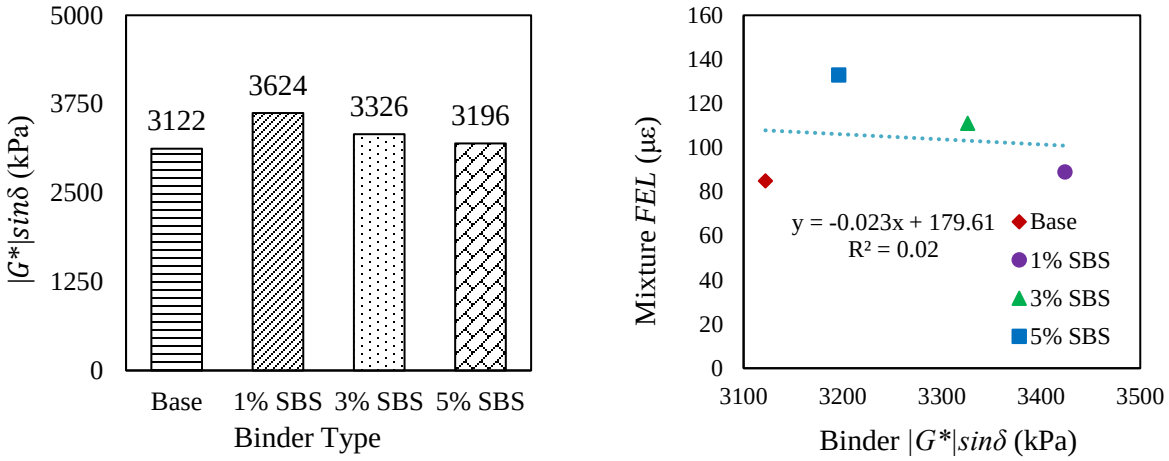

a) Binder $|G^*|sin\delta$ b) Correlation

FIGURE 31 DSR test results

Binder LVE Ranges

Since past studies showed that binder test within the LVE region is unable to represent mixture fatigue performance. This study used the Strain Sweep (SS) test to determine LVE ranges for all PAV-aged binders to use them in MSCR and TS tests. The SS test was performed in DSR device using 8 mm parallel plate geometry. In the SS test, an incremental shear strain is applied on a binder sample at a fixed loading rate and the LVE range is defined by the strain amplitude when the storage modulus starts to reduce by 5% of its initial storage modulus, *G'* (*85*). These LVE values were then used to select appropriate strain and stress levels for MSCR and LAS tests. Figure 32 shows the SS test results of all tested binders. Figure 32(a) shows the G' of the all tested binders over different strain amplitudes. From the test results, the LVE ranges have been found as 1.45%, 1.51%, 1.60% and 1.62% strain for the base binder, 1%, 3% and 5% SBS PMBs respectively. This result confirms the previous study by Bahia et. al. (1999) that SBS content increases the LVE range. As LVE ranges for all binders are within 1.62%, three higher strain values (2.50%, 5.00%, and 7.50%) were selected for later TS test. Figure 32(b) shows the stress-strain relationship for all tested binders. It is found that 5% SBS PMB followed by 3% SBS PMB has somewhat ductile property. However, 1% SBS PMB does not show any ductile behavior in case of shear loading. This is because 3% and 5% SBS PMBs have higher SBS contents those create a dense SBS reinforcing network, which may block the shear loading path and strengthen the overall binder. On the other hand, 1% SBS PMB has the lowest SBS content thus effective reinforcement network

might not establish. Thus, 1% SBS PMB and base binder failed quickly after reaching the ultimate stress. It is worth it to mention that all binders behave the same up to the LVE of the base binder and after that changes occur. From this stress-strain plot, two stress values (50 kPa and 350 kPa) were selected for later MSCR test in such a way that the smaller value is within the LVE range, and the larger value is just outside of LVE range.

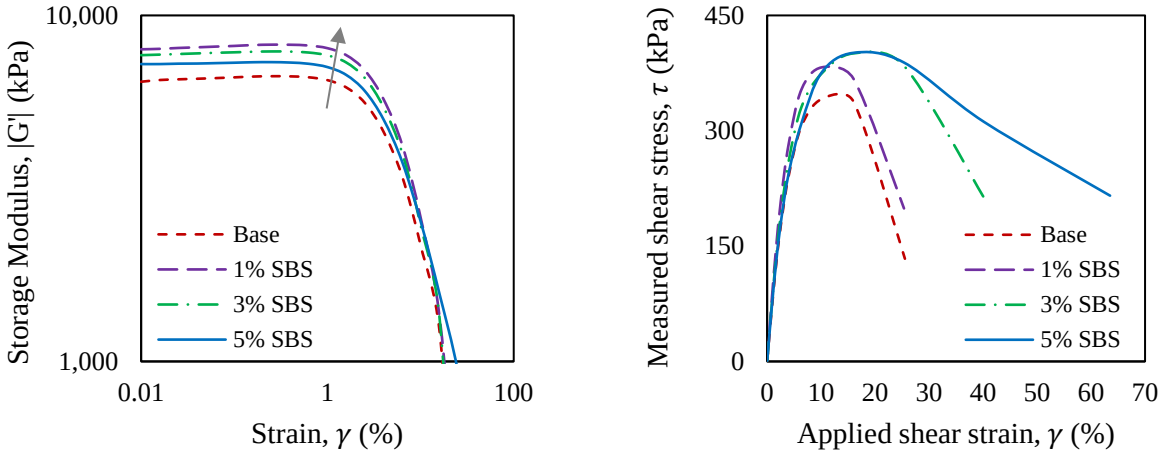

a) LVE range b) Stress-strain plot

FIGURE 32 SS test results

Alternative Binder Tests

Elastic Recovery (ER) Test

In the ER test, binder sample is stretched up to 200 mm at a rate of 50 mm/min and then the elongated sample is cut at the middle for recovery. Figure 33 shows the ductility meter used in this study to perform the ER test. Figure 34 shows the ER results and their correlation with the mixture *FEL*. Figure 34(a) shows the *%R* values of corresponding binders after 1-hour recovery period. During the stretching period, the neat binder crosses its failure point. In PMBs, the dispersed SBS globules are stretched within the binder matrix during testing. The SBS polymer has a significantly higher failure strain than the binder itself. Therefore, the globules do not reach their failure point and try to go back to their original positions after removal of the loading. As a result, the PMBs have more recovery property than the base binder. Higher SBS content leads to higher recovery potential. Thus, 5% SBS PMB has the highest *%R* and the base binder has the lowest. Figure 34(b) shows the correlation between the *%R* from ER test and mixture *FEL*. It shows that the mixture *FEL* increases with an increment of *%R*. Since the ER test is not a cyclic test, the fundamental mechanism of this test is different than the fatigue failure mechanism. Therefore, the correlation between these two parameters is not good enough to be reliable.

a) Ductility meter b) Test sample

FIGURE 33 ER test setup

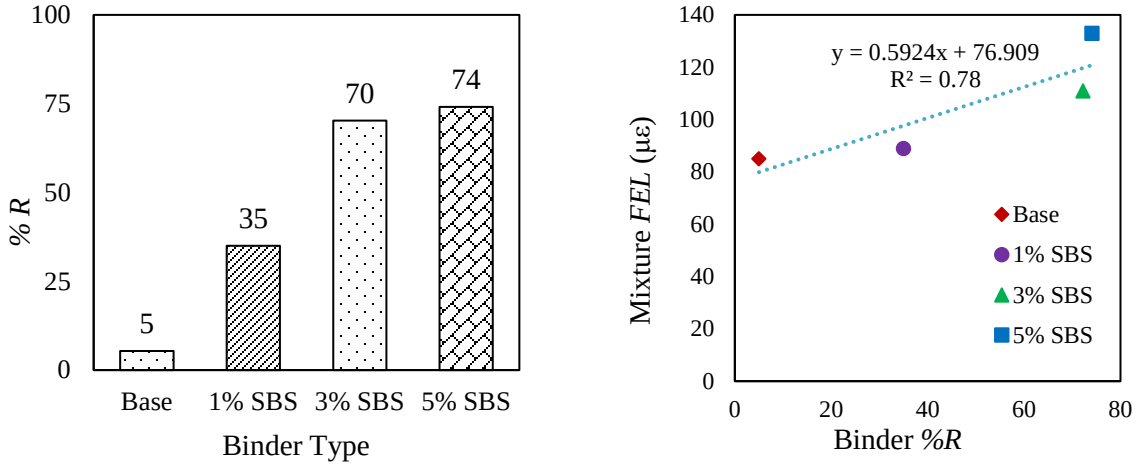

a) *%R* after 1 hour b) Correlation

FIGURE 34 ER test results

Force Ductility (FD) Test

The FD test gives an idea about the tensile strength property of the binder. In the FD test, a binder sample is stretched at a rate of 50mm/min until failure. Figure 35 shows the FD test results of all tested binders. Figure 35(a) shows the load versus displacement plots. The base binder reaches its failure point at 200 mm elongation. On the other hand, none of the PMBs completely failed at 200 mm. Since all the binder samples have the same geometry, it can be concluded from these load-displacement curves, the PMBs can take more load than the base binder. Figure 35(b) shows the correlation between the F_{max} from FD test and mixture *FEL*. It shows that the mixture *FEL* increases with an increment of F_{max}. Like the ER test, the *R*-squared (0.77) value also showed that the correlation between FD and BF tests are not good.

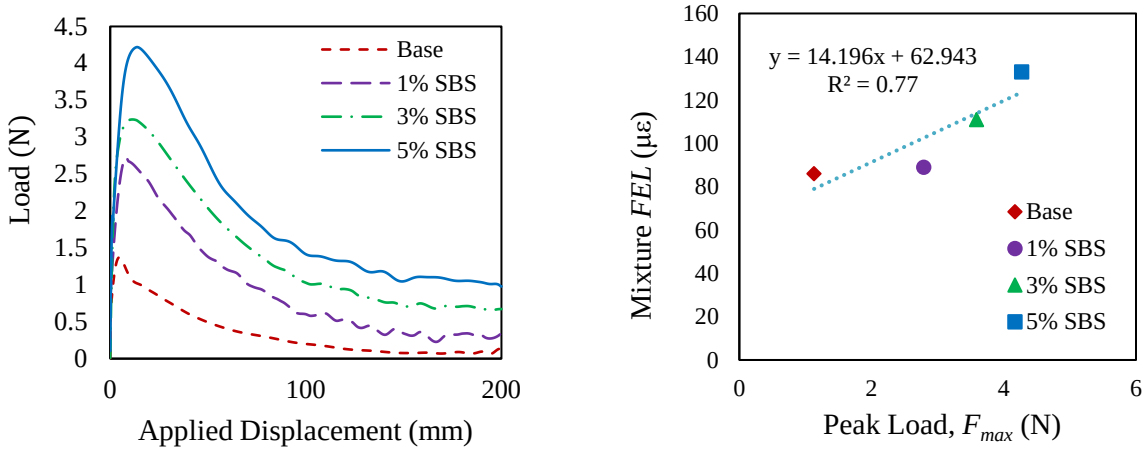

a) Load-displacement plot b) Correlation

FIGURE 35 FD test results

Multiple Stress Creep Recovery (MSCR) Test

Like the conventional MSCR test, this study also used two different stress levels in such a way that the smaller one is within the LVE range and the higher one is just outside of the LVE range. Test data for higher stress is then used for calculation of J_{nr}. Figure 36 shows the MSCR test results of all tested binders. Figure 36(a) shows the J_{nr} values for 350 kPa of all tested binders. The higher J_{nr} value indicates that the sample is prone to have more non-recoverable (plastic) strain for the same stress. The results show that the base binder has the highest J_{nr} and the 5% SBS PMB has the least J_{nr}. Figure 36(b) shows that the mixture *FEL* decreases with the increment of J_{nr} from the MSCR test. Like FD and ER tests, the MSCR test can be used as binder fatigue performance rough indicator but not a reliable one. Though the MSCR test applies cyclic stress, the number of cycles is not enough to occur the fatigue damage. Thus, MSCR failed to represent proper fatigue behavior.

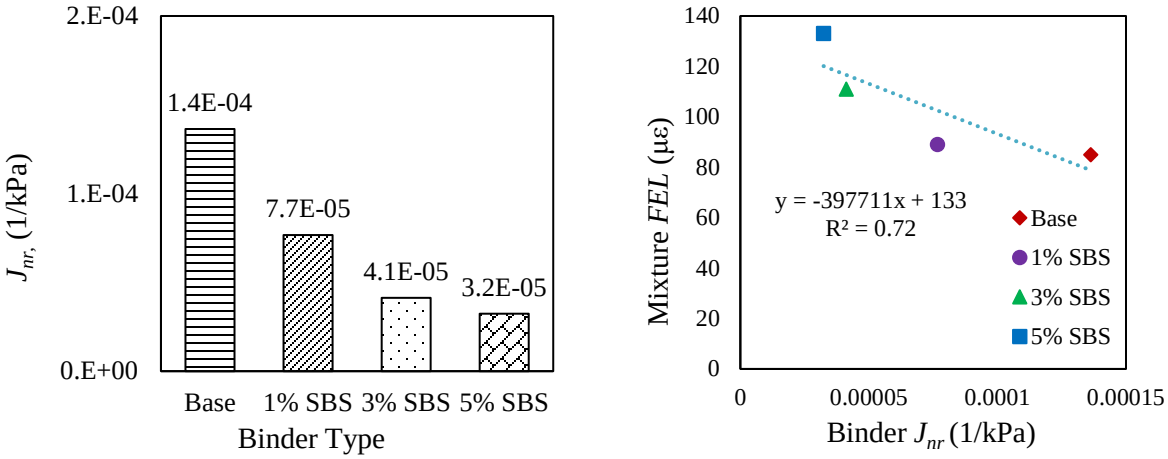

a) J_{nr} at 350 kPa b) Correlation

FIGURE 36 MSCR test results

Time Sweep (TS) Test

The TS applies a constant cyclic load on a binder sample in a DSR using 8 mm parallel plate geometry to induce damage. After each cycle of loading, it records the stiffness and computes damage of the sample. In this study, higher strain amplitudes (2.5%, 5%, and 7.5%) than the LVE range were employed to accelerate damage. The used frequency of the TS test is 10 Hz, that is same as the BF test. Figure 37 shows the TS test results for all different binders. Clearly 5% SBS PMB has significantly higher N_f than the base binder at each strain level as shown in Figure 37(a). 1% SBS PMB has fatigue life close (slightly higher) to the base binder. This study determined the *FEL* values for respective binders using Eq. (4) and correlated them to corresponding asphalt mixture *FEL*. Figure 37(b) shows the correlation between binder *FEL* and mixture *FEL*. In this case, a strong correlation was found. Though loading mode (shear) of TS test is different from BF test (flexure), both tests apply constant cyclic loadings to damage the sample. Therefore, the TS test *FEL* values match well with the BF *FEL* values.

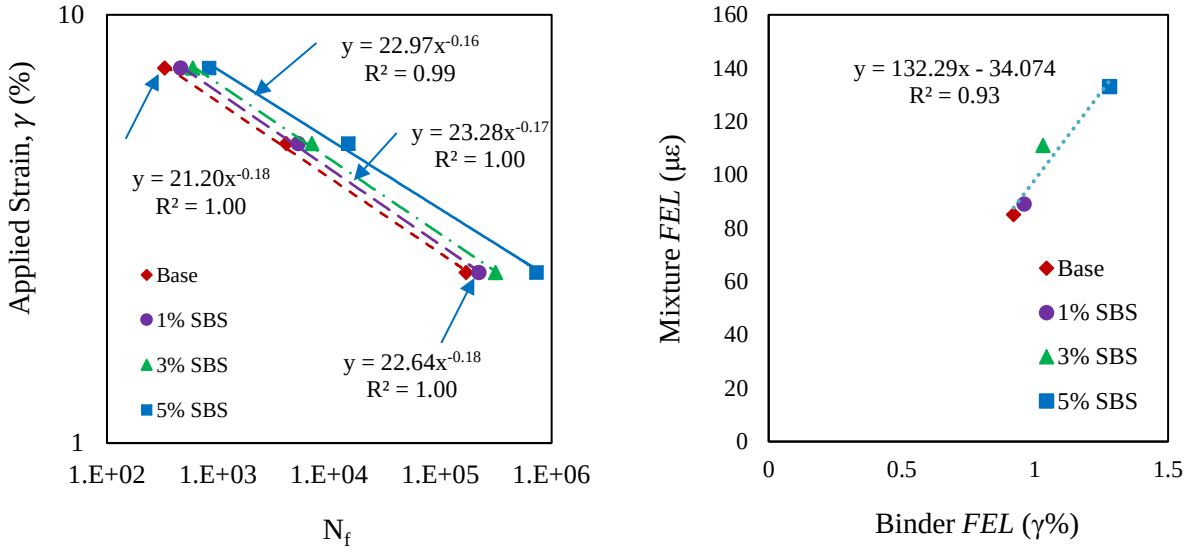

a) N_f versus applied strain b) Correlation

FIGURE 37 TS test results

Linear Amplitude Sweep (LAS) Test

The LAS test applies of a limited number of incremental load cyclic loading on the sample instead of a constant loading to accelerate damage or to reduce the testing time. This test also uses the DSR and the standard 8 mm parallel plate geometry. The LAS test includes a frequency sweep test to obtain the response of the undamaged material response, and a strain sweep test at a constant frequency of 10 Hz to induce fatigue damage at an accelerated rate. Unlike the traditional 50% reduction method, the LAS test data needs to be analyzed by the simplified viscoelastic continuum damage (S-VECD) model to capture fatigue behavior. This model uses the viscoelastic corresponding principle with the work potential theory to derive the damage parameter, *S* from the pseudo-stiffness, *C* of a sample using Eq. (5).

$$S(t) = \sum_{i=1}^{N} \left[\frac{DMR}{2} \left(\gamma_p^R\right)^2 \left(C_{i-1} - C_i\right) \right]^{\alpha/1+\alpha} \cdot \left[t_i - t_{i-1}\right]^{1/1+\alpha} \quad (5)$$

where t is the time; N is the number of load cycles; α is equal to 1+1/m, and m is slope of the logarithmic relationship between G^* and frequency, ω which can be determined from a frequency sweep test; DMR is the dynamic modulus ratio = $G^*_{fingerprint}$ /G^*_{LVE}, where $G^*_{fingerprint}$ is the initial G^* from the amplitude sweep test and G^*_{LVE} is the viscoelastic G^* from the frequency sweep test. The C can be calculated with Eq. (6).

$$C(S) = \frac{\tau_p}{\gamma_p^R \cdot DMR} \quad (6)$$

where τ_p is the peak stress in the cycle of interest; and $\gamma_p{}^R$ is the peak pseudo-strain which can be calculated with Eq. (7) using the peak strain, γ_p in the cycle of interest, and an arbitrary modulus, G_R (assumed as 1).

$$\gamma_p^R = \frac{1}{G_R} \cdot (\gamma_P \cdot G^*_{LVE}) \quad (7)$$

To evaluate the fatigue property, LAS test was conducted on PAV-aged binders. The test was conducted at 20 °C. Figure 38 compares the fatigue test results from LAS test. Figure 38(a) shows the frequency sweep test results for the PAV-aged binders. The complex modulus, $|G^*|$ over the tested frequency range, is plotted in a log-log scale. The steady-state slopes of complex modulus in log space for the base binder, 1%, 3% and 5% PMBs are found as 0.404, 0.377, 0.368 and 0.359 respectively. This indicates that the frequency dependency of the base binder is higher compared to PMBs. Figure 38(b) shows the effective stress-strain relationship for all tested binders. Clearly peak stresses of modified binders are higher than the base binder. The 1% SBS modified binder has the highest peak stress and the base binder has the lowest peak stress. Figure 38(c) compares the damage characteristics curves of the tested binders. The damage characteristics curve represents the relationship of the C with S. For a given C, a higher S value means better resistance to fatigue damage. From the C-S curves, it is observed that the base binder has higher damage compared to other PMBs. It is also observed that the damage resistance increases with an increase in polymer content. Wang et al. (*24*) reported that most appropriate failure defining for LAS is the number of cycles at which stored pseudo strain energy, $W_s{}^R$ reaches the peak value. The $W_s{}^R$ can be calculated using Eq. (8).

$$W_s^R = \frac{1}{2} \cdot C \cdot \left(\gamma_p^R\right)^2 \quad (8)$$

Figure 38(d) shows the $W_s{}^R$ values for all tested binder over the loading cycles. From this plot, the N_f is determined as the number of cycle when the curve reaches the maximum value. For example, the N_f for the base binder is 1620 cycles. In same way, N_f for other binder are determined and Figure 38(e) compares the respected N_f values of tested binders. It shows that the base binder has the lowest N_f compared to other PMBs. This results also concludes that the fatigue performance can be improved using SBS modification and fatigue life increases with an increase in SBS content. Figure 38(f) shows the correlation between binder N_f and mixture *FEL*. Like the TS test, the LAS

test results also showed a strong correlation with the BS test results which indicates that LAS test based on S-VECD model is successful to characterize the fatigue performance of an asphalt binder.

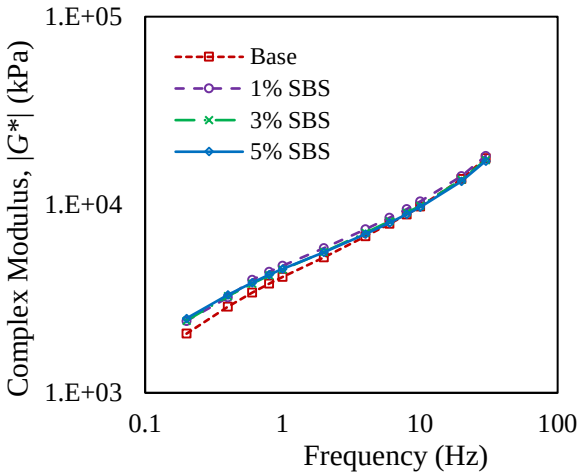

a) Frequency sweep test results

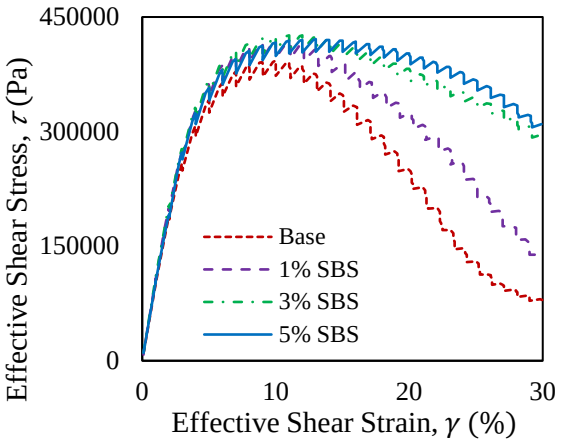

b) Amplitude sweep test result

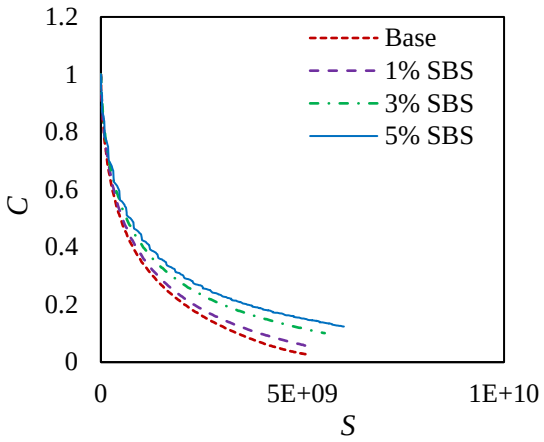

c) Damage curve

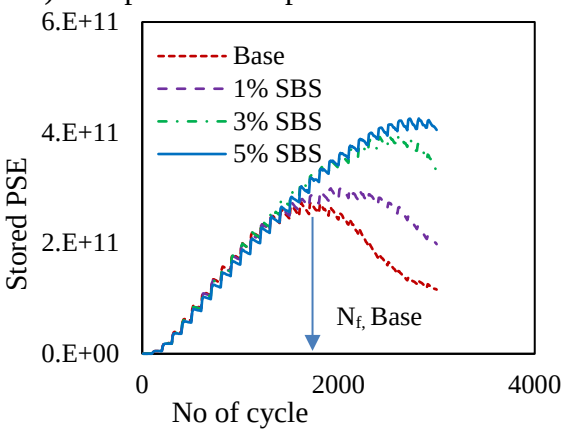

d) Stored pseudo strain energy

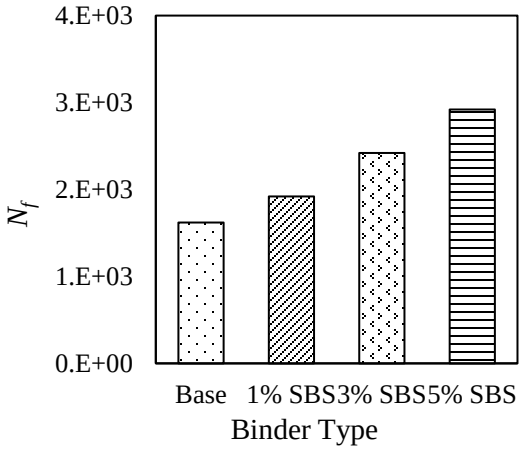

e) Fatigue life, N_f

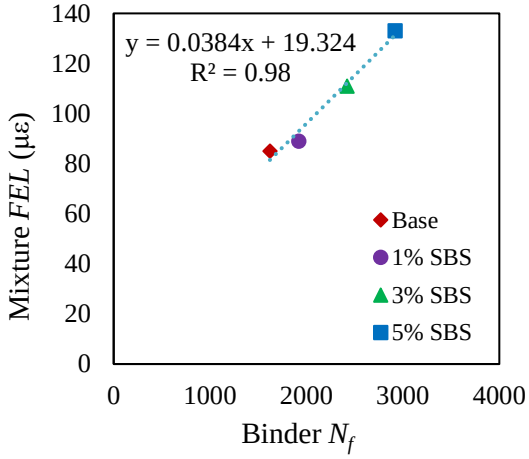

f) Correlation

FIGURE 38 LAS test results

Summary

This study explores the effectiveness of different binder tests that are available for characterizing the fatigue performance of a PMB. At the beginning, the fatigue performances of mixture samples made with four different polymer contents were investigated through a widely expected BF test. The BF test data was then used to calculate the *FEL* values of corresponding mixtures. After that, different binder tests were conducted to determine the respective parameters to correlate them with mixture *FEL*. From the test results, the following conclusions can be drawn:

- The BF test showed that the mixture N_f increases with an increment of SBS content. For this reason, the 5% SBS PMB mixture has nearly 1.5 times more *FEL* than the base mixture which indicates that the 5% SBS PMM can take similar numbers of 1.5 times greater traffic load than the base mixture or 1.5 time more lifespan.
- This study confirms again that the PG fatigue parameter, G*sinδ does not correlate with mixture *FEL*. For example, base binder and 5% SBS PMB have almost similar G*sinδ values but different *FEL*s.
- It is also found that the available performance-based tests, FD, ER, and MSCR can be used as rough indicators for ranking the binders based on their fatigue performance. However, their correlations with mixture *FEL* are not enough reliable to use.
- This study found that the *FEL* from TS test has a good correlation with the *FEL* from BF test. This is because the TS test use similar failure mechanism as used by the BF test (repeated loading and damage the sample).
- The LAS test with the help from the S-VECD model can successfully characterize the binder fatigue performance.

LOW-TEMPERATURE TEST

Low-temperature Cracking

Low-temperature cracking of asphalt concrete pavements is major distress in many regions where the temperature drops significantly. Low-temperature cracking is attributed to tensile stresses induced in pavement layer by temperature drops to extremely low levels when the temperature drops, due to contraction tensile stresses developed in the pavement layer. When this tensile stress induced in the pavement equals the strength of the asphalt concrete mixture at that temperature, a micro-crack develops at the edge and surface of the pavement (*26, 27*). To prevent low-temperature cracking, binder has to be flexible enough to avoid failure due to thermal contraction.

Mixture Performance

Thermal Stress Restrained Specimen Test (TSRST)

To simulate this scenario in a lab environment, Monismith et al. (*86*) first established the framework for using viscoelastic concepts to study the low-temperature cracking behavior of asphalt mixtures and presented the idea of the TSRST test. Later, other researchers such as Stock and Arand (*46*), and Jung and Vinson (*87*) continued this work. The TSRST test simulates the condition of asphalt pavement at low-temperatures, where the resulting thermally induced tensile

stresses primarily result in the transverse cracks in the pavement. It is a temperature-controlled test where a test specimen is glued to two end plates with an epoxy compound. The glued specimen is then cooled in an environmental chamber to a temperature of 0 °C for a sufficient amount of time to establish thermal equilibrium before testing, and then placed in the test set-up. In the test-up, two ends of the specimen are kept in constant positions to prevent the deformation of the specimen, and the temperature of the chamber is cool down at a constant rate. As the temperature reduces, thermal stress develops in the specimen because the thermal contraction is not allowed. The thermally induced stress in the specimen gradually increases as temperature decreases, until the specimen fractures. The temperature at which the specimen fails is the failure temperature of the specimen, T_{fail}. Figure 39 shows a TSRST test of sample done for this study.

a) Cracked sample

b) Fracture faces

FIGURE 39 TSRST test

TSRST Results

Figure 40 shows the TSRST result for two mixture samples made with the base binder. It shows that the thermally induced stress gradually increases as the temperature decreases under a constant rate of cooling until the specimen failures. At the breakpoint, the stress reaches its maximum value, which is referred to as the failure strength, with a corresponding failure temperature. For Sample 1, the failure strength and temperature are found 1.353 MPa and -24.84 °C respectively. For Sample 2, the failure strength and temperature are found 1.397 MPa and -21.05 °C respectively. The average failure strength and temperature for the base were calculated as 1.375 MPa and -22.94 °C. From this test, it can be concluded that the base binder can withstand up to -22.94 °C.

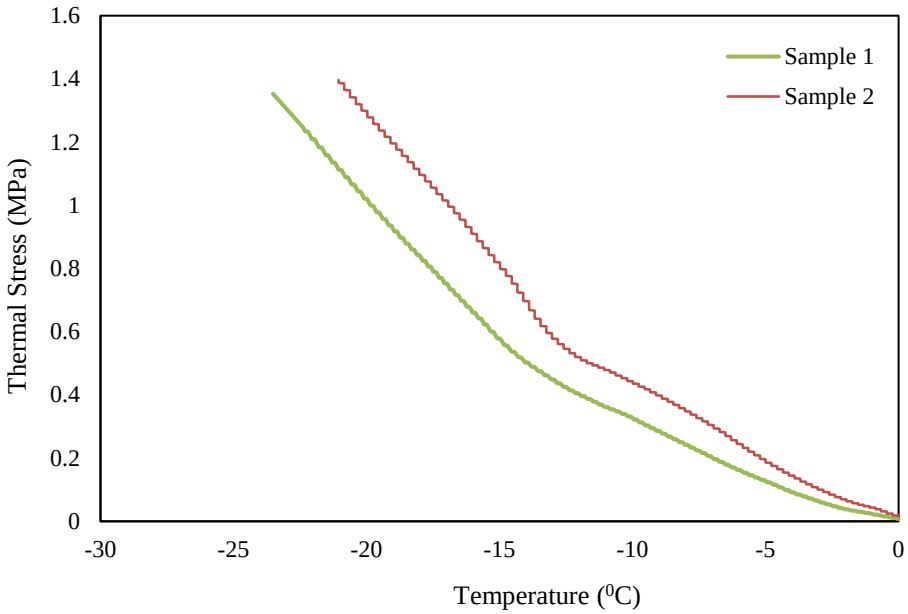

FIGURE 40 TSRST results for the base binder

Similar to the base binder, the failure temperatures of other modified binders were determined from two sample tests. Finally, the average values are shown in Table 13. It is found that the 3% SBS modified binder has the highest failure temperature and the 1% SBS modified binder has the lowest failure temperature.

TABLE 13 Summarized of TSRST results

Binder Type	Sample	Failure Strength (MPa)	Average failure strength (MPa)	Failure temperature (°C)	Average failure temperature (°C)
Base	Sample 1	1.353	1.375	-24.83	-22.94
	Sample 2	1.397		-21.05	
1% SBS	Sample 1	1.932	1.627	-17.06	-16.89
	Sample 2	1.321		-16.71	
3% SBS	Sample 1	1.973	1.968	-29.21	-28.02
	Sample 2	1.964		-26.83	
5% SBS	Sample 1	1.267	1.444	-22.27	-23.46
	Sample 2	1.622		-24.65	

PG Low-temperature Cracking Parameter

Bending Beam Rheometer (BBR) Test

In this study, AASHTO T 313 (*4*) was used to characterize the stiffness and the relaxation properties of asphalt binders at low-temperatures. As with other Superpave binder tests, this characterization is used to find out the minimum temperature at which binder can withstand against low-temperature cracking according to Superpave performance grade specification. The objective of BBR test is used to determine the creep stiffness (*S*) and rate of stress relaxation parameter (*m*-value) for PAV aged asphalt binder to find out its ability to resist low-temperature cracking by simulating creep test at different low-temperatures. According to PG specification, binder has to have a stiffness lower than 300 MPa and *m*-value at least 0.30. Figure 41 shows the BBR test apparatus.

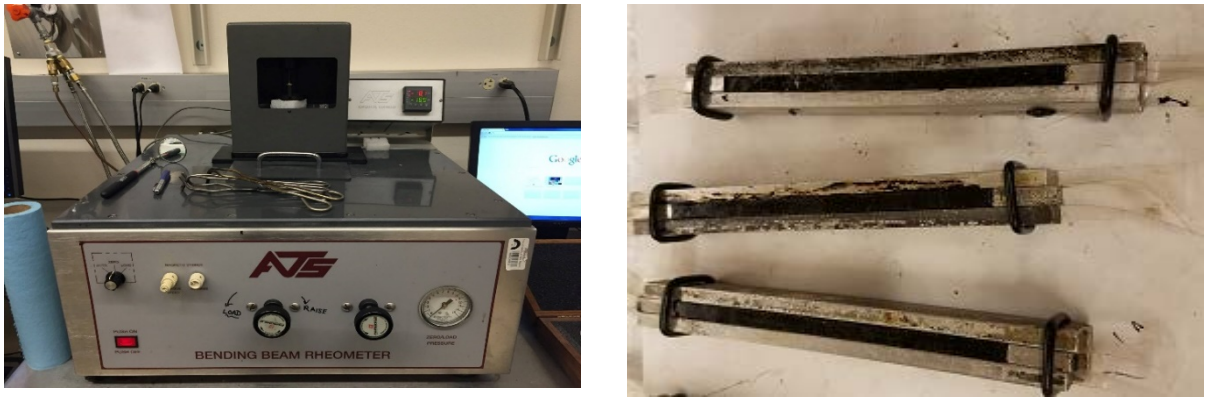

a) BBR apparatus b) Asphalt binder beam samples

FIGURE 41 BBR test setup

BBR Test Results

In the BBR test, the sample is subjected to a flexural creep loading over a total time of 240 sec. at any tested temperature. As a viscoelastic material, creep defection, $\delta(t)$ occurs in the binder over the time. Hence, the defection data was used to determine the flexural stiffness values using Eq. (9).

$$S(t) = \frac{Pl^3}{bh^3\delta(t)} \tag{9}$$

where *P* is the applied load; *l*, *b*, and *h* are the length, width, and depth of the sample; *t* represents the time. Usually, the *S* was determined at 6 different times of loading: 8, 15, 30, 60, 120 and 240 sec. In this study, the BBR test was done at four different temperature levels: 0, -6, -12 and -18 °C and *S* was calculated using Eq. (9). Figure 42 shows the BBR result for different PAV aged binders at four different temperatures. As expected, the stiffness increases with lowering the temperature and decreases with time. It is also found that at 0 °C, the base binder has the lowest stiffness as shown in Figure 42(a) compared to modified binders regardless of time. However, at -18 °C, the

base binder has slightly higher stiffness than the 5% SBS modified binder. This result indicates that the base binder is more susceptible to temperature.

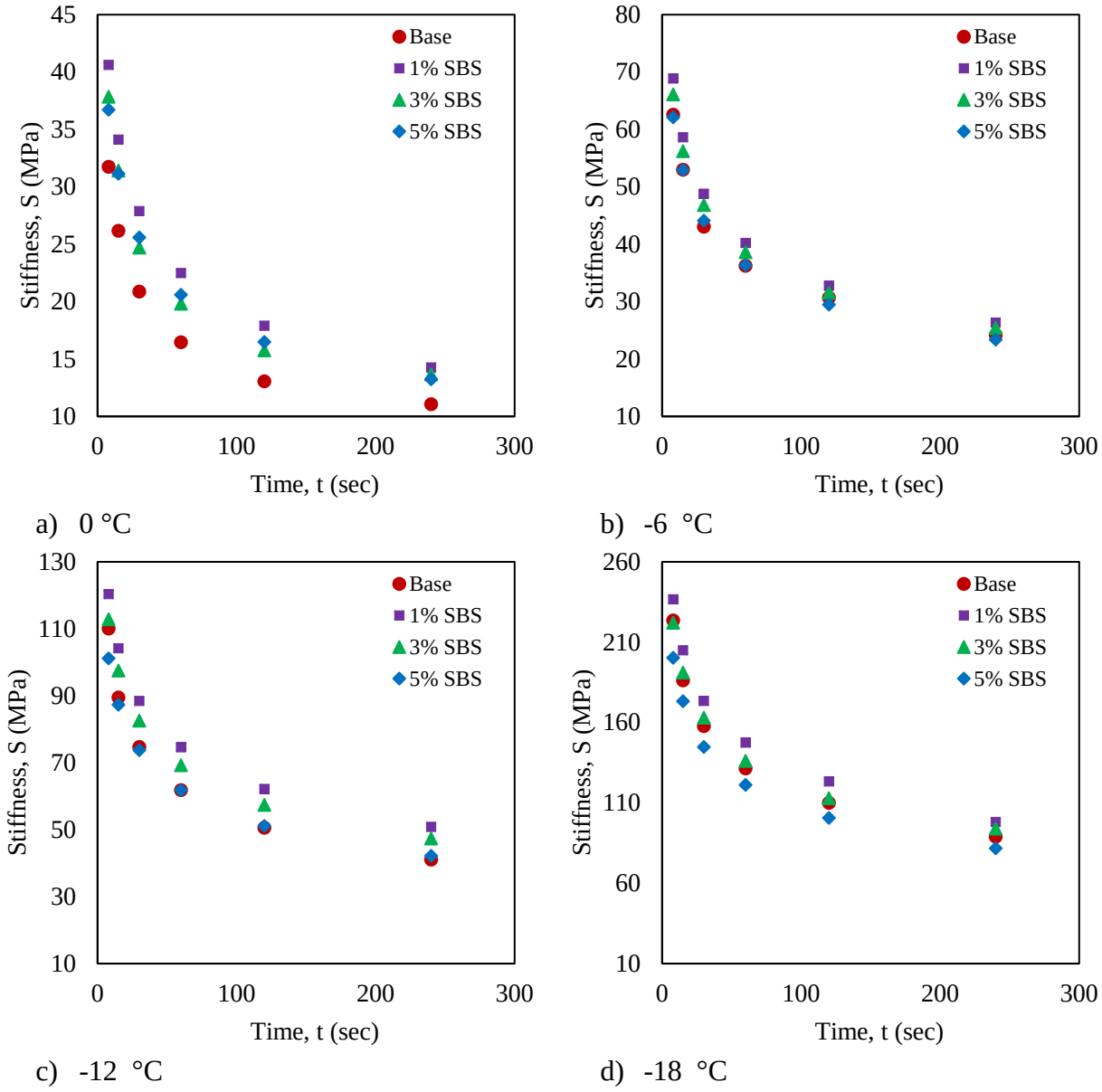

FIGURE 42 BBR Results

Figure 43 shows the PG low-temperature cracking parameters for different PAV aged binders. Its shows that for same temperature stiffness values for modified binders greater than the base binder. In addition, stiffness values for modified binders decreases with increase of polymer content. The increment is not significant. All tested binders passed the lower temperature stiffness criteria (Stiffness ≤ 300 MPa) based on the Superpave classification requirement. However, Figure 44 shows that the *m*-value (≥ 0.3) passing condition for base binder and the modified binders are different. For example, PAV aged base binder meets the PG *m*-value criteria at -12 °C, binder with

1% SBS meets the criteria at -2 °C, binder with 3% SBS meets the criteria at -3 °C and binder with 5% SBS meets the criteria at -4 °C. The actual low-temperature grades of all binders are shown in Table 14.

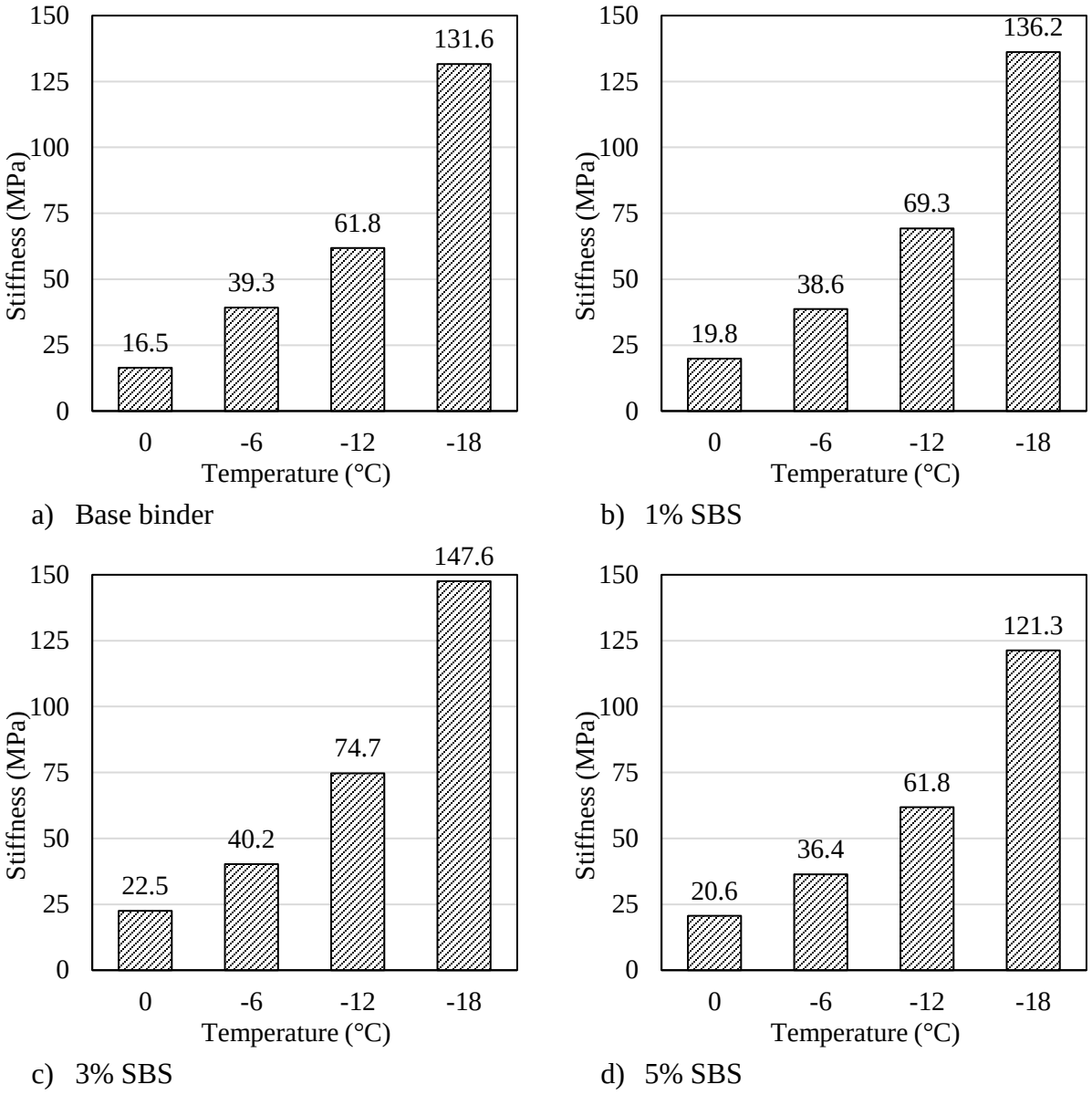

FIGURE 43 BBR results, stiffness versus temperature

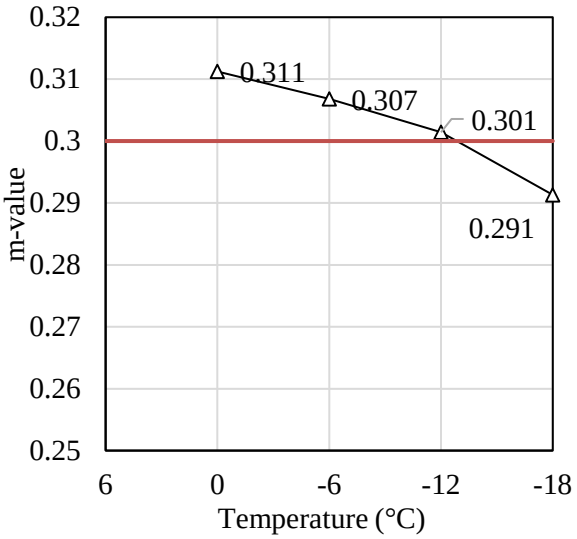

a) Base binder

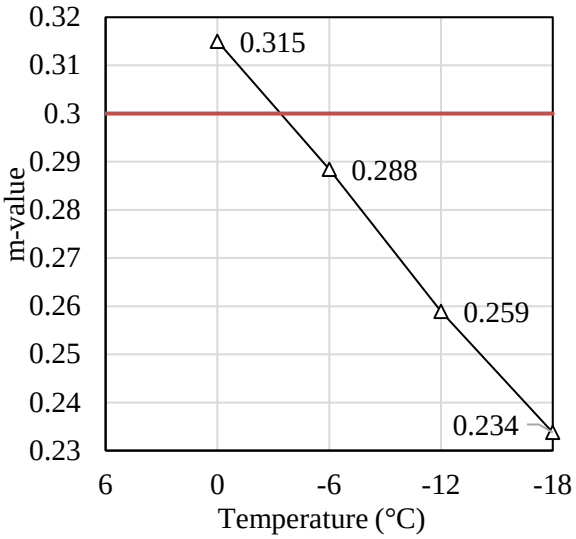

b) 1% SBS

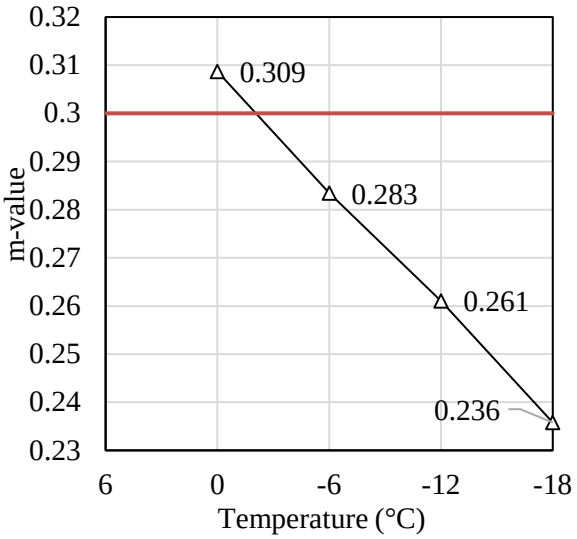

c) 3% SBS

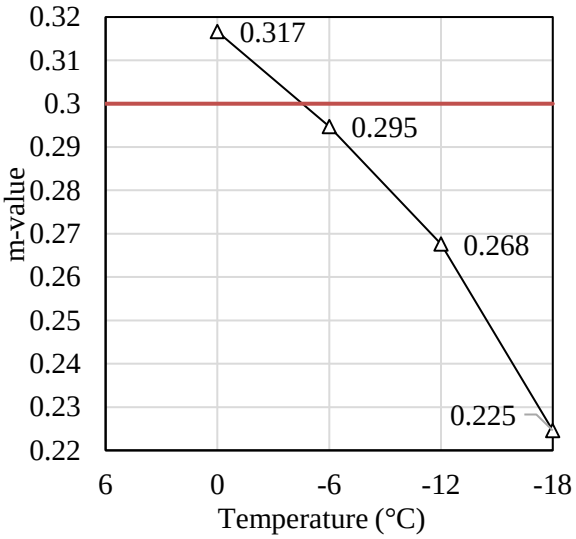

d) 5% SBS

FIGURE 44 BBR results, *m*-value vs temperature

TABLE 14 Actual low-temperature grade of the tested binders

Binder type	Low-temperature grade (°C)
Base binder (PG 64-22)	-22
1 % SBS	-12
3% SBS	-13
5 % SBS	-14

Correlation between TSRST Test and BBR Test

Figure 45 shows the correlation between the low-temperature grade from the BBR test and failure temperature from the TSRST test. It reveals that there is no specific correlation between the binder low-temperature grade and failure temperature. For example, base binder and 5% SBS PMB has almost similar failure temperature but significantly different low-temperature grades.

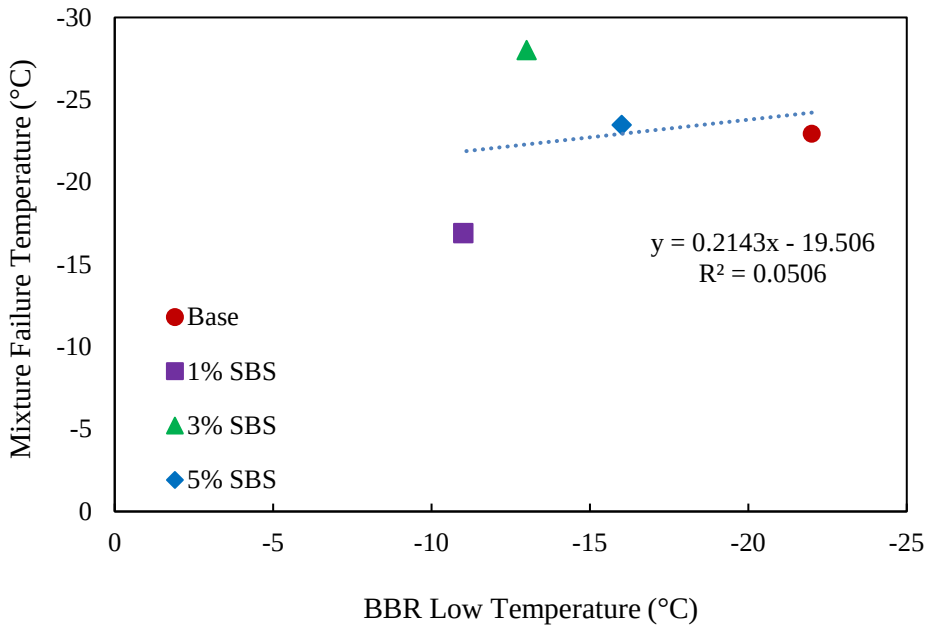

FIGURE 45 Correlation between BBR test and TSRST

Alternative Binder Test or Parameter

Binder Critical Temperature

Since BBR based low-temperature grade does not represent the low-temperature performance of the PMBs, many researchers proposed to use critical temperature instead of low-temperature grade. The critical temperature represents the lowest temperature at which tensile stress in binder phase due to thermal contraction exceeds the binder tensile strength. Both BBR and Direct Tension (DT) test data are required to determine the critical temperature of a binder (*88*). The DT test gives directly the tensile strength of a binder at a different temperature. From the BBR test, thermal stress for thermal contraction can be calculated. The BBR test gives the flexural stiffness of a binder, which depends on both time and temperature. Therefore, the time-temperature superposition (TTS) principle was employed to develop the master curves. After that, the developed relaxation master curve was converted into thermal stresses considering cooling rate as -10 °C/hr. Finally, the critical temperature was determined as the temperature where BBR and DT data intersects.

Direct Tension (DT) Test

In addition to BBR test, the PG specification recommends performing the DT test to characterize the failure properties of asphalt binder in direct tension if the flexural stiffness, *S* exceeds 300 MPa. The basic DT test measures the stress and the strain at failure of a specimen of asphalt binder pulled apart at a constant rate of elongation. The test temperatures are such that the failure will be from brittle or brittle-ductile failure. The DT test is also conducted on PAV aged asphalt binder samples. Figure 46 shows the DT test device used for this study.

a) Sample mold

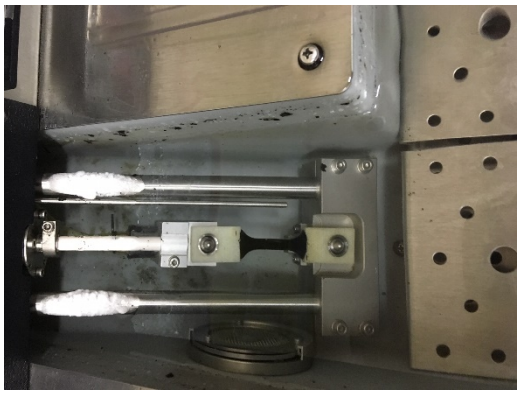

b) sample in the chamber

FIGURE 46 DT sample preparation and testing

DT Test Results

The DT test was done at three different temperatures depending on the binder type. Figure 47 shows the 3% SBS modified binder at -24 °C. It shows that the 3% SBS modified binder has a tensile strength of 1.94 MPa at -24 °C. Tensile strengths of all tested binders at each testing temperature are listed in Table 15.

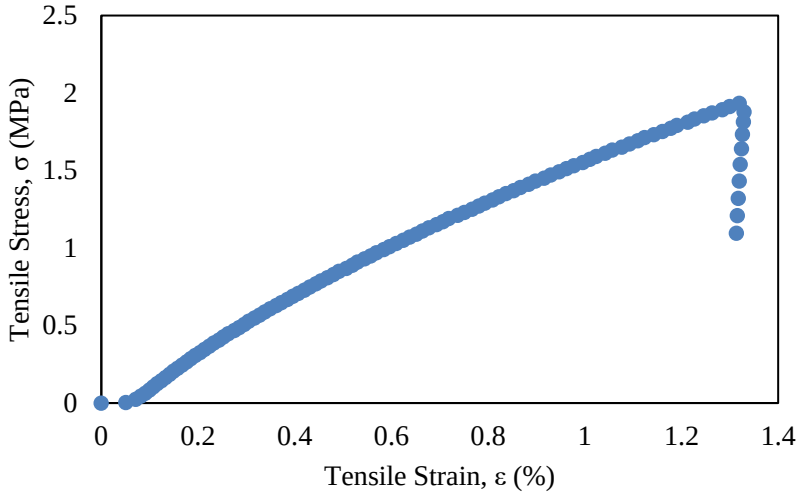

FIGURE 47 DT test result for 3% SBS at -24 °C

TABLE 15 DT test results

Binder Type	Temperature -6 °C	Temperature -12 °C	Temperature -18 °C	Temperature -24 °C
Base	0.985	1.129	0.988	
1% SBS	1.115	1.048	0.767	
3% SBS		2.003	1.850	1.933
5% SBS		1.066	0.989	1.205

Time-Temperature Superposition (TTS) Principle

In this study, the Christensen-Anderson-Marasteanu (CAM) model was used to develop the relaxation master curves using the BBR test data. The CAM model can be expressed as following Eq. (10):

$$S(t) = S_g \left[1 + \left(\frac{\zeta}{\lambda} \right)^{\beta} \right]^{-\kappa/\beta} \tag{10}$$

where, S_g is the glassy modulus (assume as 3 GPa); ζ is the reduced time; β, λ, and κ are the fitting parameters. ζ can be calculated using time and the shift factor, a_T using Eq. (11).

$$\zeta = \frac{t}{a_T} \tag{11}$$

The a_T is calculated using Eq. (12).

$$\ln a_T = \frac{-C_1 (T - T_{ref})}{C_2 + (T - T_{ref})} \tag{12}$$

where T is the testing temperature; T_{ref} is the reference temperature (0 °C); C_1 and C_2 are the fitting parameters.

Converting relaxation modulus into thermal stress

If the average shrinkage rate is α of asphalt pavement, then the thermal stress was calculated using a numerical approach to solve the Eq. (13).

$$\sigma(\zeta) = -\alpha \int_0^t E(\zeta - \zeta^i) \frac{\partial(\Delta T)}{\partial \zeta'} \partial \zeta' \tag{13}$$

Critical Temperatures

Figures 48 shows the thermal stress from the BBR test data and tensile stress from the DT test for the base binder. As mentioned in an earlier section that the critical temperature is the intersection of the BBR and the DT data. Figure 48(a) shows that the critical temperature for the base binder is -16.7 °C. In the similar way, critical temperatures for other binders are shown in Figures 48(b)-(d). The found critical values for the 1%, 3% and 5% SBS modified binders are -14.5, -20.4 and -

16.5 °C. This result indicates that 3% SBS modified binder is most suitable for preventing low-temperature cracking. It was shown in the previous quarterly report that the binder got aged during mixing of the polymer. However, the addition of polymer induced the flexibility in a binder. The 1% SBS modified binder performs poor due to lack of polymeric reinforcement. On the other hand, the 3% SBS modified binder has sufficient polymeric reinforcement that helps it to perform better against thermal stress. The excessive polymer in 5% SBS modified binder leads to lose the tenacity of the binder. Therefore, all 5% SBS modified binder samples breaks at the joints of the end insert of the mold. Thus, tensile strength from the DT test of 5% SBS modified binders are lower compared to 3% SBS modified binders.

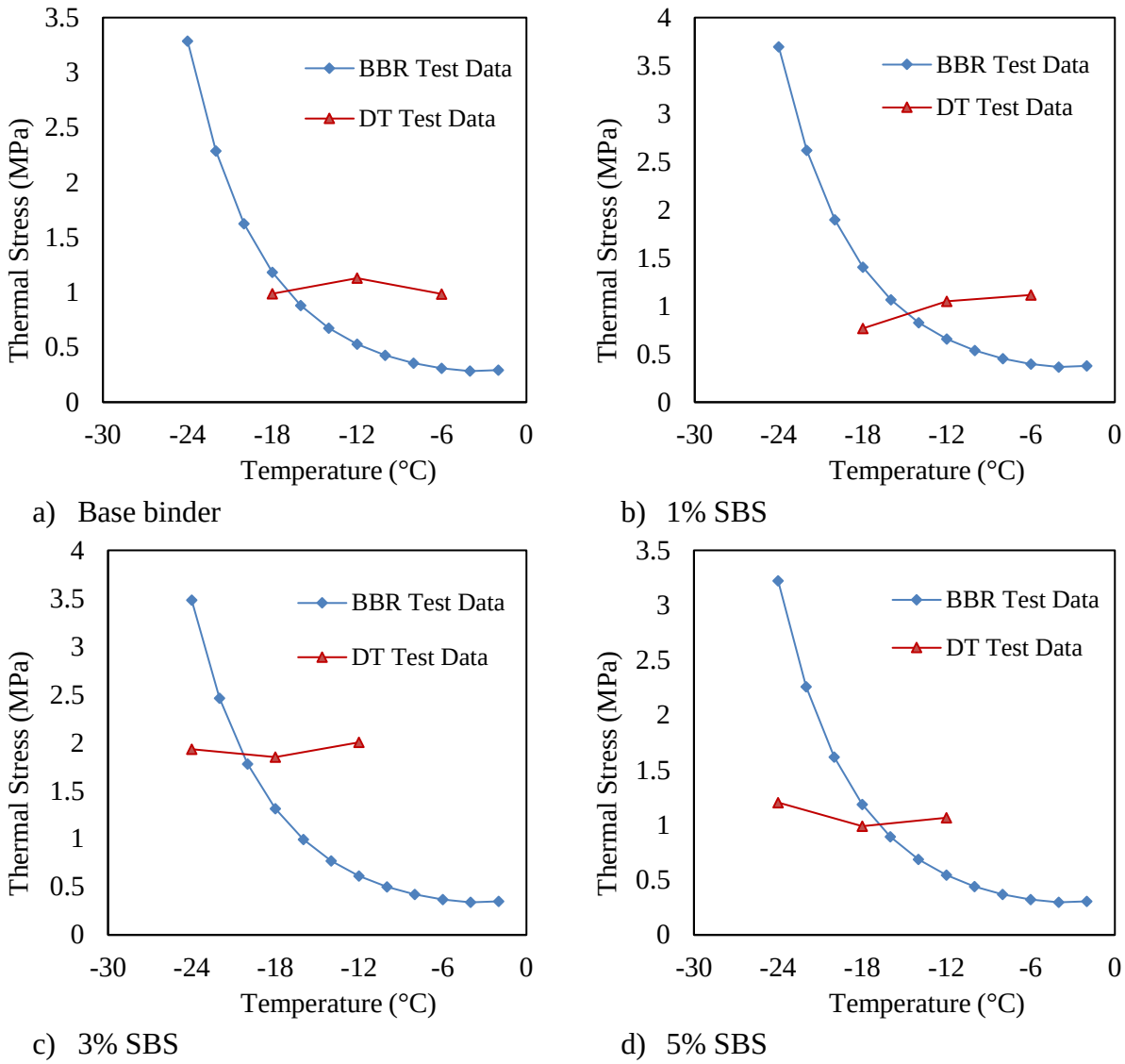

FIGURE 48 Determination of critical temperatures

Correlation between Binder and Mixture Performance

In this section, the correlation between binder critical temperature and the mixture failure temperature was determined. A good linear correlation observed between binder critical temperature and the mixture failure temperature as shown in Figure 49.

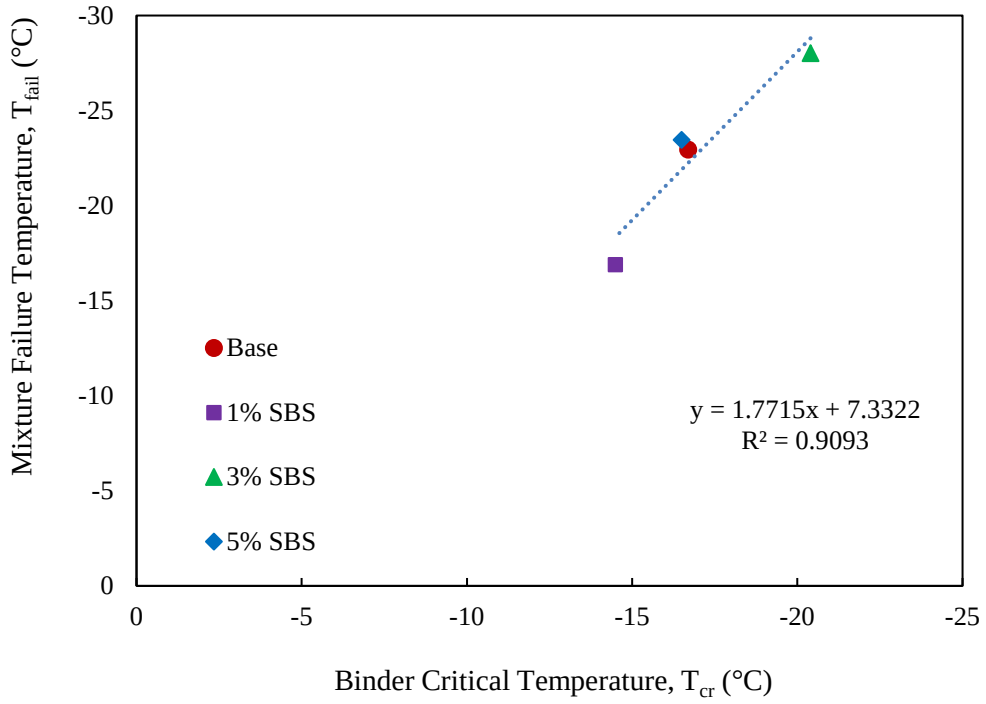

FIGURE 49 Binder critical temperature versus mixture failure temperature

Summary

In this section, low-temperature performances of the lab-produced binders were investigated through BBR and DT tests. Time-temperature superposition principle was to develop the relaxation master curves using the BBR test data. After that, relaxation master curves were used to generate the thermal stress diagram for each test binders. The DT test data was used to determine the critical temperature of the binder. TSRST test was performed to determine the failure temperature of the mixture sample made with a tested binder. This study found that there is a good correlation between binder critical temperature and mixture failure temperature.

THIS PAGE LEFT BLANK INTENTIONALLY

PERFORMANCE OF PMBs USING ME-DESIGN

INTRODUCTION

The AASHTOWare Pavement ME-design software offers several dramatic improvements over the old pavement design procedure (*89*). It considers all input parameters that influence pavement performance, including traffic, climate, pavement structure and material properties, and applying the principles of engineering mechanics to predict critical pavement responses. One of the key advantages of the ME-design is that, it can utilize the dynamic responses of the pavement materials. This section describes the performances of PMBs using the ME-design software.

DESIGN INPUTS

This study evaluated the ME-design predicted performances of the trial sections for the base and other three lab-produced PMBs. The ME-design needs the mixtures' *E** data from the dynamic modulus (DM) test. Instead of performing the DM test on the mixture samples, this study performed the DM test on the binder samples and determines the binders' *G**. After that, it used the Witczak and Bari (*90*) model to predict the mixtures' |*E**| using the mix-volumetrics and the binders' *G**.

Binder Master Curves

This study performed the DSR test to determine the *G** values at different frequencies at different temperature, and then, used to the DSR and the BBR test data to generate the master curves with help of the TTS principle. Following approximation as considered to convert the BBR flexural stiffness, *S* to *G** and time, *t* to tested angular frequency, ω.

$$G^* \approx \frac{S}{3} \tag{14}$$

$$\omega = \frac{1}{t} \tag{15}$$

It is known that the binder response, *G** over the reduced angular frequency, ω_r can be expressed using a sigmoidal function (*91*) as shown in Eq. (16).

$$\log(G^*) = \delta + \frac{\alpha}{1+e^{\beta+\gamma\log(\omega_r)}} \tag{16}$$

where, α, β, δ, and γ are the fitting parameters. The ω_r can be calculated from the tested angular frequency, ω and a shift factor, a_T using Eq. (17).

$$\omega_r = \omega \cdot a_T \tag{17}$$

The purpose of a_T is to convert the ω of any temperature, T to the reference temperature, T_r. The fitting parameters α, β, and γ can be used to represent the phase angle master curve as shown in Eq. (18).

$$\delta_b = -\xi \cdot 90\alpha\gamma \frac{e^{\beta+\gamma\log(\omega_r)}}{\left(1+e^{\beta+\gamma\log(\omega_r)}\right)^2} \tag{18}$$

where, δ_b is the phase angle, and ξ the material fitting parameter.

There are many different shift factor functions found in the literature. One of the widely used shift factor functions is the Williams, Landel, and Ferry (WLF) equation as shown in Eq. (19).

$$\log a_T = \frac{-C_1(T-T_{ref})}{C_2+(T-T_{ref})} \tag{19}$$

where, C_1, and C_2 are the material fitting parameters that depends on T_r. The Arrhenius equation (Eq. (20)) is another shift factor function that is also popular.

$$\log a_T = C\left(\frac{1}{T}-\frac{1}{T_r}\right) \tag{20}$$

where, C is the material constant; and T and T_r are in Kelvin scale. However, second order polynomial equation is most popular for mixture samples as shown in Eq. (21).

$$\log a_T = aT^2 + bT + c \tag{21}$$

where, a, b, and c are the fitting parameters. This study used Eq. (19) for developing binder master curves and used Eq. (21) for the mixture master curves.

Figure 50 shows the developed master curves in frequency (f = ω/2π) for all tested binders. It shows that G^* increases with polymer content at lower frequencies (which also represents the higher temperatures). However, at higher frequencies all binder has almost similar G^* values. Figure 51 shows the phase angle master curves for the tested binders.

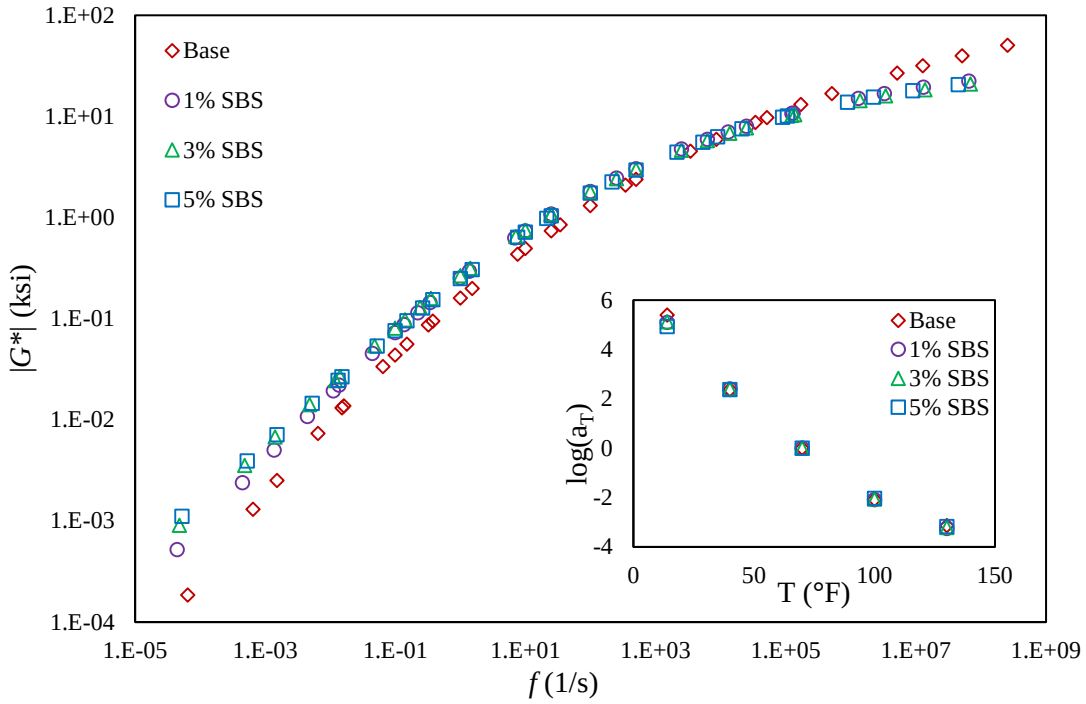

FIGURE 50 *G master curves of the tested binders**

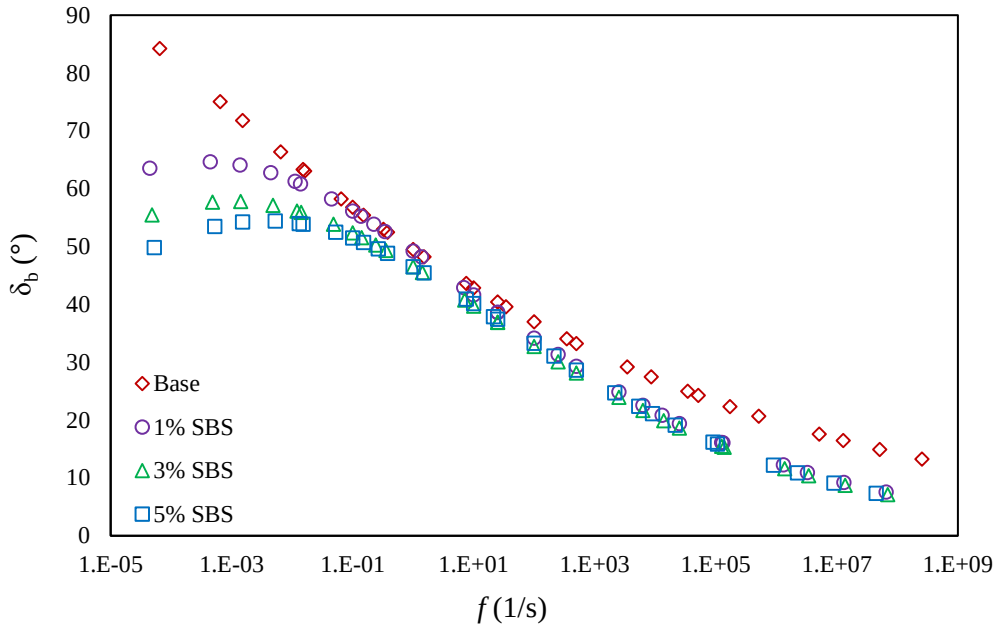

FIGURE 51 Phase angle master curves of the tested binders

Mixture Master Curves

The Witczak and Bari model was used to predict the mixtures' |*E**| values from the binders' *G** values and the mix-volumetrics (*92*). The used model is expressed in Eq. (22). The found *E** values were then used to generate the master curves with help of TTP principle. Figure 52 shows the developed master curves in frequency for all tested mixtures.

$$\log(E^*) = -0.49 + 0.754((G^*)^{-0.0052})[6.65 - 0.032P_{200} + 0.0027P_{200}^{\ 2} + 0.011P_4 - 0.0001P_4^{\ 2} + 0.006P_{3/8} - 0.00014P_{3/8}^{\ 2} - 0.08V_a - 1.06(\frac{V_{be}}{V_{be}+V_a})] + \frac{2.56 + 0.03V_a + 0.71(\frac{V_{be}}{V_{be}+V_a}) + 0.012P_{3/8} - 0.0001P_{3/8}^{\ 2} - 0.01P_{3/4}}{1 + e^{[-0.7814 - 0.5785\log(G^*) + 0.8834\log(\delta_b)]}} \quad (22)$$

where,

E^* = mixture dynamic modulus (psi)
G^* = binder dynamic shear modulus (psi)
δ_b = binder phase angle
V_a = air void
V_{be} = effective binder content by volume
P_{200} = passing No. 200 sieve
P_4 = cumulative % retained on No. 4 sieve
$P_{3/8}$ = cumulative % retained on 3/8 in sieve
$P_{3/4}$ = cumulative % retained on 3/4 in sieve

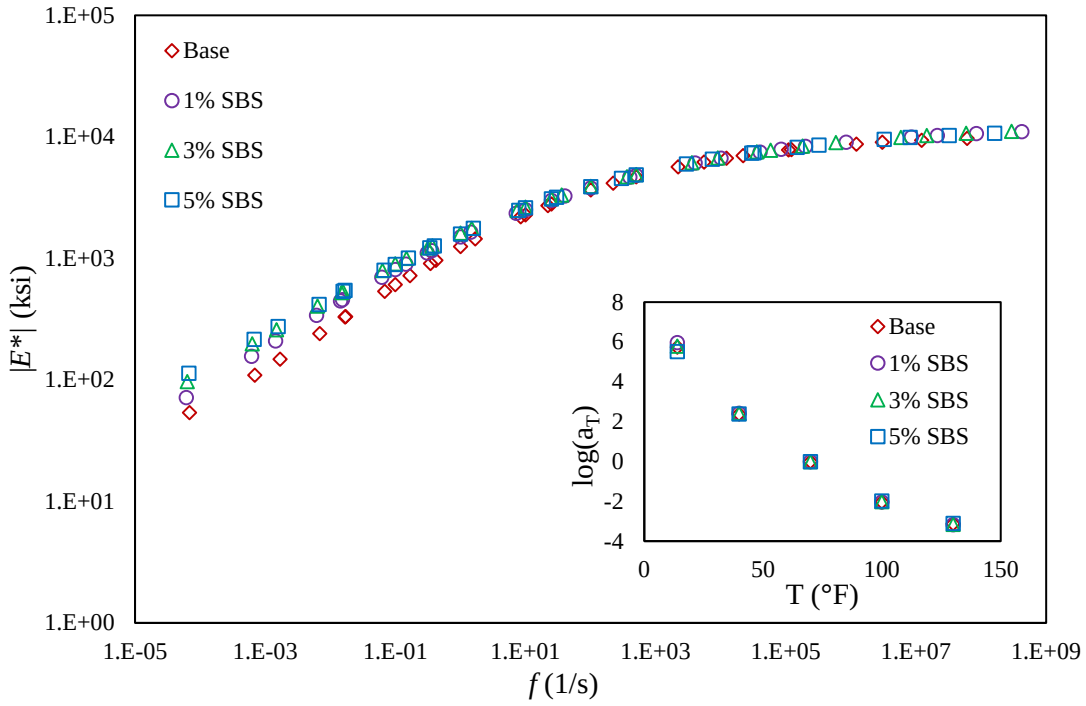

FIGURE 52 *E master curves of the tested binders**

Final Inputs

A trial pavement section with 200 mm AC, 250 mm crushed stone base course underlain by natural subgrade was considered for all sites. In this comparative study, all input parameters were kept constant except the binder and mixture parameters. For each mixture type, the respective G^* and δ_b values from the DSR test was used as the binder input, and the respective E^* values from the Witczak and Bari model was used as the mixture input. The base course modulus was chosen as 280 MPa for crushed stone. Subgrade was chosen as A-3 ME software default subgrade with resilient modulus 170 MPa. Climate data were generated using the weather station of Albuquerque, New Mexico. A traffic growth factor of 3% with a compound rate was used for all analysis. The analysis period was 20 years for all cases. The Annual Average Daily Truck Traffic (AADTT) was chosen as 4,000.

ME ANALYSIS

All three major pavement distresses were considered for this comparative analysis. The predicted distresses are here:

Rutting

Figure 53 compares the predicted rutting found from the ME design software. Since the polymer content increases the stiffness, the rutting value decreases in an increment of polymer content. The base binder has highest rutting and the 5% SBS PMB has the lowest rutting.

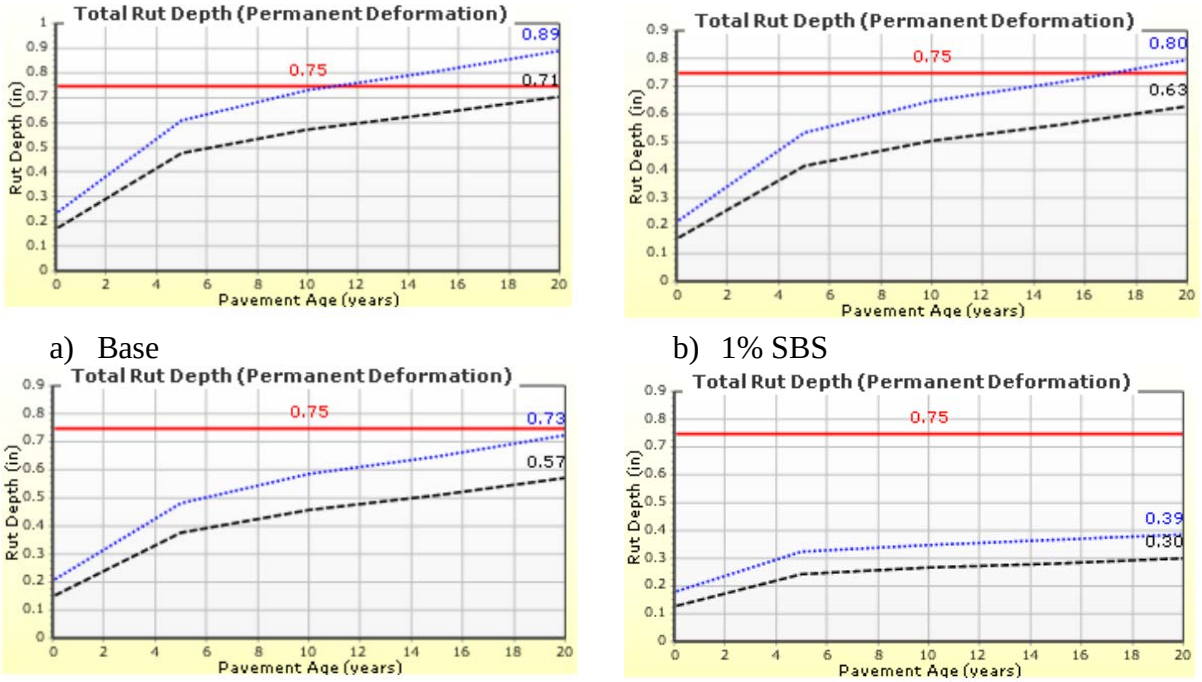

a) Base b) 1% SBS

c) 3% SBS d) 5% SBS

FIGURE 53 Comparison of rutting performance

Fatigue Cracking

Figure 54 compares the predicted fatigue cracking found from the ME design software. The fatigue cracking performance does not follow any pattern with the polymer content because the ME-design uses the empirical model that was developed for the neat binders.

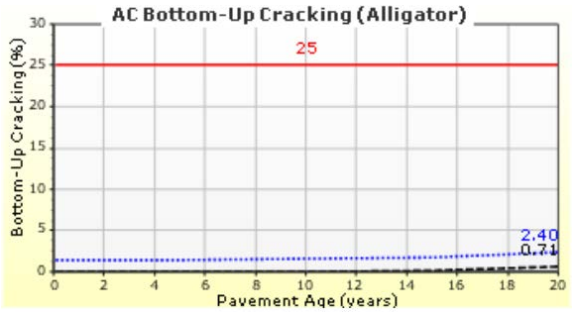

a) Base

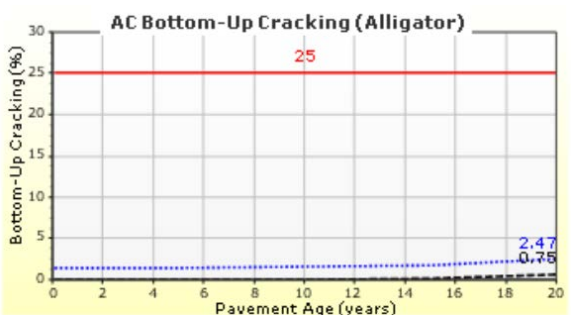

b) 1% SBS

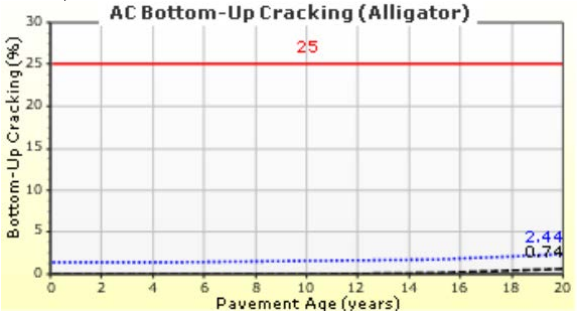

c) 3% SBS

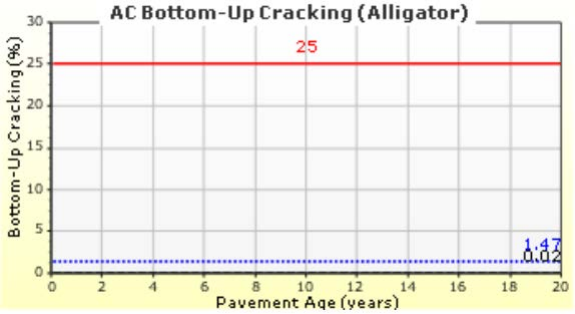

d) 5% SBS

FIGURE 54 Comparison of fatigue cracking performance

Low-temperature Cracking

Figure 55 compares the predicted low-temperature cracking found from the ME design software. There is no difference observed among the binder types. This is because the low-temperature cracking model is still under development.

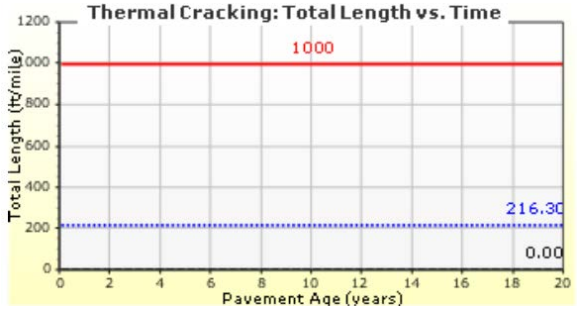

a) Base

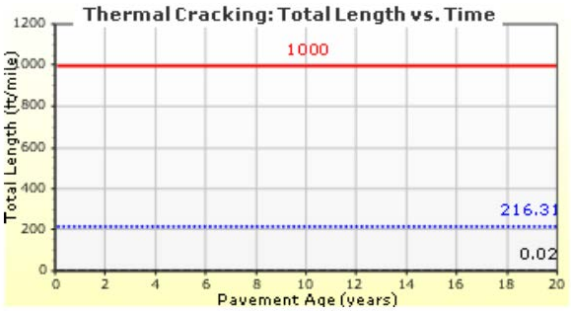

b) 1% SBS

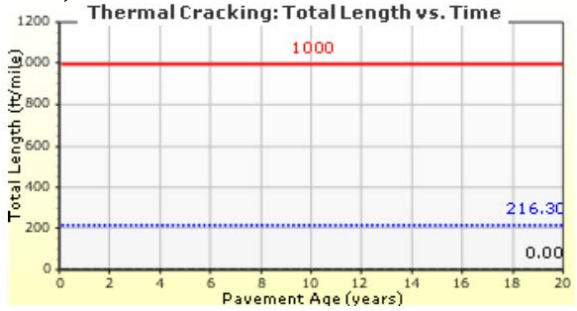

c) 3% SBS

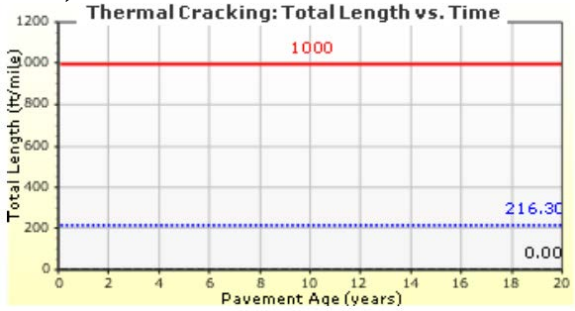

d) 5% SBS

FIGURE 55 Comparison of low-temperature cracking performance

SUMMARY

In this section, the ME-design predicted performances of the trial sections for the base and other three lab-produced PMBs were evaluated. It is found that only predicted rutting follows the same trends as the mixture performance.

EVALUATION OF FIELD PERFORMANCE

INTRODUCTION

Pavement performance can be complicated by some uncontrollable/un-documented factors in the field. Therefore, it is important to evaluate the performance of the polymer modified pavements.

SELECTION OF FIELD SITE

It is known that pavement performance can be significantly affected by a small change in mix volumetrics and layer thickness. In addition, climate and traffic are also very important parameter those directly controls the pavement performance (*93, 94*). To evaluate the field performance of the PMBs compare to the neat binders, it is essential to select the pair of pavement sites in which both sites have all same properties except the binder type. However, practically, it is very difficult to find such pair sites. Furthermore, the use of PMBs in main pavement layers is rare in New Mexico and only one pair was found that meets the abovementioned criteria. The interested pavement sections are in District 4 of central New Mexico and were constructed in fall of 2014 along the westbound lane of Interstate 40 near Santa Rosa, New Mexico. Both pavement sections were constructed with ceca based Warm Mix Asphalt (WMA) incorporating approximately 20% Reclaimed Asphalt Material (RAP). The used binder grades of these sections are PG 70-28 and PG 70-28+ respectively. Both pavements have an AC layer of nearly 12 inch with a 13 inch granular subbase underlined a treated subbase. The performance data was extracted from the LTPP database. Figure 56 compares the measure distresses between two sites. It shows that both pavements only have some rutting after their construction. However, none of them has the fatigue and the low-temperature cracking. This may be due to a large AC layer thickness. Moreover, both pavements are newly constructed and might not experience enough traffic loading or environment adversity.

SUMMARY

The field data is not adequate to make a conclusion.

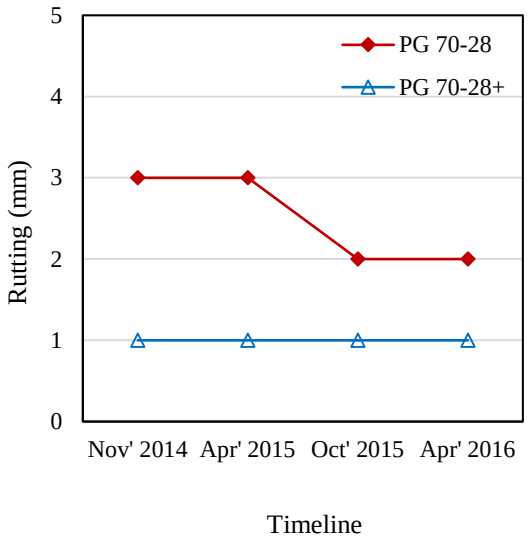

a) Rutting

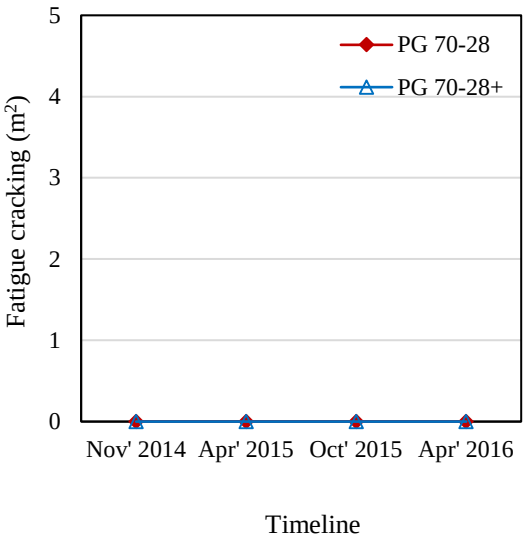

b) Fatigue cracking

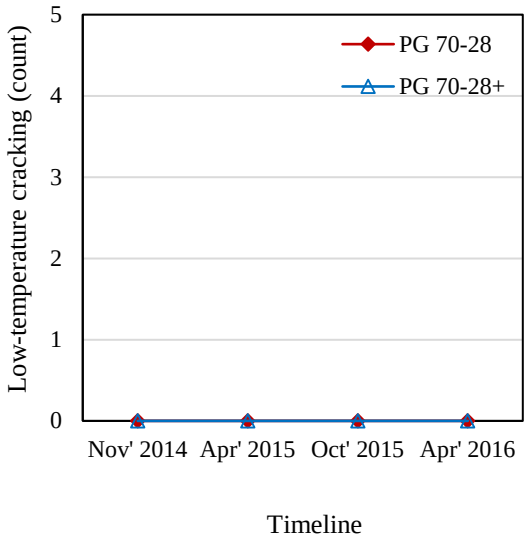

c) Low-temperature cracking

FIGURE 56 Investigation of field performance of PMB

CONCLUSIONS AND RECOMMENDATION

CONCLUSIONS

This study explored the effectiveness of different binder tests for characterizing performance of PMBs against three major pavement distresses such as rutting, fatigue cracking and low-temperature cracking. At the beginning, a neat binder was blended with SBS polymer at three different percentages: 1%, 3% and 5%. The blended binders were used to generate a calibration curve using FTIR spectroscopy for detecting SBS content in an unknown PMB. The lab produced binders were also used to prepare the mixture samples for performance tests. All the mixture samples have same volumetric properties other than the binder type. HWTD, BF and TSRST tests were performed on mixture samples made with different binders to investigate the rutting, fatigue cracking and low-temperature performance respectively. Binder performance was evaluated through current PG tests and other performance based-tests to determine the representative parameter for the above-mentioned distresses. After that, this study evaluated the linear correlation between the mixture test data and respective binder tests data. Based on the results following conclusions can be drawn:

a) The FTIR spectroscopy shows that the PMBs have noticeable peak values for the presence of different polymetric functional groups. It is also found that the peak values also increase with an increment of polymer content and this study developed a calibration based on this relationship. This calibration curve will be an effective tool for detecting the presence of polymer as well as polymer content.
b) None of the PG parameters works for the PMBs. For example, the rutting parameter, $G^*/\sin\delta$ does not correlate good with the rut depth from the HWDT test. The fatigue cracking parameter, $G^*\sin\delta$ also has a very poor correlation with the *FEL* from the BF test. Similarly, the low-temperature grades do not correlate with the failure temperature, T_{fail} from the TSRST test.
c) The MSCR is most appropriate test for characterizing rutting potential of a PMB because the J_{nr} from the MSCR test has a very strong correlation with the rut depth from the HWDT test.
d) This study found that both TS and LAS tests are appropriate for representing fatigue performance of a PMB.
e) Critical temperature from the BBR and DT tests can be a good option for characterizing the low-temperature cracking performance of a PMB.

RECOMMENDATION FOR FUTURE STUDIES

The following tasks can be recommended for the future studies:

a) This is a preliminary study on the PMBs based on a single polymer type and a single aggregate gradation. Adding different polymers and different aggregate gradation will make the conclusion more valid and acceptable.
b) This study evaluated the correlations between different binder tests' parameters and laboratory mixture performances. However, the correlations between different binder

tests' parameters and field pavement performances were not investigated here, which can be pursued in another research.

c) Use of reclaimed asphalt pavement (RAP) became popular these days. As RAP materials are aged and may increase the possibility of fatigue and low-temperature cracking. It would be interesting to see whether PMBs survive this drawback after adding RAP.

REFERENCES

1. AASHTO, M 320-14. Standard Specification for Performance Graded Asphalt Binder." American Association of State Highway and Transportation Officials, Washington, DC, 2014.
2. AASHTO, T 315-14. Standard Method of Test for Determining the Rheological Properties of Asphalt Binder Using a Dynamic Shear Rheometer (DSR)." American Association of State Highway and Transportation Officials, Washington, DC, 2014.
3. AASHTO, T 240-14. Standard Method of Test for Effect of Heat and Air on a Moving Film of Asphalt (Rolling Thin-Film Oven Test). American Association of State Highway and Transportation Officials, Washington, DC, 2014.
4. AASHTO T 313-14. Standard Method of Test for Determining the Flexural Creep Stiffness of Asphalt Binder Using the Bending Beam Rheometer (BBR). American Association of State Highway and Transportation Officials, Washington, DC, 2014.
5. AASHTO, R. 28-14 Standard Practice for Accelerated Aging of Asphalt Binder Using a Pressurized Aging Vessel (PAV)." American Association of State Highway Transportation Officials, Washington, DC, 2014.
6. AASHTO T 314-14. Determining Fracture Properties of Asphalt Binder in Direct Tension (DT). American Association of State Highway and Transportation Officials, Washington, DC, 2014.
7. Yildirim, Y. Polymer Modified Asphalt Binders. Construction and Building Materials, Vol. 21, No. 1, 2007, pp. 66–72.
8. Hasan, M. A., Manna, U. A., and Tarefder, R. A. Exploring the Alternative Binder Tests to Assess the Fatigue Performance of a Polymer Modified Binder. In *98th Annual Meeting of Transportation Research Board*, Washington D.C., paper 19-04966, 2019.
9. Airey, G. D. Styrene Butadiene Styrene Polymer Modification of Road Bitumens. *Journal of Materials Science*, Vol. 39, No. 3, pp. 951–959, 2004.
10. Airey, G. D. Rheological Properties of Styrene Butadiene Styrene Polymer Modified Road Bitumens. *Fuel*, Vol. 82, No. 14, pp. 1709–1719, 2003.
11. Chen, J.-S., M.-C. Liao, and M.-S. Shiah. Asphalt Modified by Styrene-Butadiene-Styrene Triblock Copolymer: Morphology and Model. *Journal of Materials in Civil Engineering*, Vol. 14, No. 3, pp. 224–229, 2002.
12. Sengoz, B., and G. Isikyakar. Evaluation of the Properties and Microstructure of SBS and EVA Polymer Modified Bitumen. *Construction and Building Materials*, Vol. 22, No. 9, pp. 1897–1905, 2008.
13. Sengoz, B., A. Topal, and G. Isikyakar. Morphology and Image Analysis of Polymer Modified Bitumens. *Construction and Building Materials*, Vol. 23, No. 5, pp. 1986–1992, 2009.
14. Bahia, H. U., H. Zhai, K. Bonnetti, and S. Kose. Non-Linear Viscoelastic and Fatigue Properties of Asphalt Binders. *Journal of the Association of Asphalt Paving Technologists*, Vol. 68, pp. 1–34, 1999.
15. Anderson, M., J. D'Angelo, and D. Walker. MSCR: A Better Tool for Characterizing High Temperature Performance Properties. *Asphalt*, Vol. 25, No. 2, 2010.
16. AASHTO T 350-14. "Multiple Stress Creep Recovery (MSCR) Test of Asphalt Binder Using a Dynamic Shear Rheometer." American Association of State Highway and Transportation Officials, Washington, DC, 2014.

17. Bahia, H. U., D. I. Hanson, M. Zeng, H. Zhai, M. A. Khatri, and R. M. Anderson. *Characterization of Modified Asphalt Binders in Superpave Mix Design*. NCHRP No. 459, Project 9-10 FY'96, 2001.
18. AASHTO, TP 101. "Standard Method of Test for Determining the Fatigue Life of Compacted Asphalt Mixtures Subjected to Repeated Flexural Bending." American Association of State Highway and Transportation Officials, Washington, DC, 2014.
19. Johnson, C. M. Estimating Asphalt Binder Fatigue Resistance using an Accelerated Test Method. PhD dissertation. University of Wisconsin–Madison, 2010.
20. Hintz, C., R. Velasquez, C. Johnson, and H. U. Bahia. Modification and Validation of the Linear Amplitude Sweep Test for Binder Fatigue Specification. In *Transportation Research Record: Journal of the Transportation Research Board*, No. 2207, Washington, D.C., pp. 99–106, 2011.
21. Hintz, C., and H. U. Bahia. Simplification of Linear Amplitude Sweep Test and Specification Parameter. In *Transportation Research Record: Journal of the Transportation Research Board*, No. 2370, Washington, D.C., pp. 10–16, 2013.
22. Micaelo, R., Pereira, A., Quaresma, L. and Cidade, M.T., 2015. Fatigue resistance of asphalt binders: Assessment of the analysis methods in strain-controlled tests. *Construction and Building Materials*, 98, 703-712.
23. Safaei, F., Castorena, C., and Kim, Y. R. (2016). "Linking asphalt binder fatigue to asphalt mixture fatigue performance using viscoelastic continuum damage modeling." *Mechanics of Time-Dependent Materials*, Springer, 20(3), 299–323.
24. Wang, C., Castorena, C., Zhang, J., & Richard Kim, Y. (2015). Unified failure criterion for asphalt binder under cyclic fatigue loading. *Road Materials and Pavement Design*, 16, 125-148.
25. Hasan, M. A., Hasan, M. M., Bairgi, B. K., Mannan, U. A., and Tarefder, R. A. Utilizing Simplified Viscoelastic Continuum Damage Model to Characterize the Fatigue Behavior of Styrene-Butadiene-Styrene (SBS) Modified Binders. *Construction and Building Materials*, 159–169, 2019.
26. Marasteanu, M., Zofka, A.; Turos, M., Li, X.; Velasquez, R., Xue, L., Buttlar, W., Paulino, G., Braham, A., Dave, E. Investigation of Low Temperature Cracking in Asphalt Pavements. A Transportation Pooled Fund Study; Report No MN/RC 2007-43; University of Minnesota: Minneapolis, MN, USA, 2007.
27. Marasteanu, M., Buttlar, W., Bahia, H., Williams, C. Investigation of Low Temperature Cracking in Asphalt Pavements, National Pooled Fund Study—Phase II; Report No MN/RC 2012-23; University of Minnesota: Minneapolis, MN, USA, 2012.
28. Lu, X., and U. Isacsson. Chemical and Rheological Evaluation of Ageing Properties of SBS Polymer Modified Bitumens. *Fuel*, Vol. 77, No. 9–10, pp. 961–972, 1998.
29. Tarefder, R. A., and A. M. Zaman. Nanoscale Evaluation of Moisture Damage in Polymer Modified Asphalts. *Journal of Materials in Civil Engineering*, Vol. 22, No. 7, 2009, pp. 714–725.
30. Molenaar, A.A.A., Hagos, E.T. and Van de Ven, M.F.C. Effects of aging on the mechanical characteristics of bituminous binders in PAC. *Journal of Materials in Civil Engineering*, 22(8), pp.779-787, 2010.

31. Naskar, M., Reddy, K.S., Chaki, T.K., Divya, M.K. and Deshpande, A.P. Effect of ageing on different modified bituminous binders: comparison between RTFOT and radiation ageing. *Materials and Structures*, 46(7), pp.1227-1241, 2013.
32. Tarefder, R. A., and S. S. Yousefi. Rheological Examination of Aging in Polymer-Modified Asphalt. *Journal of Materials in Civil Engineering*, Vol. 28, No. 2, p. 4015112, 2015.
33. Ameri, M., Mansourian, A. and Sheikhmotevali, A.H. Investigating effects of ethylene vinyl acetate and gilsonite modifiers upon performance of base bitumen using Superpave tests methodology. *Construction and Building Materials*, 36, pp.1001-1007, 2012.
34. Bulatović, V.O., Rek, V. and Marković, K.J. Rheological properties and stability of ethylene vinyl acetate polymer-modified bitumen. *Polymer Engineering & Science*, 53(11), pp.2276-2283, 2013.
35. Bahia, H.U. and Davies, R. Effect of crumb rubber modifiers (CRM) on performance related properties of asphalt binders. *Asphalt Paving Technology*, 63, pp.414-414, 1994.
36. Navarro, F.J., Partal, P., Martínez-Boza, F.J. and Gallegos, C. Influence of processing conditions on the rheological behavior of crumb tire rubber-modified bitumen. *Journal of Applied Polymer Science*, 104(3), pp.1683-1691, 2007.
37. Kök, B.V. and Çolak, H. Laboratory comparison of the crumb-rubber and SBS modified bitumen and hot mix asphalt. *Construction and Building Materials*, 25(8), pp.3204-3212, 2011.
38. Robinson, H. (2005). "*Polymers in Asphalt"* (Vol. 15, No. 11). iSmithers Rapra Publishing.
39. Navarro, F.J., Partal, P., Martinez-Boza, F. and Gallegos, C. Influence of crumb rubber concentration on the rheological behavior of a crumb rubber modified bitumen. *Energy & Fuels*, 19(5), pp.1984-1990, 2005.
40. Utracki, L.A. History of commercial polymer alloys and blends (from a perspective of the patent literature). Polymer Engineering & Science, 35(1), pp.2-17, 1995.
41. Rostler, F.S., White, R.M. and Cass, P.J. Modification of Asphalt Cements for Improvement of Wear Resistance of Pavement Surfaces. Report No.: FHWA-RD-72-24, Washington, D.C., 1972.
42. Chaffin, C. W., O'Connor, D. L., & Hughes, C. H. Evaluation of the use of certain elastomers in asphalt. Report No.: FHWA-TX-78180-1F, Washington, D.C., 1978.
43. Piazza, S., Arcozzi, A., & Verga, C. Modified bitumens containing thermoplastic polymers. *Rubber Chemistry and Technology*, 53(4), 994-1005, 1980.
44. Reese, R., & Predoehl, N. H. Evaluation of Modified Asphalt Binders. Interim Report. Report No.: FHWA/CA/TL-89/15, Washington, D.C., 1989.
45. Krutz, N. C., Siddharthan, R., & Stroup-Gardiner, M. Investigation of rutting potential using static creep testing on polymer-modified asphalt concrete mixtures. *Transportation Research Record: Journal of the Transportation Research Board*, (1317), 100-108, 1991.
46. Stock, A. F., & Arand, W. Low temperature cracking in polymer modified binders. *Journal of the Association of Asphalt Paving Technologists*, 62, 1993.
47. Lu, X., Isacsson, U., & Ekblad, J. Phase separation of SBS polymer modified bitumens. *Journal of Materials in Civil Engineering*, 11(1), 51-57, 1999.
48. Wen, G., Zhang, Y., Zhang, Y., Sun, K., and Fan, Y. Rheological characterization of storage-stable SBS-modified asphalts. Polymer Testing, Elsevier, 21(3), 295–302, 2002.

49. Li, Y., Li, L., Zhang, Y., Zhao, S., Xie, L., and Yao, S. Improving the aging resistance of styrene-butadiene-styrene tri-block copolymer and application in polymer-modified asphalt. *Journal of Applied Polymer Science*, 116(2), 754-761, 2010.
50. Navarro, F. J., Partal, P., Martınez-Boza, F., & Gallegos, C. Thermo-rheological behaviour and storage stability of ground tire rubber-modified bitumens. *Fuel*, 83(14), 2041-2049, 2004.
51. Lu, X., and U. Isacsson. Rheological Characterization of Styrene-Butadiene-Styrene Copolymer Modified Bitumens. *Construction and Building Materials*, Vol. 11, No. 1, pp. 23–32, 1997.
52. Lu, X., and U. Isacsson. Chemical and Rheological Evaluation of Ageing Properties of SBS Polymer Modified Bitumens. *Fuel*, Vol. 77, No. 9–10, pp. 961–972, 1998.
53. Lu, X., & Isacsson, U. Modification of road bitumens with thermoplastic polymers". *Polymer Testing*, 20(1), 77-86, 2002.
54. Khattak, M., and Baladi, G. Fatigue and permanent deformation models for polymer-modified asphalt mixtures. *Transportation Research Record: Journal of the Transportation Research Board*, (1767), 135-145, 2001.
55. Navarro, F. J., Partal, P., Martınez-Boza, F., Valencia, C., and Gallegos, C. Rheological characteristics of ground tire rubber-modified bitumens. *Chemical Engineering Journal*, 89(1), 53-61, 2002.
56. Ruan, Y., Davison, R. R., & Glover, C. J. Oxidation and viscosity hardening of polymer-modified asphalts". *Energy & Fuels*, 17(4), 991-998, 2003.
57. Glanzman, T. Quantifying the Benefits of Polymer Modified Asphalt. *Asphalt*, 20, no. 1 2005.
58. Von Quintus, H. L., Mallela, J., and Buncher, M. S. Quantification of Effect of Polymer-Modified Asphalt on Flexible Pavement Performance. *Transportation Research Record: Journal of the Transportation Research Board*, No 2001, 2007, pp. 141-154, 2005.
59. Dreessen, S., Planche, J. P., Ponsardin, M., Pittet, M., and Dumont, A. G. Durability study: field aging of conventional and polymer-modified binders. In *Transportation Research Board 89th Annual Meeting*, Washington, D.C.: Transportation Research Board, Paper No. 10-2127, 2010.
60. Bahia, H., Perdomo, D., & Turner, P. Applicability of Superpave binder testing protocols to modified binders. *Transportation Research Record: Journal of the Transportation Research Board*, (1586), 16-23, 1997.
61. Bahia, H. U., Hislop, W. P., Zhai, H., and Rangel, A. Classification of asphalt binders into simple and complex binders. *Journal of the Association of Asphalt Paving Technologists*, 67, 1–41, 1999.
62. D'Angelo, J., Kluttz, R., Dongre, R. N., Stephens, K., & Zanzotto, L. Revision of the superpave high temperature binder specification: The multiple stress creep recovery test (with discussion). *Journal of the Association of Asphalt Paving Technologists*, 76, 2007.
63. Harmelink D., Special Polymer Modified Asphalt Cement". Colorado Department of Transportation, Final Report: CDOT -DTD-R -97-3, 1997.
64. Greene, J., Chun, S., Choubane, B. Evaluation and Implementation of a Heavy Polymer Modified Asphalt Binder through Accelerated Pavement Testing. Florida Department of Transportation, Research Report: FL/DOT/SMO/14-564, 2014.
65. Loucks, D. A., and Seguin, F. P. Analysis of Asphalt. U. S. Patent No. 4,990,456, 1991.

66. Mansoori, G. A. A unified perspective on the phase behaviour of petroleum fluids. *International Journal of Oil, Gas and Coal Technology*. 2:141–167, 2009.
67. Kosińska, J., Boczkaj, G., Gałęzowska, G., Podwysocka, J., Przyjazny, A., & Kamiński, M. Determination of modifier contents in polymer-modified bitumens and in samples collected from the roads using high-performance gel permeation/size-exclusion chromatography. *Road Materials and Pavement Design*, 1-16, 2015.
68. Chen, J-S., and Lin, C-H. Construction of Test Road to Evaluate Engineering Properties of Polymer-Modified Asphalt Binders. *International Journal of Pavement Engineering*, Vol. 1, No. 4, pp. 285-295, 2000.
69. Han, S., Yuan, J. A., Cheng, D. H., and Gao, W. (2009). A method to determine polymer content in asphalt based viscosity-temperature curve. Chinese Patent No. 101694450 A (in Chinese).
70. Molenaar, J.M.M., Hagos, E.T., Van de Ven, M.F.C., and Hofman, R. An Investigation into the Analysis of Polymer Modified Bitumen (PMB). In *Proceedings of the 3rd Eurasphalt and Eurobitume Congress*, Book I, Eurasphalt and Eurobitume Congress, Vienna, Austria, pp. 666-682, 2004.
71. Hasan, M. A., Mannan, U. A., and Tarefder, R. A. (2017). "Determination of Polymer Content in SBS Modified Asphalt Binder using FTIR Analysis." In *The Ninth International Conference on Construction in the 21st Century (CITC-9), Revolutionizing the Architecture, Engineering and Construction Industry through Leadership, Collaboration and Technology*, March 5th-7th, 2017, Dubai, United Arab Emirates.
72. Yen, T. F., and G. V Chilingarian. Asphaltenes and Asphalts, 2. Elsevier, 2000.
73. Zubeck, H. K., L. Raad, S. Saboundjian, and Minassian. Workability and Performance of Polymer-Modified Asphalt Aggregate Mixtures in Cold Regions. *International Journal of Pavement Engineering*, 4:1, 25-36, 2013.
74. Cong, Y., W. Huang, K. Liao, and Y. Zhai. Study on Storage Stability of SBS Modified Asphalt. *Petroleum Science and Technology*, Vol. 23, No. 1, pp. 39–46, 2005.
75. Fernandes, M. R. S., M. M. C. Forte, and L. F. M. Leite. Rheological Evaluation of Polymer-Modified Asphalt Binders. *Materials Research*, Vol. 11, No. 3, pp. 381–386, 2008.
76. Kou, C., A. Kang, and W. Zhang. Methods to Prepare Polymer Modified Bitumen Samples for Morphological Observation. *Construction and Building Materials*, Vol. 81, pp. 93–100, 2015.
77. Kou, C., P. Xiao, A. Kang, P. Mikhailenko, H. Baaj, and Z. Wu. Protocol for the Morphology Analysis of SBS Polymer Modified Bitumen Images Obtained by Using Fluorescent Microscopy. *International Journal of Pavement Engineering*, pp. 1–7, 2017.
78. AASHTO T 316-14. Standard Method of Test for Viscosity Determination of Asphalt Binder Using Rotational Viscometer (RV). American Association of State Highway and Transportation Officials, Washington, DC, 2014.
79. AASHTO T 324-11. Standard Method of Test for Hamburg Wheel-Track Testing of Compacted Hot Mix Asphalt (HMA). American Association of State Highway and Transportation Officials, Washington, DC, 2011.
80. AASHTO T 350-16. Multiple Stress Creep Recovery (MSCR) Test of Asphalt Binder Using a Dynamic Shear Rheometer. American Association of State Highway and Transportation Officials, Washington, DC, 2016.

81. Mannan, U. A., M. R. Islam, and R. A. Tarefder, Effects of Recycled Asphalt Pavements on the Fatigue Life of Asphalt under Different Strain Levels and Loading Frequencies. *International Journal of Fatigue*, Vol. 78, pp. 72–80, 2015.
82. AASHTO, T 321-14. Standard Method of Test for Determining the Fatigue Life of Compacted Asphalt Mixtures Subjected to Repeated Flexural Bending. American Association of State Highway and Transportation Officials, Washington, DC, 2014.
83. Tarefder, R. A., D. Bateman, and A. K. Swamy. Comparison of Fatigue Failure Criterion in Flexural Fatigue Test". *International Journal of Fatigue*, Vol. 55, pp. 213–219, 2013.
84. Prowell, B. D., Brown, E. R., Anderson, R. M., Daniel, J. S., Swamy, A. K., Quintus, H. V., Shen, S., Carpenter, S. H., Bhattacharjee, S. and Maghsoodloo, S. Validating the fatigue endurance limit for hot mix asphalt". Final NCHRP Rep. 646, National Cooperative Highway Research Program, Washington, DC, 2010.
85. Peterson, J. C., R. E. Robertson, J. F. Branthaver, P. M. Harnsberger, J. J. Duvall, and S. S. Kim. Binder Characterization and Evaluation, Volume 4: Test Methods. Rep. No. SHRP-A-367, Strategic Highway Research Program, National Research Council, Washington, DC, 1994.
86. Monismith, C.L.; Secor, G.A.; Secor, K.E. Temperature induced stresses and deformations in asphalt concrete. *Journal of the Association of Asphalt Paving Technologists*. 34, 248–285, 1965.
87. Jung, D.; Vinson, T.S. Low temperature cracking resistance of asphalt concrete mixtures. *Journal of the Association of Asphalt Paving Technologists*. 62, 54–92, 1993.
88. Moon, Ki Hoon. Comparison of thermal stress calculated from asphalt binder mixture creep compliance data. Masters Thesis, University of Minnesota, 2010.
89. *Guide for Design of Pavement Structures*. American Association of State Highway and Transportation Officials, Washington, D.C., 1993.
90. Bari, J., and Witczak, M.W. Development of a New Revised Version of the Witczak E* Predictive Model for Hot Mix Asphalt Mixtures. *Journal of the Association of Asphalt Paving Technologists*, Vol. 75, pp. 381-423, 2006.
91. Oshone, M., Dave, E., Daniel, J.S. and Rowe, G.M. Prediction of phase angles from dynamic modulus data and implications for cracking performance evaluation. *Road Materials and Pavement Design*, 18, pp.491-513, 2017.
92. Giuliana, G., Nicolosi, V., & Festa, B. Predictive Formulas of Complex Modulus for High Air Void Content Mixes". In *Transportation Research Board 91st Annual Meeting*, Washington, DC, 2012.
93. Hasan, M. A., M. R. Islam, and R. A. Tarefder. Clustering Vehicle Class Distribution and Axle Load Spectra for Mechanistic-Empirical Predicting Pavement Performance. *Journal of Transportation Engineering*, DOI: 10.1061/(ASCE)TE.1943-5436.0000876, 05016006, 2016.
94. Hasan, M.A. and Tarefder, R.A., 2018. Development of Temperature Zone Map for Mechanistic Empirical (ME) Pavement Design. *International Journal of Pavement Research and Technology*, 11(1), pp.99-111, 2018.

New Mexico Department of Transportation
RESEARCH BUREAU
7500B Pan American Freeway NE
PO Box 94690
Albuquerque, NM 87199-4690
Tel: (505) 841-9145